SLAC-PUB-1851
December 1976

ψ SPECTROSCOPY*

Gary J. Feldman

Stanford Linear Accelerator Center
Stanford University, Stanford, California

CONTENTS

* Work supported by the Energy Research and Development Administration

(Lectures 1 and 2 of a three-lecture series given at the Summer Institute on Particle Physics, Stanford Linear Accelerator Center, Stanford, California, August 1976. Lecture 3 is available as SLAC-PUB-1852.)

I. Introduction

These first two lectures will cover the properties of the various members of the ψ family, the bound states of a charmed quark and a charmed anti-quark. The recent identification of charmed mesons in e^+e^- annihilation[1-4] has effectively removed other explanations of the origin of the ψ particles as viable alternatives. Accordingly, whenever it is convenient to do so in these lectures, we will freely assume that members of the ψ family are states of charmonium.

As an introduction, we will investigate what can be learned by studying the e^+e^- spectrum, that is, the total cross section for e^+e^- annihilation into hadronic final states as a function of energy. Then after a brief description of a few detectors, we will start on the main topic of these lectures, the properties of the ψ's and χ's as determined from their production and decay.

II. The e^+e^- spectrum

II.A. The s-channel resonances

Figure 1 shows the ratio, R, of the total cross section for hadron production to the total cross section for μ pair production as a function of center-of-mass energy. The data come from Novosibirsk,[5-8] Orsay,[9-15] Frascati,[16-20] CEA,[21,22] and SPEAR.[23-27] The most obvious features of this spectrum are a series of resonances. We can understand these resonances as bound states of quark-antiquark pairs. For each type of quark, we can form an s-wave state with quark spins parallel. Such states will have the quantum numbers of a photon and can be produced as s-channel resonances in e^+e^- annihilations as illustrated in Fig. 2.

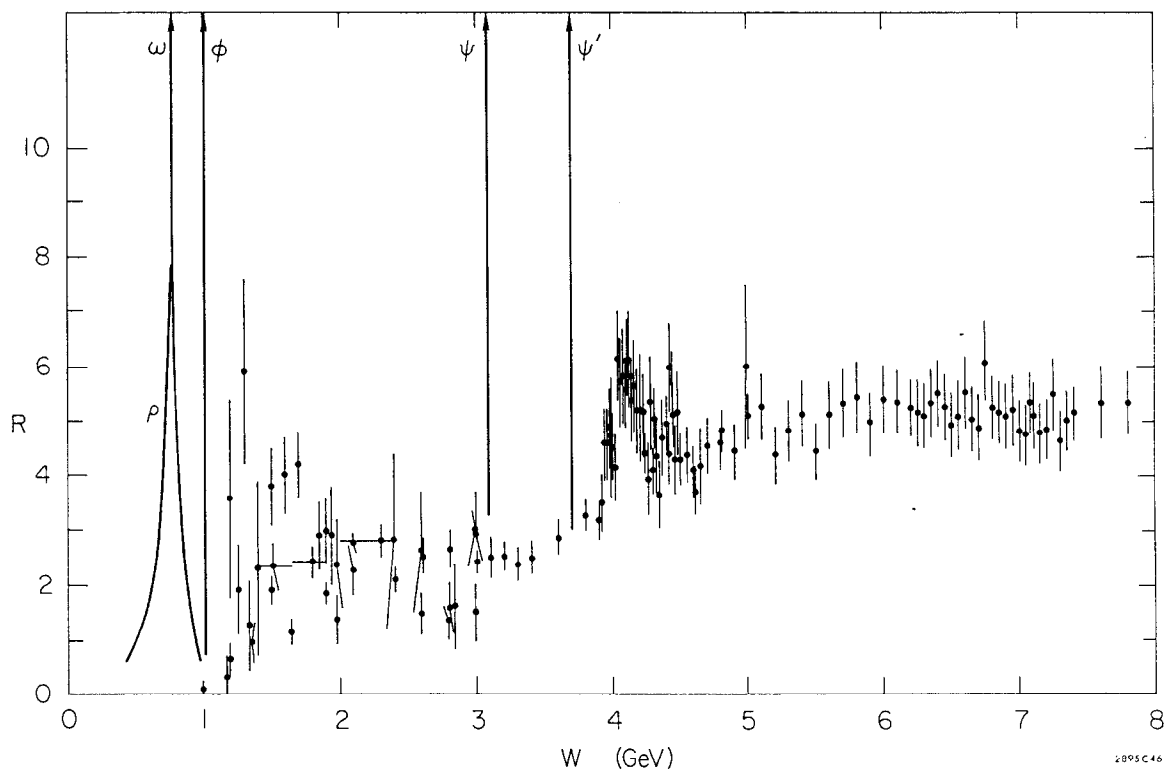

FIG. 1. Ratio, R, of the total cross section for hadron production to the total cross section for μ pair production as a function of center-of-mass energy.

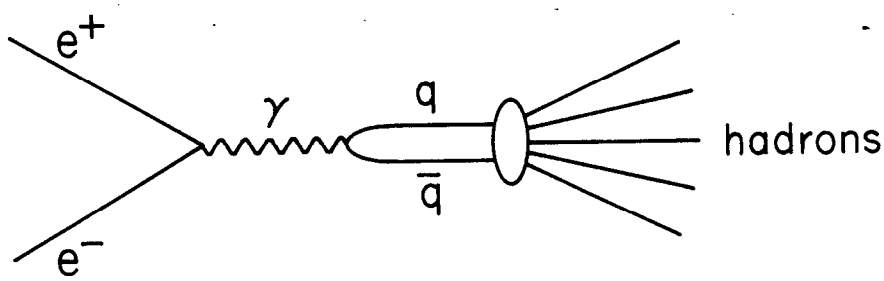

FIG. 2. Production of s-channel resonances in e^+e^- annihilation.

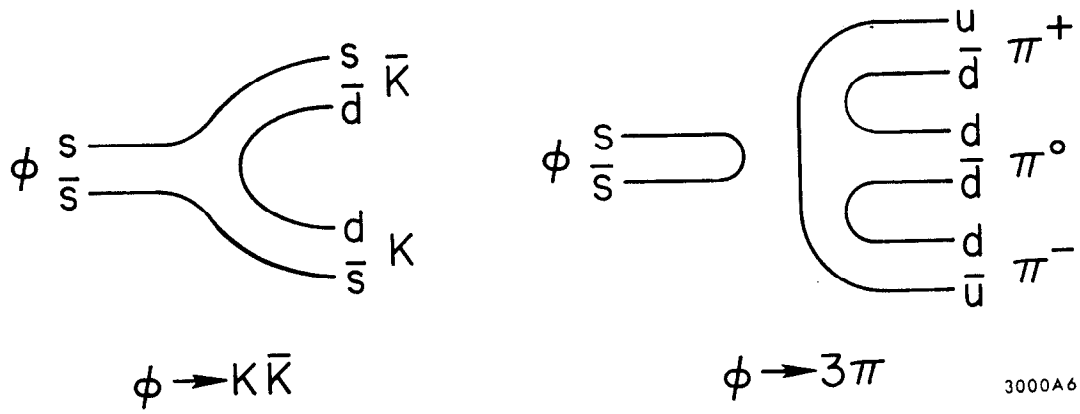

FIG. 3. Quark diagrams illustrating Zweig's rule in ϕ decays.

Table I lists the narrow s-channel resonances, their quark composition and their Q values, where, in this case, the Q value is the maximum kinetic energy released in the decay of the resonance to the lowest mass state which contains the constituent quarks of the resonance.

TABLE I. Quark content of vector mesons. Q value is the kinematic energy released in the decay to the lowest lying mesons containing the constituent quarks.

Meson	Quark content	Q value (MeV)
ρ	$\frac{1}{\sqrt{2}}(u\bar{u} - d\bar{d})$	491
ω	$\frac{1}{\sqrt{2}}(u\bar{u} + d\bar{d})$	369
ϕ	$s\bar{s}$	32
ψ	$c\bar{c}$	-635
ψ'	$c\bar{c}$	-46
$\psi''(4.03)$	$c\bar{c}$	300

The ϕ meson has a small Q value for decaying into two K mesons; nevertheless, this is its dominant decay mode. The suppression of the three pion mode was explained phenomenologically a decade ago by the Okubo-Zweig-Iizuka rule[28-30] (which we'll call the Zweig rule for short). The rule is illustrated in Fig. 3. Quark diagrams which are disconnected are suppressed relative to diagrams which are not. A disconnected diagram is one in which one or more particles can be isolated by drawing a line which does not cross any quark lines. The

Zweig rule will be a key concept in understanding much of the ψ spectroscopy. It will be covered in detail in Dave Jackson's lectures.[31]

When we come to the ψ we find a new phenomenon in nature -- a resonance with only Zweig suppressed decays. Nature has given us an even greater gift in the ψ' -- a radially excited state with only Zweig suppressed decays. If the ψ' had been 100 MeV/c^2 higher in mass, the rich spectroscopy of the χ states, the $C = +1$ intermediate states, would not have been experimentally accessible to us.

It is not until we get to the second radial excitations in the 4 GeV region that we find charmonium states whose decays are not Zweig suppressed, that is, states which can decay to charmed particles. The e^+e^- spectrum for this region is shown in Fig. 4.[26] This region is quite complicated and is not well understood. There are probably several resonances and many thresholds for charmed meson production conspiring to create the complex structure seen in Fig. 4. There appears to be an isolated resonance at 4414 MeV/c^2, shown in more detail in Fig. 5, but we do not yet understand very much about it.

II.B. Limits on other narrow states.

From the first four types of quarks we have learned that we can expect at least one narrow vector meson in the e^+e^- spectrum for each type of quark. The question then immediately arises: Are there more types of quarks in the energy range accessible to SPEAR?

Before we look at the data on limits on narrow states, we should ask what we would expect for a new quark. While there is no rigorous way to specify this, it is worth noting that there seems to be a regularity in the first four vector mesons.[32] The leptonic width of the

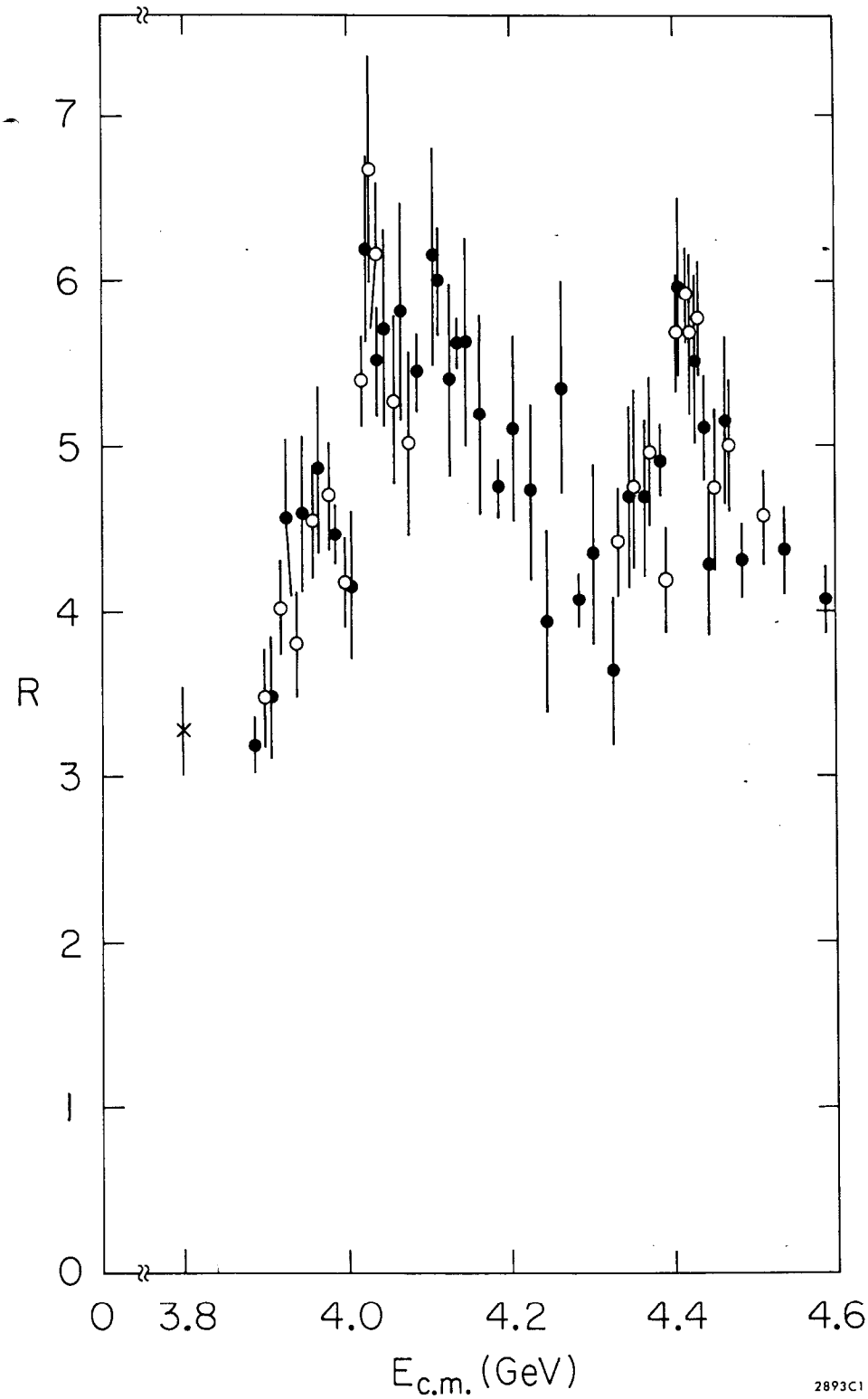

FIG. 4. R as a function of center-of-mass energy in the region 3.9 to 4.6 GeV. Open and closed circles represent data taken at different times.

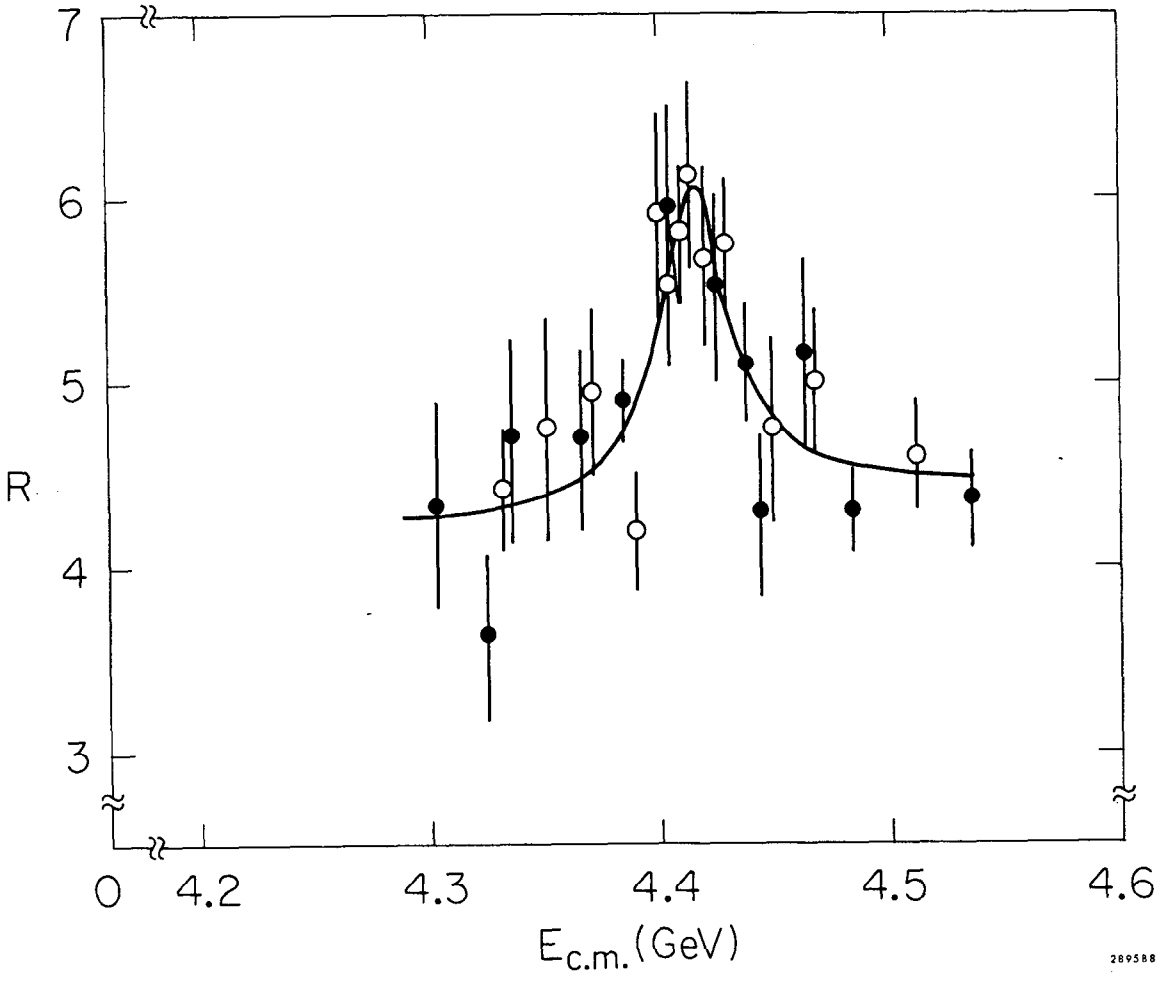

FIG. 5. R as a function of center-of-mass energy in the vicinity of the $\psi(4414)$. The curve is the fit to the $\psi(4414)$ line shape.

mesons divided by a unitary symmetry factor, which is equivalent to the square of the constituent charge, is almost constant:

$$\frac{\Gamma(\rho \to e^+e^-)}{1/2} \qquad \frac{\Gamma(\omega \to e^+e^-)}{1/18} \qquad \frac{\Gamma(\phi \to e^+e^-)}{1/9} \qquad \frac{\Gamma(\psi \to e^+e^-)}{4/9}$$

$$= 13.0 \pm 1.8 \ : \ 13.7 \pm 1.4 \ : \ 12.1 \pm 1.3 \ : \ 11.3 \pm 0.8 \quad (1)$$

This relationship holds to about 20% and so one might expect it to hold approximately for the next quark also. Thus we expect leptonic widths of 4.8 or 1.2 KeV depending on whether the quark charge is 2/3 or 1/3. The leptonic width is a convenient quantity to consider since, as we will derive in Sec. IV, it is proportional to the total integrated cross section for the production of the vector meson,

$$\Gamma_{ee} = \frac{m^2}{6\pi^2} \int \sigma_{tot} \, dE. \qquad (2)$$

The way one searches for narrow vector mesons is to increase the storage ring energy a few MeV at a time and measure the cross section at each energy. The first search of this type was rather crude -- a few hadronic events a point (Fig. 6).[33] However, it proved that the technique worked since the ψ' was discovered by it.[34] More recently, the region between 5.7 and 7.4 GeV was studied in much greater detail,[35] partially in response to reports of possible new resonances around 6 GeV found in hadronic interactions.[36,37] Part of these data are displayed in Fig. 7. The data for $6.4 < E_{cm} < 7.0$ were taken quite recently and have not been fully analyzed yet.

Limits on Γ_{ee} of possible narrow resonances are summarized in

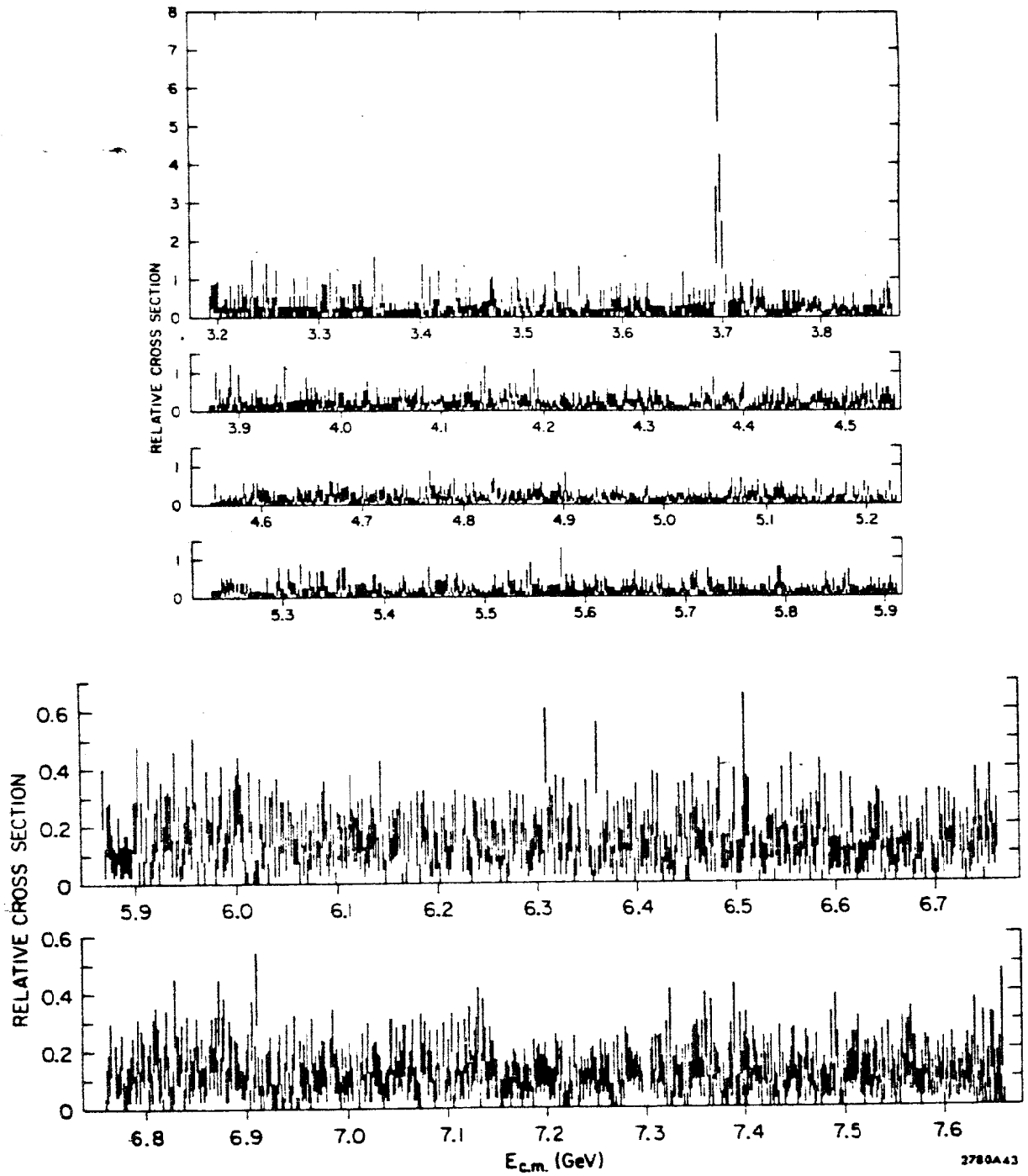

FIG. 6. Fine scan cross section (1 unit ≈ 100 nb) as a function of center-of-mass energy.

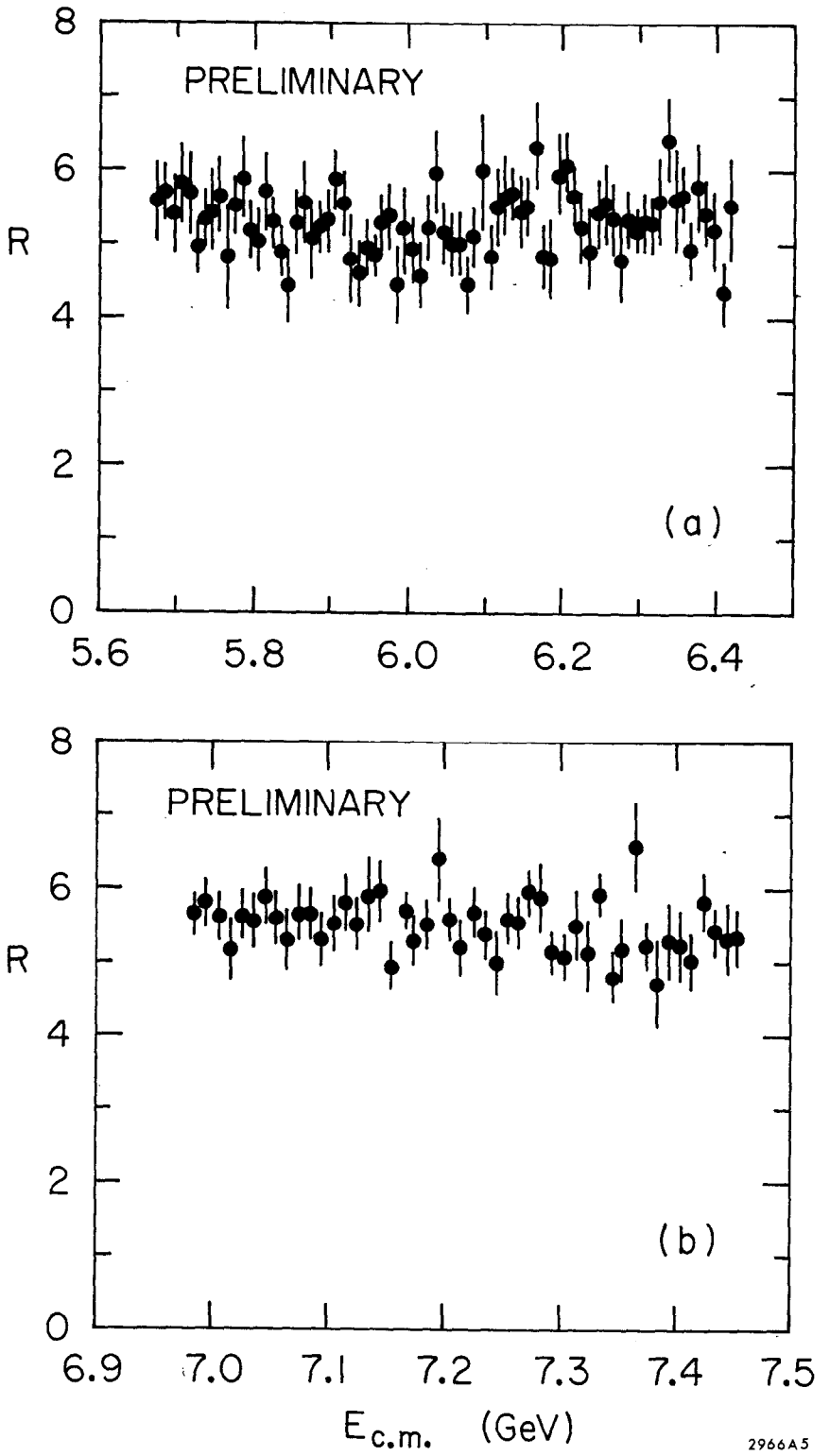

FIG. 7. Preliminary fine scan R as a function of center-of-mass energy plotted in 10 MeV bins.

Table II. From the considerations we just discussed, it is unlikely that a bound state of a charge 2/3 quark exists below 7.6 GeV. However, it is quite possible that a bound state of a charge 1/3 quark could exist in the mass range 4.9 to 5.7 GeV, and we just missed it in the coarse scan. We plan to study this region in detail in the coming year.

TABLE II. Limits on narrow resonances.

E_{cm}	Γ_{ee}(eV)(90% c.l.)
3.2 - 4.9	600 [a]
4.9 - 5.7	1100
5.7 - 6.4	150
6.4 - 7.0	∿100-200 [b]
7.0 - 7.4	70

a. The region between 3.2 and 4.5 GeV has been well studied, but not systematically.

b. Preliminary estimate based on on-line results.

II.C. The continuum

The total e^+e^- annihilation cross section in the continuum is one of the basic measurements of physics. In the parton picture, the ratio, R, of the total cross section to the μ pair production cross section measures the sum of charges squared of the fundamental fermions. (Conventionally the electron and muon are excluded from this sum since experimentally they are easy to separate out in the total cross section.)

Measurements of R from SPEAR are shown in Fig. 8.[27] As an ex-

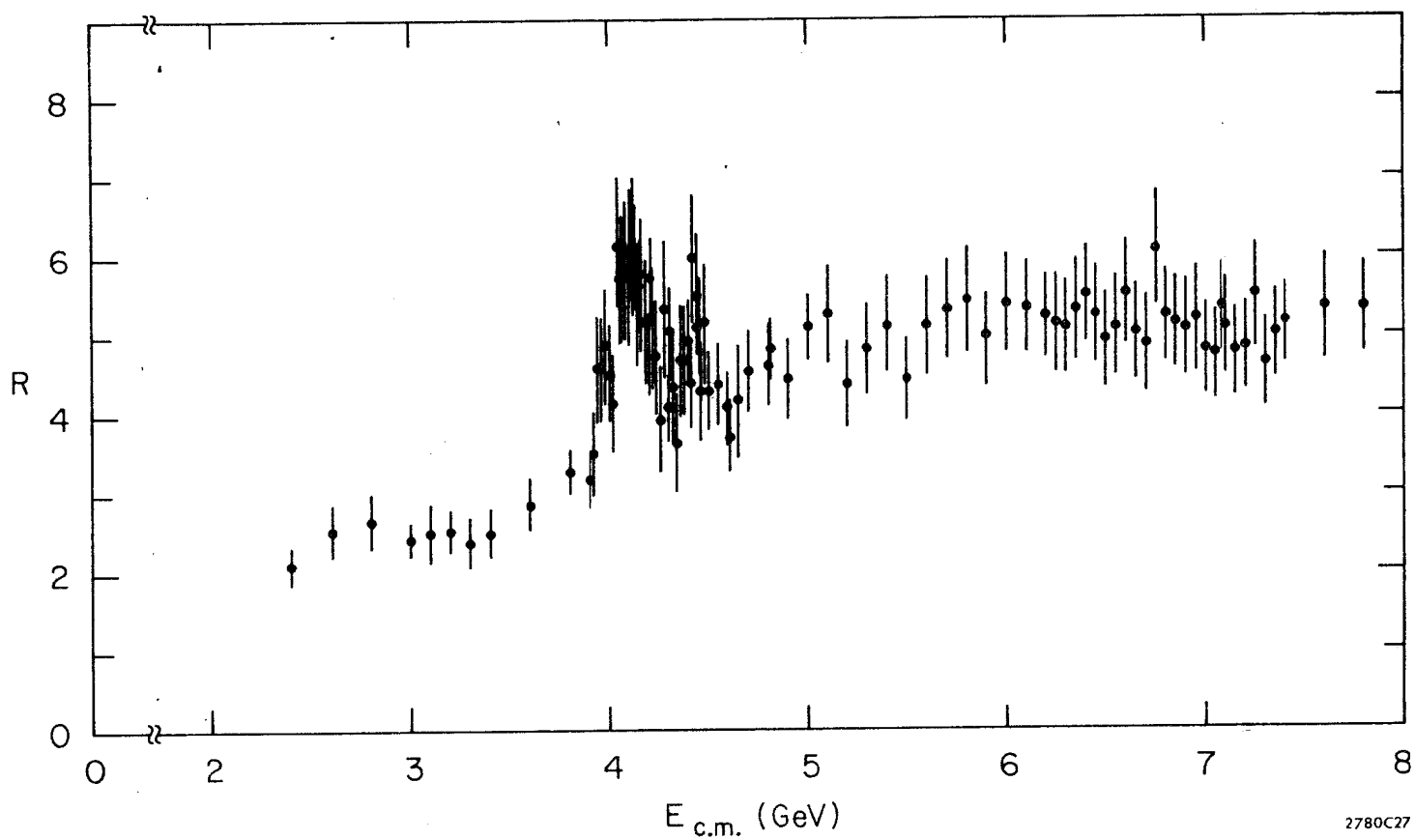

FIG. 8. SPEAR measurements of R as a function of center-of-mass energy.

ercise, let's take these results seriously and follow them to their logical conclusion. There are two plateaus in R, the region below 3.5 GeV and the region above 5 GeV. In these two regions we observe values of R about 2.5 and 5.2. But from the standard three-color quark model we expect values of 2 and 3 1/3. There are two sources of error. First, there is a 15% systematic uncertainty in the experiment, and second, the theory may have corrections at non-asymptotic energies.[38] We will assume, without any justification, that these errors are energy independent and use a combined experimental-theoretical fudge factor of 1.25 to make the lower plateau agree with experiment. Now we expect R to be 4.1 in the higher plateau from the quark model, leaving a difference of 1.1 units between the measurements and the fudged theory.

We need another fundamental fermion to resolve this discrepancy. A charge 1/3 quark will only contribute 1/3 to R, which is not enough. Therefore, we need either a charge 2/3 quark which will contribute 1 1/3 (1 2/3 after applying the fudge factor) or a new lepton which will contribute one unit.

The lepton is preferred for a number of reasons. First, if there is a new quark, t, then there should be a narrow $t\bar{t}$ bound state in the 4-5 GeV region with a leptonic width of 4 to 5 KeV, but limits presented in the previous section clearly exclude this. This difficulty, however, can be avoided if the $t\bar{t}$ state has some mixture of $c\bar{c}$ and is broad.

Second, in order to retain lepton-hadron symmetry, if we have any additional fermions, we need both leptons and quarks. In the two cases we have so far the lepton is lighter than the corresponding quarks.

Third, (and this is probably the only convincing reason), we have

direct experimental evidence for a new lepton. This will be the topic of the third lecture.

III. Detectors

Before we get down to the main business of these lectures, the properties of the ψ family, it is worthwhile spending a few minutes describing two general detectors which provide most of the data which we will discuss.

The SLAC-LBL magnetic detector[39,40] at SPEAR is a general purpose, large solid angle, charged particle detector. It is shown in a telescoped view in Fig. 9a and in more detail in a side view in Fig. 9b. The detector has a solenoidal coil which produces a magnetic field parallel to the incident beams. A set of cylindrical spark chambers measures trajectories of charged particles over about 70% of the full solid angle. Two cylindrical arrays of 48 trigger counters and 24 lead-scintillator sandwich shower counters detect charged particles and γ-rays over about 65% of the solid angle. The trigger for an event is two or more charged particles which each fire a trigger and shower counter. Separation of π's, K's, and p's is accomplished by time-of-flight measurements in the trigger counters. π-K separation is possible to momenta of about 700 MeV/c and K-p separation is possible to momenta of about 1 GeV/c. Electrons can be identified as particles which cause large pulse heights in the shower counters and muons can be identified as particles which penetrate the flux return and fire the muon spark chambers. Additional muon detection is provided by barite-loaded concrete absorbers above the main detector.

The DASP detector[41,42] at DORIS, shown in Fig. 10, is in several ways

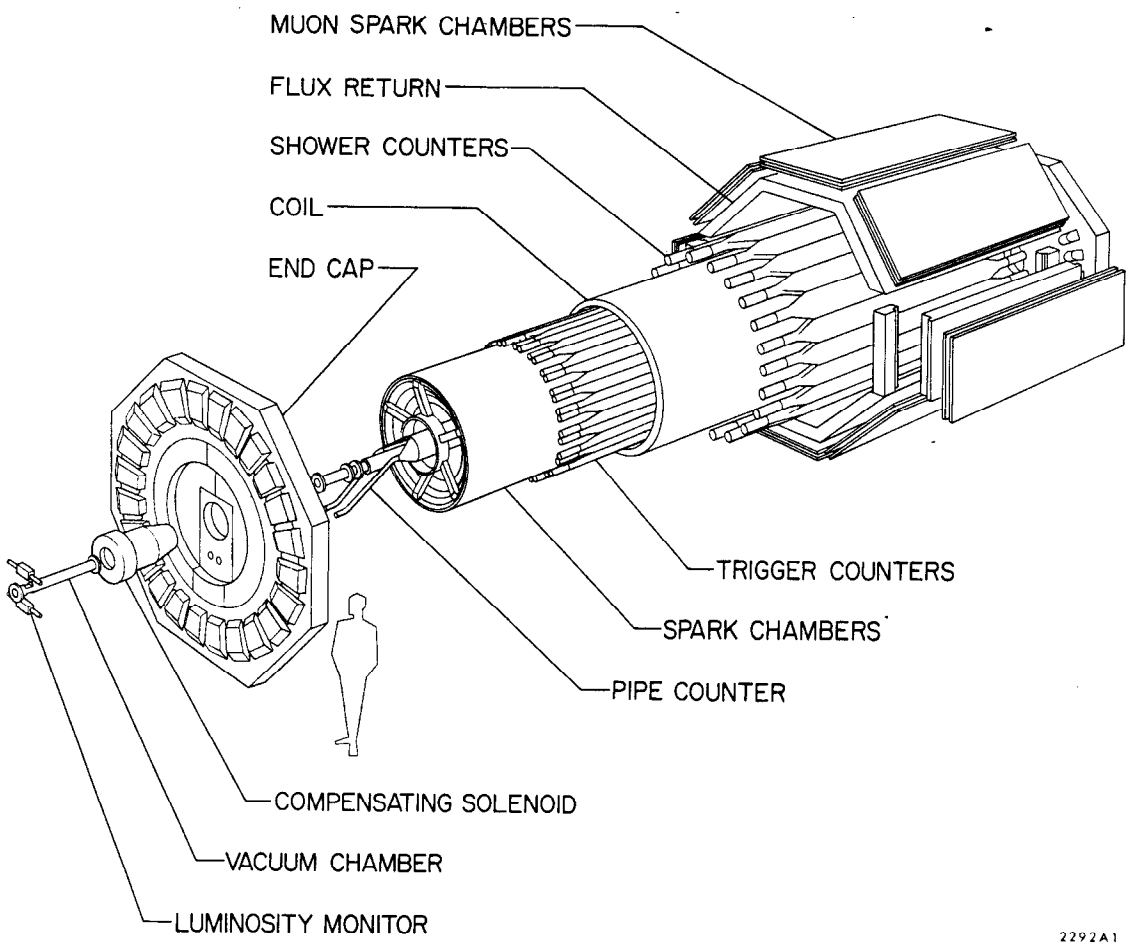

FIG. 9a. Telescoped view of the SLAC-LBL magnetic detector at SPEAR.

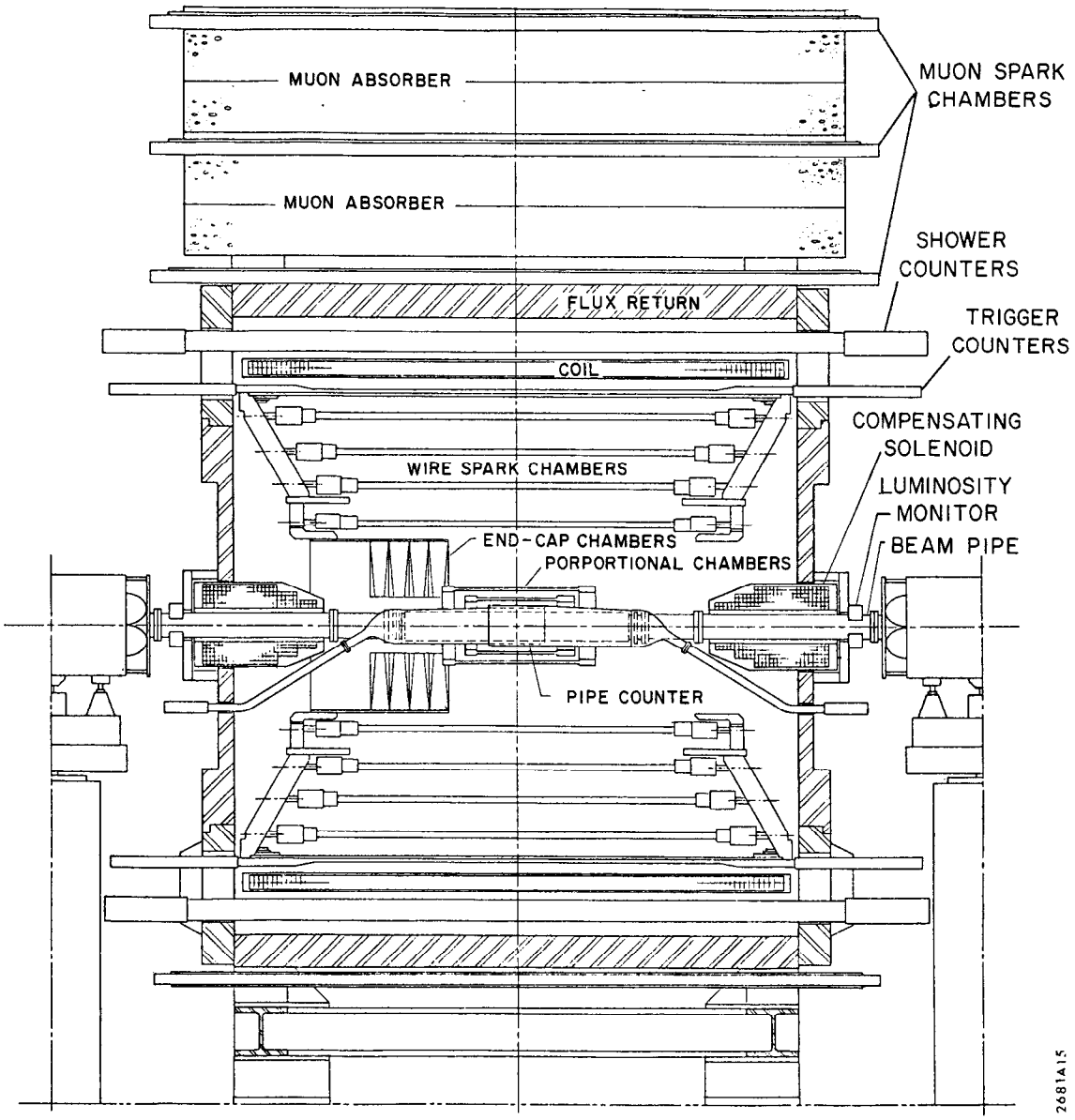

FIG. 9b. Side view cross section of the SLAC-LBL magnetic detector at SPEAR.

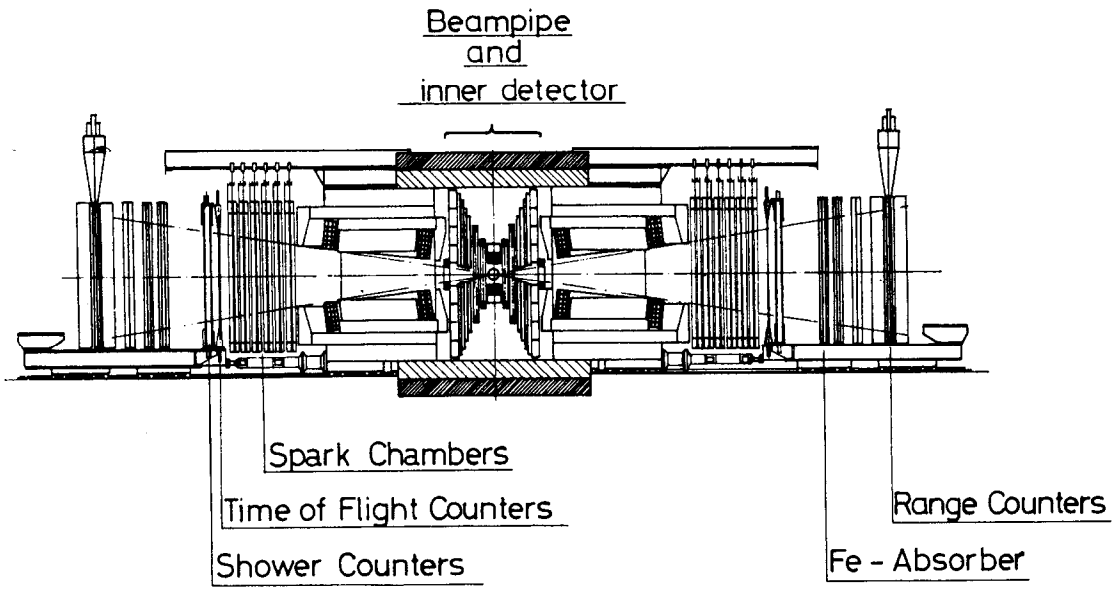

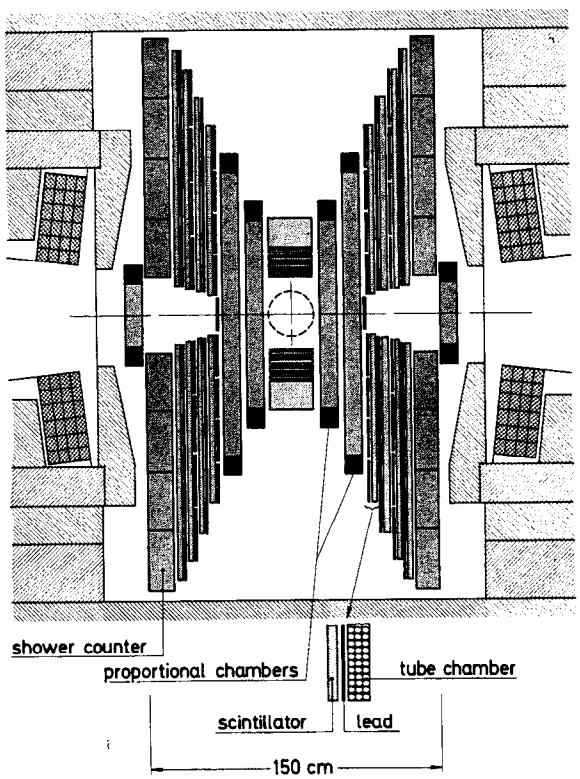

DASP — Inner Detector

3000A7

FIG. 10. DASP detector at DORIS.

complementary to the SLAC-LBL detector. It consists of two parts: two magnetic spectrometers on either side of the interaction region covering about 10% of the solid angle and a non-magnetic inner detector covering about 70% of the solid angle.

The magnetic spectrometers have better momentum resolution than the SLAC-LBL detector and much better time-of-flight resolution due to a 5 m flight path. Pions can be separated from kaons up to 1.5 GeV/c and kaons from protons up to 3 GeV/c.

The inner detector is well suited for photon direction and energy measurements. It is composed of an eight radiation length thick lead-scintillator shower counter preceded by four units, each of which contains a scintillation counter hodoscope, 5mm of lead, and two to three layers of proportional tubes. The direction of a shower is determined to about $\pm 2^{o}$. The efficiency of the detector is 50% for 50 MeV photons rising to about 90% for 100 MeV photons.

IV. Widths of the ψ and ψ'

Figures 11 and 12 show the measured cross sections for hadron production, μ pair production, and e pair production (or scattering) in the vicinity of the ψ and ψ'.[24,25] These are only apparent cross sections because in both cases the true widths of the resonances are considerably smaller than the experimental resolution.

In cases such as this the true widths must be determined by a "trick". Here the trick is that we measure ψe^+e^- coupling two different ways. As can be seen from Fig. 13, $e^+e^- \to \psi \to$ anything is proportional to this coupling, while $e^+e^- \to \psi \to e^+e^-$ is proportional to the square.

The formalism is fairly simple. For any state f, the resonant

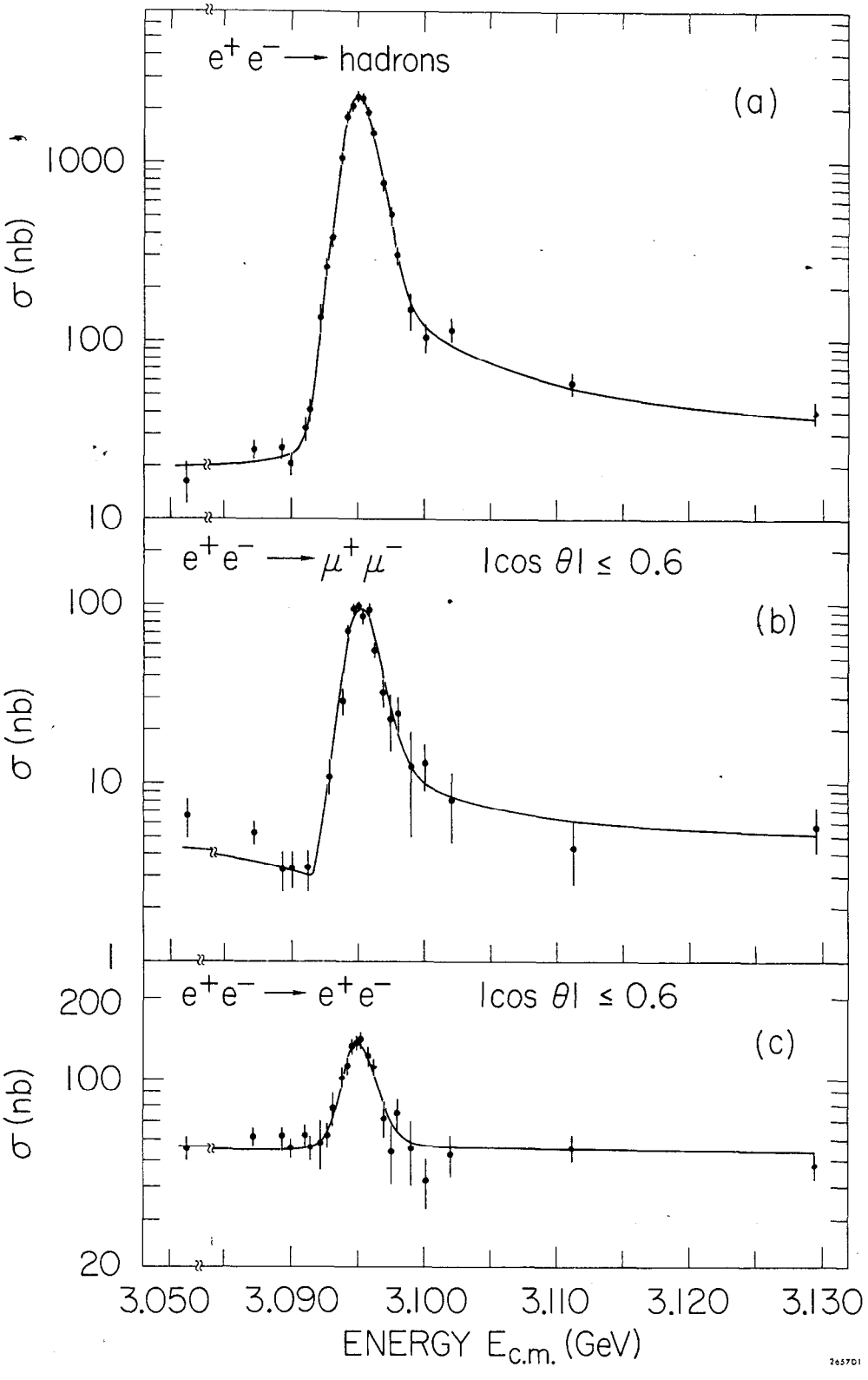

FIG. 11. Cross sections for a) hadron production, b) μ pair production, and c) e pair production and scattering in the vicinity of the ψ(3095).

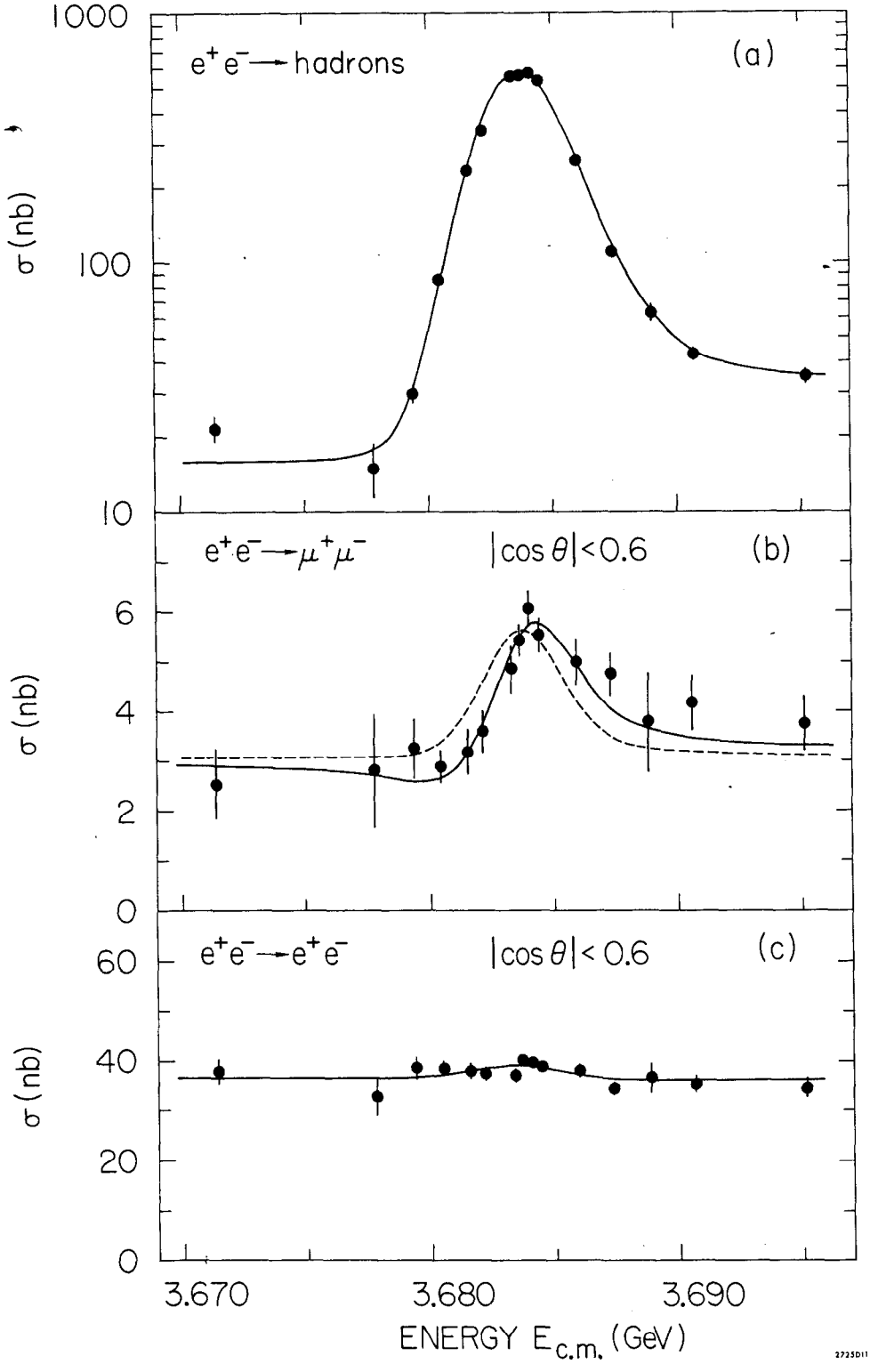

FIG. 12. Cross sections for a) hadron production, b) μ pair production, and c) e pair production and scattering in the vicinity of the ψ'(3684).

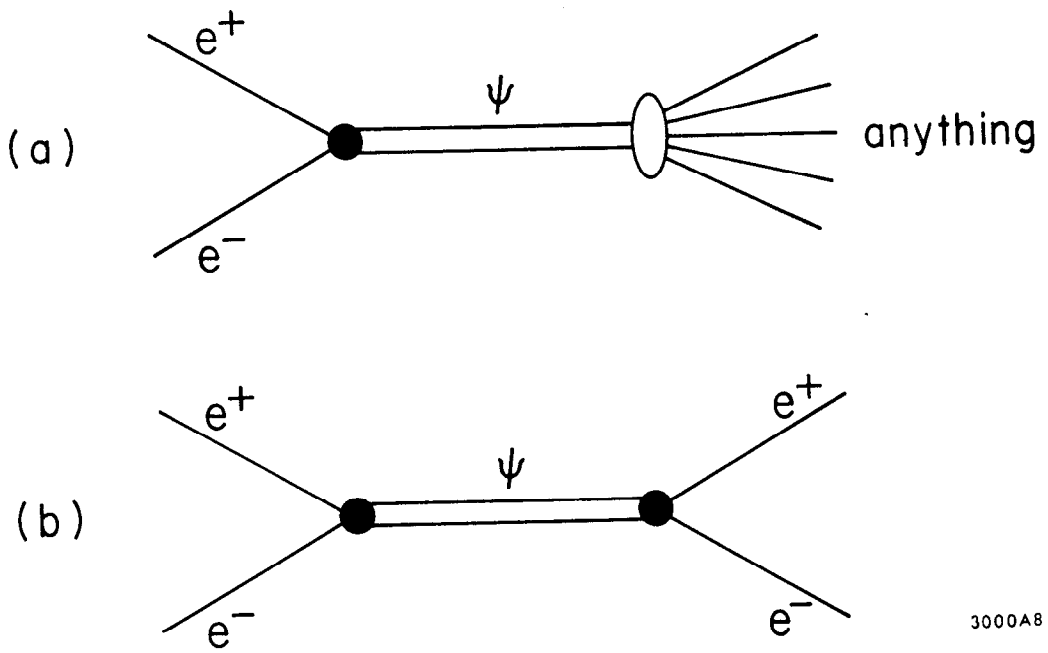

FIG. 13. Diagrams for a) $e^+e^- \to \psi \to$ anything and b) $e^+e^- \to \psi \to e^+e^-$.

cross section will be given by

$$\sigma_{\psi,f} = \frac{\pi(2J+1)}{m^2} \frac{\Gamma_{ee}\Gamma_f}{(E-m)^2 + \Gamma^2/4} , \tag{3}$$

where m is the mass of the ψ, J is its spin, Γ_f is the partial decay width to the state f, and Γ is the total decay width.

Integrating Eq. (3) and using J = 1 (which we will establish in a few minutes), we obtain

$$\Sigma_{\psi,f} \equiv \int \sigma_{\psi,f}\, dE = \frac{6\pi^2}{m^2} \frac{\Gamma_{ee}\Gamma_f}{\Gamma} . \tag{4}$$

We can now use Eq. (4) to obtain all the widths. In particular,

$$\Gamma_{ee} = \frac{m^2}{6\pi^2} \Sigma_{\psi,all} \tag{5}$$

and

$$\Gamma = \frac{\Sigma_{\psi,all}}{\Sigma_{\psi,ee}} \Gamma_{ee} . \tag{6}$$

For simplicity we have ignored radiative effects and interference between ψ decays and the direct channel $e^+e^- \to f$. These effects can be included in a straightforward way.

The widths determined by the SLAC-LBL collaboration for the ψ,ψ', and higher resonances are given in Table III.[24-26] (The world averages for the ψ and ψ', which are only slightly different, will be given later in a complete list of decay modes.) Note that although we don't know how many resonances are in the 4.1 GeV region or their locations and widths, we can still determine that the branching fractions to electron pairs are of order 10^{-5} since they are only proportional to the peak cross sections.

TABLE III. Widths of the ψ particles. SLAC-LBL values.[24-26]

	$\psi(3095)$	$\psi'(3684)$	"4.1 region"	$\psi'''(4414)$
Γ(MeV)	0.069 ± 0.015	0.228 ± 0.056	~ 200	33 ± 10
Γ_{ee}(KeV)	4.8 ± 0.6	2.1 ± 0.3	~ 2	0.44 ± 0.14
$B_{ee} = \frac{\Gamma_{ee}}{\Gamma}$	0.069 ± 0.009	0.0093 ± 0.0016	$\sim 10^{-5}$	$(1.3 \pm 0.3) \times 10^{-5}$

V. Spin, parity, and charge conjugation of the ψ and ψ'

If the ψ particles are states of charmonium, they should be produced in e^+e^- annihilations by coupling to the photon, in which case they would have the same quantum numbers, $J^{PC} = 1^{--}$. This would not have to be the case, however, if they coupled directly to leptons, so an experimental check is clearly important.

We can determine the quantum numbers directly by observing the interference between the leptonic decays of the ψ particles,

$$e^+e^- \to \psi \to e^+e^- \tag{7}$$

and

$$e^+e^- \to \psi \to \mu^+\mu^- \tag{8}$$

and the direct production of lepton pairs,

$$e^+e^- \to e^+e^- \tag{9}$$

and

$$e^+e^- \to \mu^+\mu^- \quad . \tag{10}$$

The amplitude for reaction (10) is

$$A(e^+e^- \to \mu^+\mu^-) = \left(\frac{3\pi}{E^2}\right)^{\frac{1}{2}} \left(-\frac{2\alpha}{3}\right) \quad , \tag{11}$$

and the amplitude for reaction (8) is

$$A(e^+e^- \to \psi \to \mu^+\mu^-) = \left(\frac{(2J+1)\pi}{E^2}\right)^{\frac{1}{2}} \frac{\Gamma_{ee}}{m - E - i\Gamma/2} \quad . \tag{12}$$

If the ψ particles have the quantum numbers of the photon, the cross section will have the form

$$\frac{d\sigma}{d\theta} = \frac{9\pi}{8E^2}(1 + \cos^2\theta) \left| -\frac{2\alpha}{3} + \frac{\Gamma_{ee}}{m - E - i\Gamma/2} \right|^2 \quad . \tag{13}$$

The sum of the amplitudes which go into Eq. (13) is shown graphically in Fig. 14. As the resonance proceeds around the diagram, it is clear that there will be destructive interference below the resonant energy.

The ratio of muon pairs to electron pairs as a function of energy is shown for the ψ and the ψ' in Fig. 15. This ratio is used because it is least sensitive to normalization effects and because the electron pairs are expected to have a small constructive interference below the resonance (due to interference with the spacelike diagram). The data are inconsistent with no interference by 2.7 standard deviations in the ψ region and by 4.9 standard deviations in the ψ' region. This is sufficient to confirm that the quantum numbers of both the ψ and ψ' are those of the photon, $J^{PC} = 1^{--}$.

VI. Hadronic decays of the ψ

VI.A. Table of results

Table IV contains a compendium of the world measurements of ψ decays. The cutoff date for inclusion of data in this table (and other tables in these lectures) was July 26, 1976, although in a few important cases, new data presented during the topical conference have been included.

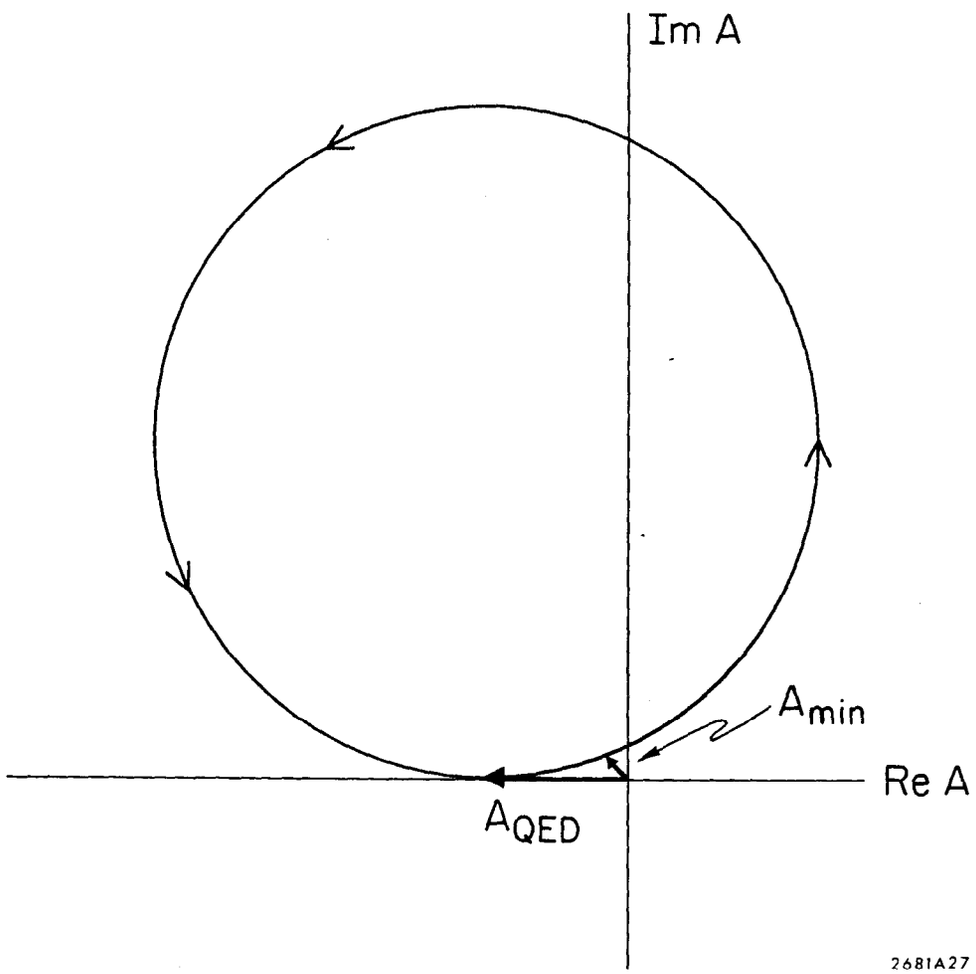

FIG. 14. Amplitude for μ pair production in the vicinity of a vector meson. A_{QED} is the amplitude for μ pair production far below and far above the resonant energy.

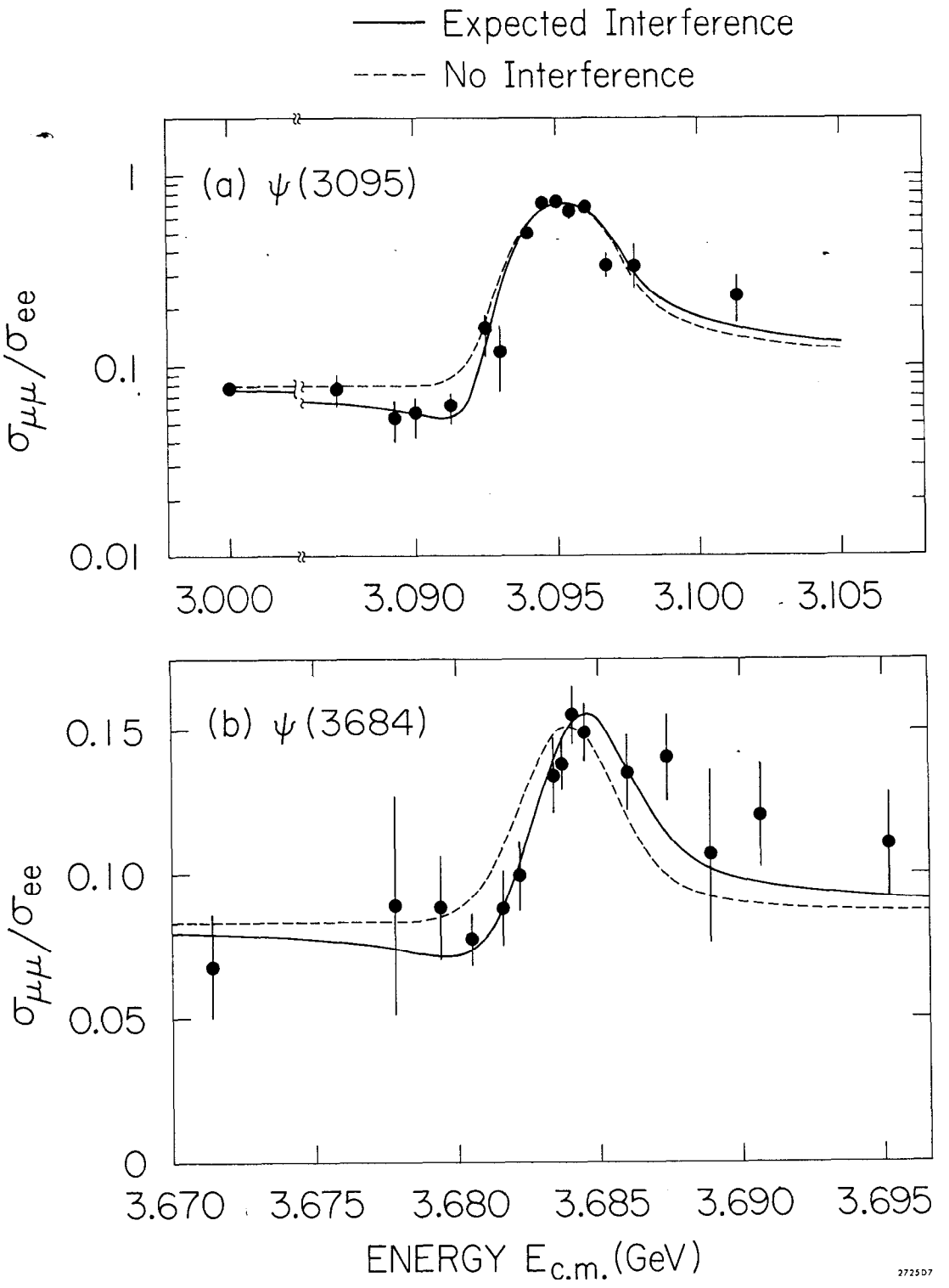

FIG. 15. The ratio of μ pair yield to e pair yield in the vicinity of a) the ψ(3095) and b) the ψ(3684) for $|\cos\theta| \lesssim 0.6$.

TABLE IV. Decay modes of ψ (3095)

General modes include resonant contributions, e.g. $K^+K^-\pi^+\pi^-$ includes a contribution from $\phi\pi^+\pi^-$. The branching fraction always refers to the mode plus its charge conjugate state and unless qualified to the sum of all possible charge states, e.g. $\rho\pi = \Sigma(\rho^+\pi^- + \rho^o\pi^o + \rho^-\pi^+)$. Upper limits are at the 90% confidence level. References not used in determining a branching fraction are listed in parentheses.

Mode	Fraction (%)	Ref.	Footnotes
e^+e^-	7.3 ± 0.5	24,42-48	a
$\mu^+\mu^-$	7.4 ± 0.5		
$\pi^+\pi^-$	0.01 ± 0.007	49,(50,51)	b
$\pi^+\pi^-\pi^o$	1.6 ± 0.6	52	c
$2\pi^+ 2\pi^-$	0.4 ± 0.1	52	d
$2\pi^+ 2\pi^- \pi^o$	4.0 ± 1.0	52	
$3\pi^+ 3\pi^-$	0.4 ± 0.2	52	d
$3\pi^+ 3\pi^- \pi^o$	2.9 ± 0.7	52	
$4\pi^+ 4\pi^- \pi^o$	0.9 ± 0.3	52	
$\rho\pi$	1.25 ± 0.2	49,52	e
$A_2^+ \pi^-$	<0.43	49	f
$\omega \pi \pi$	1.0 ± 0.3	53,(52)	g
$\rho \pi \pi \pi$	1.8 ± 0.45	52	g
ρA_2	0.9 ± 0.6	53	g
$\omega 2\pi^+ 2\pi^-$	0.85 ± 0.34	53	
$K^+ K^-$	<0.015	49,51	h,i
$K_S K_L$	<0.008	54	h,j
$K^+ K^- \pi^+ \pi^-$	0.72 ± 0.23	53,(55)	
$2K^+ 2K^-$	0.07 ± 0.03	53	
$K^+ K^- 2\pi^+ 2\pi^-$	0.3 ± 0.1	55	

TABLE IV continued

Mode	Fraction (%)	Ref.	Footnotes
K^+K^{-*}	0.34 ± 0.06	49,53,(54)	k
$K^o\ \bar{K}^{o*}$	0.27 ± 0.06	53,(54)	k
$K^+\ K^{-**}$	<0.15	53,(49,54)	h,k
$K^o\ \bar{K}^{o**}$	<0.20	53,(54)	h,k
$K^{o*}\ \bar{K}^{o*}$	<0.5	53,(54)	h,k
$K^{o*}\ \bar{K}^{o**}$	0.67 ± 0.26	53,(54)	k
$K^{o**}\ \bar{K}^{o**}$	<0.29	53,(55)	h,k
$\phi\ \pi\ \pi$	0.21 ± 0.09	53,(55)	g
$\omega\ K^+\ K^-$	0.03 ± 0.02	53	
$\phi\ K^+\ K^-$	0.09 ± 0.04	53	
$\phi\ \eta$	0.07 ± 0.04	53	
$\phi\ \eta'$	0.05 ± 0.04	53	l
$\phi\ f'$	0.08 ± 0.05	53	
$p\ \bar{p}$	0.22 ± 0.02	47,49,56	m
$p\ \bar{n}\ \pi^-$	0.38 ± 0.08	57,(55)	
$p\ \bar{p}\ \pi^o$	0.10 ± 0.02	57,(55)	
$p\ \bar{p}\ \eta$	0.19 ± 0.04	56	
$p\ \bar{p}\ \pi^+\ \pi^-$	0.41 ± 0.08	57	
$p\ \bar{p}\ \pi^+\ \pi^-\ \pi^o$	0.11 ± 0.04	57	
$p\ \bar{p}\ \omega$	0.05 ± 0.01	57	
$\Lambda\ \bar{\Lambda}$	0.16 ± 0.08	55	m
$\Lambda\ \bar{\Sigma}$	<0.04	58	f
$\Xi^-\ \bar{\Xi}^-$	∿0.04	59	n
$\gamma\ \gamma$	<0.03	50,(41,46)	o
$\gamma\ \pi^o$	<0.016	65,(41,60)	
$\gamma\ \eta$	0.10 ± 0.02	65,(61)	
$\gamma\ \eta'$	0.24 ± 0.06	65,66,(50,61-63)	

Mode	Fraction	Ref.	Footnotes
γ X(2800)	<3.0	67	
γ X(2800)$\rightarrow 3\gamma$	$\sim$0.015	50,62,(61)	p
γ X(2800)$\rightarrow \gamma p\bar{p}$	<0.004	56	

a. From a simultaneous fit to measurements on leptonic and total widths. The fit value for the total width is 69 ± 7 KeV.

b. Based on 2 observed events with a calculated background of 0.24 events. This decay is isospin violating and thus presumably proceeds via a second-order electromagnetic interaction. With this assumption, $|F_\pi(q^2 = m_\psi^2)|^2 = (5.6 \pm 4.0) \times 10^{-3}$.

c. Mainly $\pi\rho$.

d. Proceeds via a second-order electromagnetic interaction. The total hadronic decay fraction via this type of interaction is (17 ± 3)%. (Ref. 24).

e. $\Gamma(\rho^o\pi^o)/\ (\rho^+\pi^-) + \Gamma(\rho^+\pi^-) = 0.59 \pm 0.17$. (Ref. 52).

f. Forbidden by isospin.

g. Isospin invariance used to calculate modes with more than one neutral.

h. Forbidden by SU(3).

i. Implies $|F_{K^\pm}(q^2 = m_\psi^2)|^2 < 8.6 \times 10^{-3}$

j. Implies $|F_{K^o}(q^2 = m_\psi^2)|^2 < 4.3 \times 10^{-3}$.

k. $K^* \equiv K^*(892)$ and $K^{**} \equiv K^*(1420)$.

l. Based on 2 events observed in $K^+K^-\pi^+\pi^-$ + (η missing).

m. Angular distribution of $1 + \cos^2\theta$ assumed. This is in agreement with measurements of the $\psi \rightarrow p\bar{p}$ mode.

n. Four events observed.

o. Forbidden for a spin 1 particle.

p. The existence of this state needs confirmation.

VI.B. Techniques

We will not have time to discuss all of the results presented in Table IV, much less discuss the data on which they are based. However, it is worthwhile to spend a few minutes examining some examples, so that one obtains a feeling for the quality and limitations of the data.

With a few important exceptions, the shower counters in the SPEAR magnetic detector do not have sufficient position or energy resolution to be useful for photon measurements. Thus, most of the hadronic final state analysis from this device uses techniques familiar in bubble chamber physics. If there are no neutral particles in the event and all the charged particles are detected, the event is over constrained and a four-constraint (4-C) fit is possible. If there is only one neutral particle, a 1-C fit is possible. An example of the latter is shown in Fig. 16, $\psi \to \pi^+\pi^-\pi^+\pi^-\pi^o$, the largest of the ψ hadronic decay modes. The missing mass squared of the missing neutral is plotted and a prominent peak is seen at the π^o mass squared. This decay can then be isolated with about 20% background. After isolating this decay, we can investigate it further by plotting the invariant mass of each $\pi^+\pi^-\pi^o$ combination (Fig. 17). A strong peak appears at the ω mass and we can isolate $\psi \to \omega\pi^+\pi^-$ also with about 20% background. In Sec. VI.E., we will go one step further and examine the $\pi^+\pi^-$ mass spectrum in the $\omega\pi^+\pi^-$ final state as part of our study of Zweig's rule.

The decay $\psi \to K\bar{K}^*$ offers a good example of different techniques studying the same reaction. In the SPEAR magnetic detector one of the ways this decay has been studied is to search for final states containing $K_S^o K^+\pi^-\pi^+$, where the K_S^o decays to $\pi^+\pi^-$. This is a 4-C situation and kine-

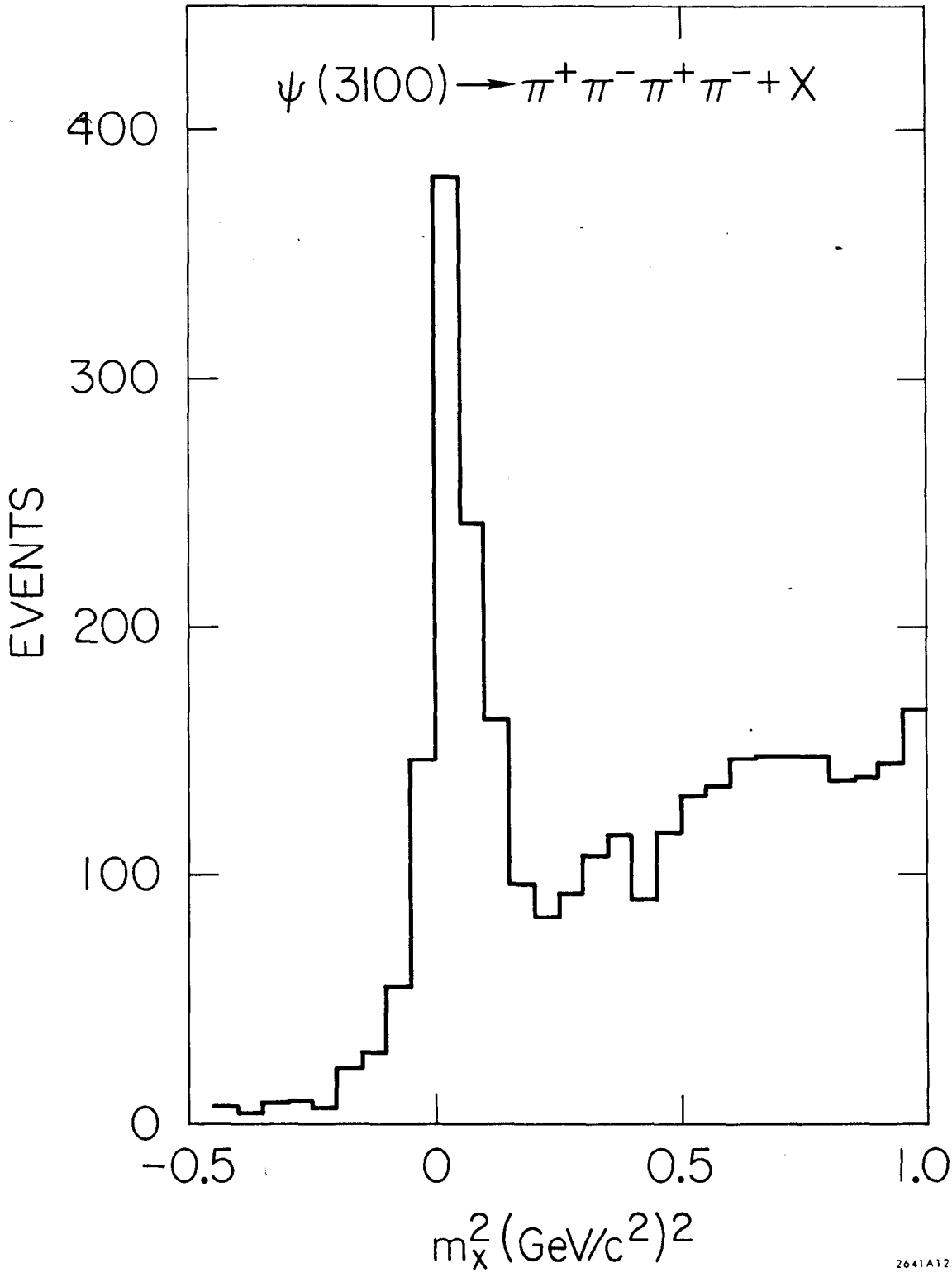

FIG. 16. The invariant mass squared recoiling against four charged pions in ψ decays.

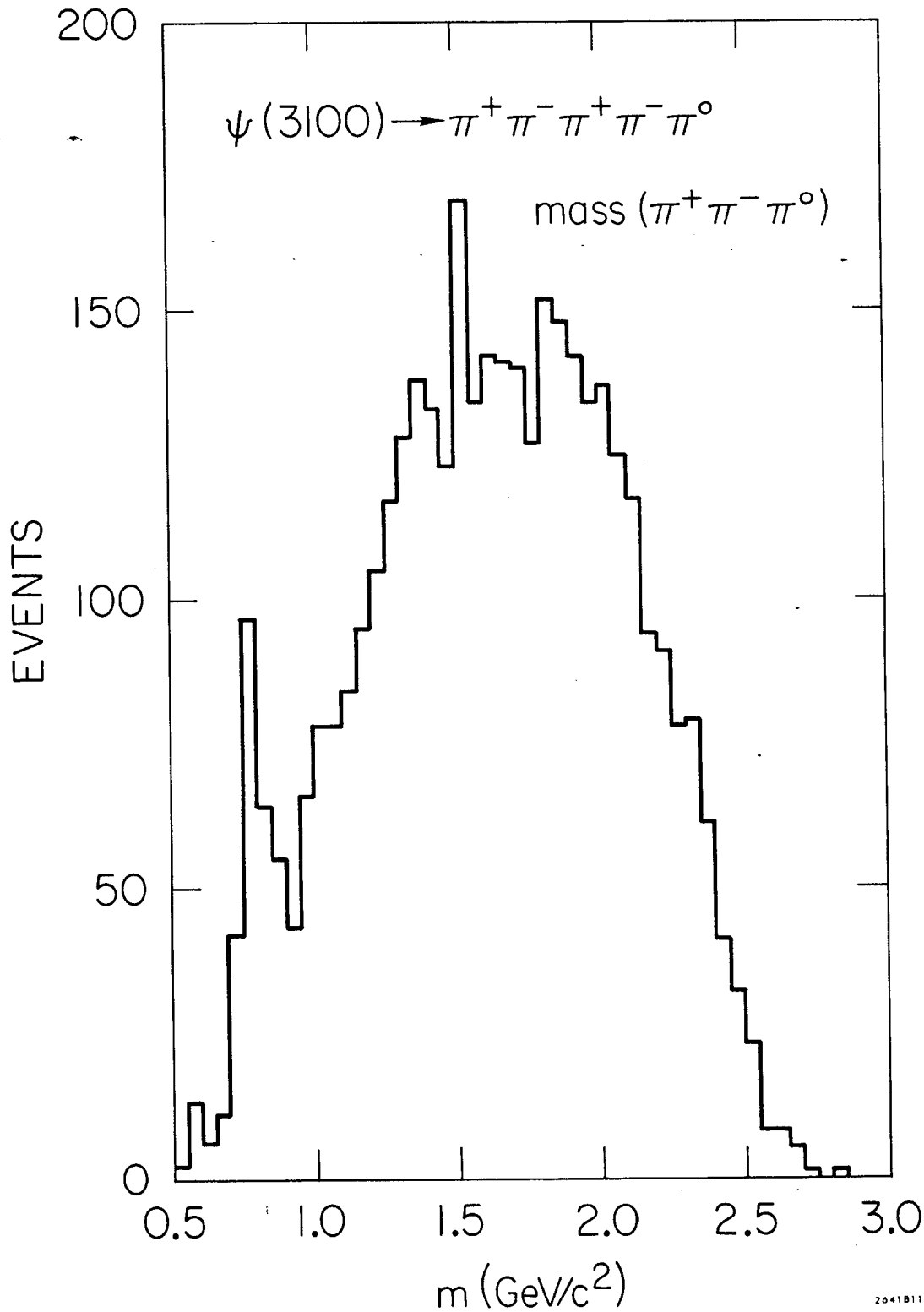

FIG. 17. The invariant mass of $\pi^+\pi^-\pi^o$ combinations from the decay $\psi \rightarrow 2\pi^+2\pi^-\pi^o$.

matics alone is sufficient to identify the final state. The Dalitz plot shown in Fig. 18 clearly displays both the charged and neutral $K\bar{K}^*$ modes.[53]

In the DASP spectrometer at DORIS, the charged mode of this decay was measured by detecting the charged K with good momentum and time-of-flight resolution and observing the K^* in the recoil mass spectrum (Fig. 19).[49] The two experiments obtained consistent results. This decay will be important in Sec. VI.D, where we study the SU(3) properties of the ψ.

VI.C. Isospin and G parity

We can determine the G parity of the ψ by observing whether it decays into even or odd numbers of pions. It turns out that the ψ decays into both even and odd numbers of pions -- a violation of I spin. However, this violation occurs in precisely the way we expect it to occur, and in the way it is required to occur, if the ψ couples to a photon.

Consider the three diagrams in Fig. 20. Figure 20(a) shows the direct decay of the ψ into hadrons, (b) shows the decay of the ψ into hadrons via an intermediate photon, and (c) shows the decay into μ pairs. In (b), the nature of the final state, except for a phase factor, must be the same as the non-resonant final state produced in e^+e^- annihilation at the same energy. This state need not conserve isospin and may be quite different from the state produced by (a). Furthermore, we know what contribution (b) must make because the ratio between (b) and (c) must be the same as it would be if the ψ were not in the diagram, about 2.5. Thus, from the data in Table IV, we deduce that if the ψ couples to a photon (a) contributes 68% to the width of the ψ, (b) contributes 18%, and the leptonic modes contribute 14%.

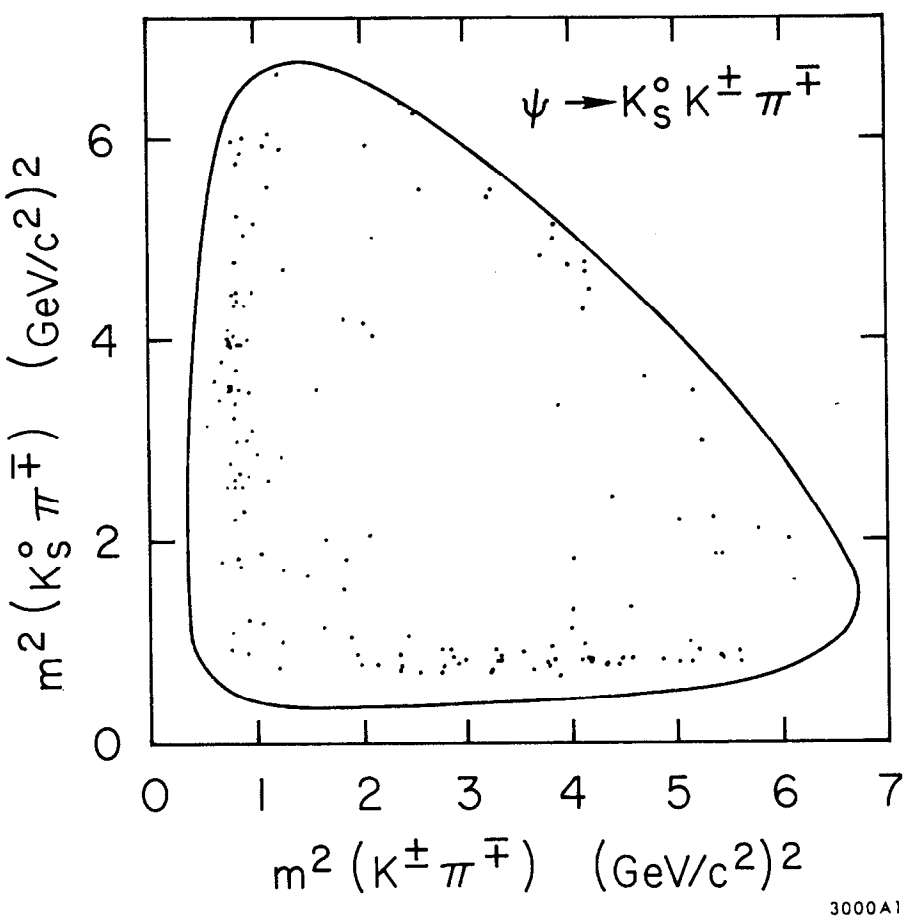

FIG. 18. Dalitz plot for $\psi \to K_S^o K^\pm \pi^\mp$.

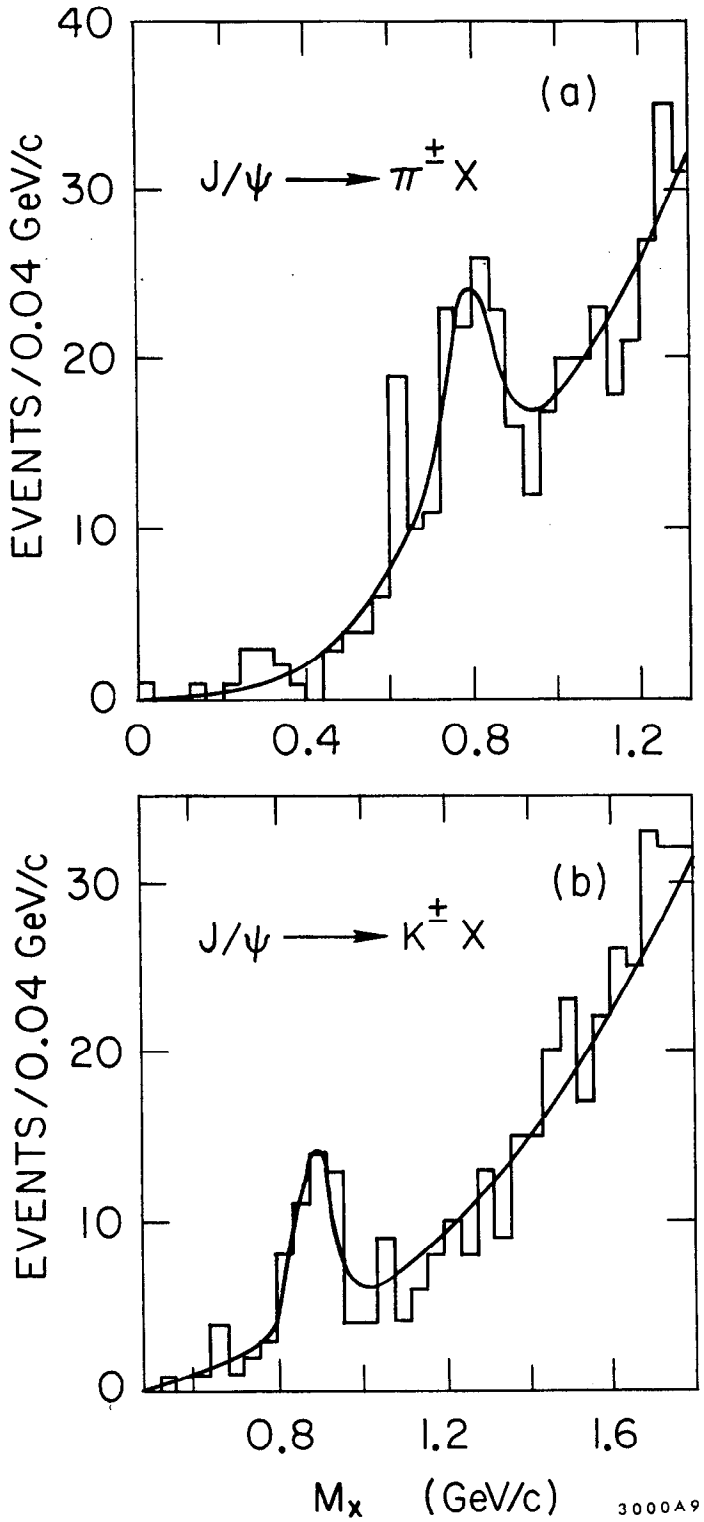

FIG. 19. Missing mass spectrum recoiling against single a) pions and b) kaons in ψ decays as measured by DASP.

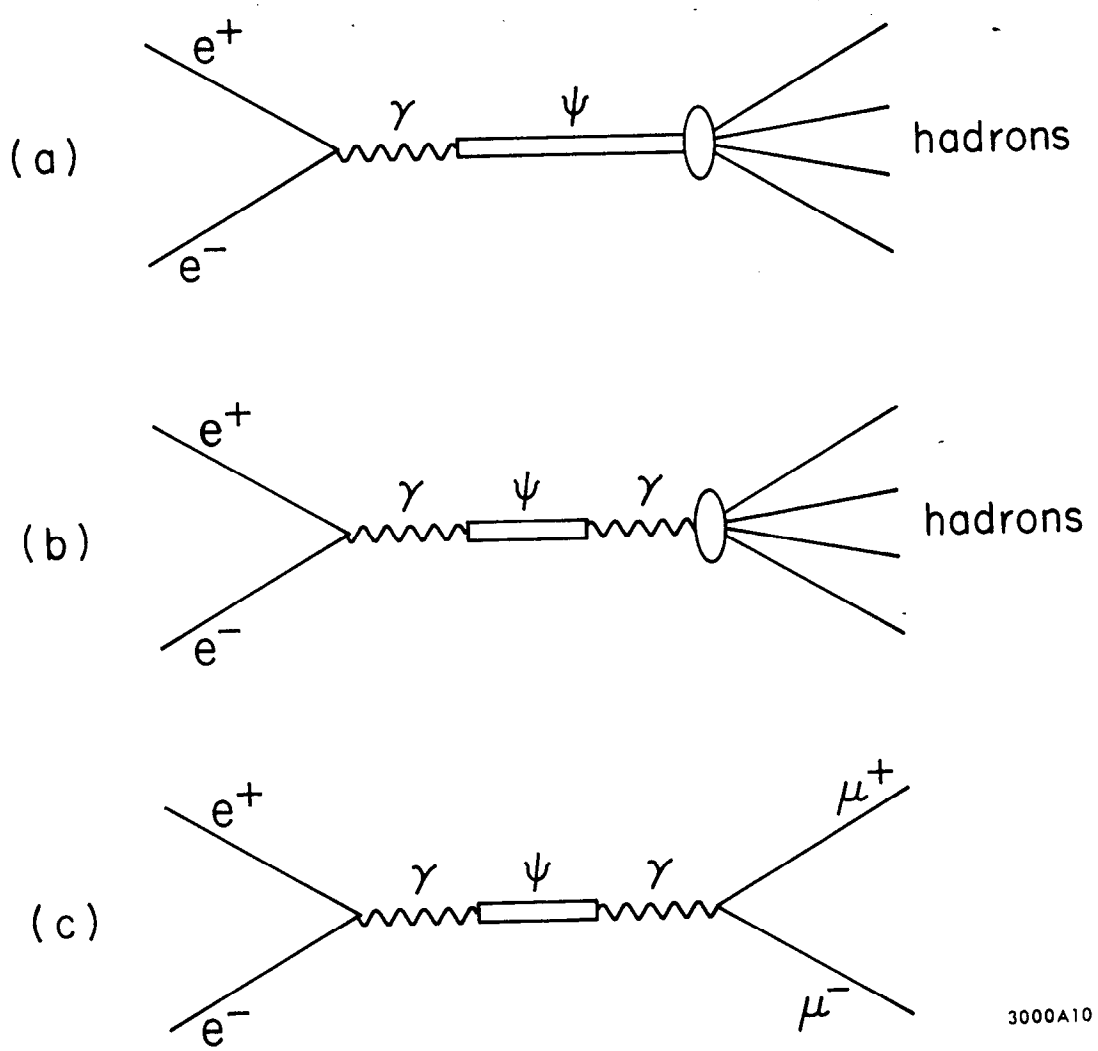

FIG. 20. Diagrams for a) direct ψ decays to hadrons, b) ψ decays to hadrons via an intermediate photon, and c) ψ decay to μ pairs.

To test this hypothesis we want to compare the ratio of all pion final state cross sections to μ pair cross sections on-and off-resonance. we compute the ratio α, defined

$$\alpha = \frac{\sigma^{\psi}_{n\pi}}{\sigma^{\psi}_{\mu\mu}} \Bigg/ \frac{\sigma^{3.0}_{n}}{\sigma^{3.0}_{\mu\mu}} , \qquad (14)$$

where data at 3.0 GeV are used as the off-resonance sample. Values of α for three to seven pion production are shown in Fig. 21.[52] The results are consistent with all of the even number of pion production (G even, I odd) coming from the intermediate photon decay, Fig. 20b. Most of the odd pion production comes from the direct ψ decay, Fig. 20a, and the ψ appears to decay directly into a pure $I^G = (\text{even})^-$ state.

It is relatively easy to show that I = 0. We will give just one argument here. Figure 22 shows the Dalitz plot for $\psi \to 3\pi$. This channel is clearly dominated by $\psi \to \rho\pi$, which implies that either I = 0 or I = 2. If I = 0, then $\Gamma_{\rho^o\pi^o} = \Gamma_{\rho^o\pi^o}$, whereas for I = 2, $\Gamma_{\rho^o\pi^o} = 4\Gamma_{\rho^+\pi^-}$. The data indicate that $\Gamma_{\rho^o\pi^o} = (1.18 \pm 0.34)\Gamma_{\rho^+\pi^-}$, strongly favoring I = 0. These properties, the coupling to photon pairs via a photon, the conservation of isospin in direct decays, and I = 0, are just the properties we expect of a state of charmonium.

VI.D. SU(3)

If the ψ is a state of charmonium, then we expect it to behave as a singlet with respect to the approximate SU(3) symmetry of the three lighter quarks. For each SU(3) multiplet there is a generalized charge conjugation, $\mathscr{C}$, which is equal to C of the I = 0 part of the multiplet. If the ψ is an SU(3) singlet, then it cannot decay into two mesons with the same $\mathscr{C}$.[68]

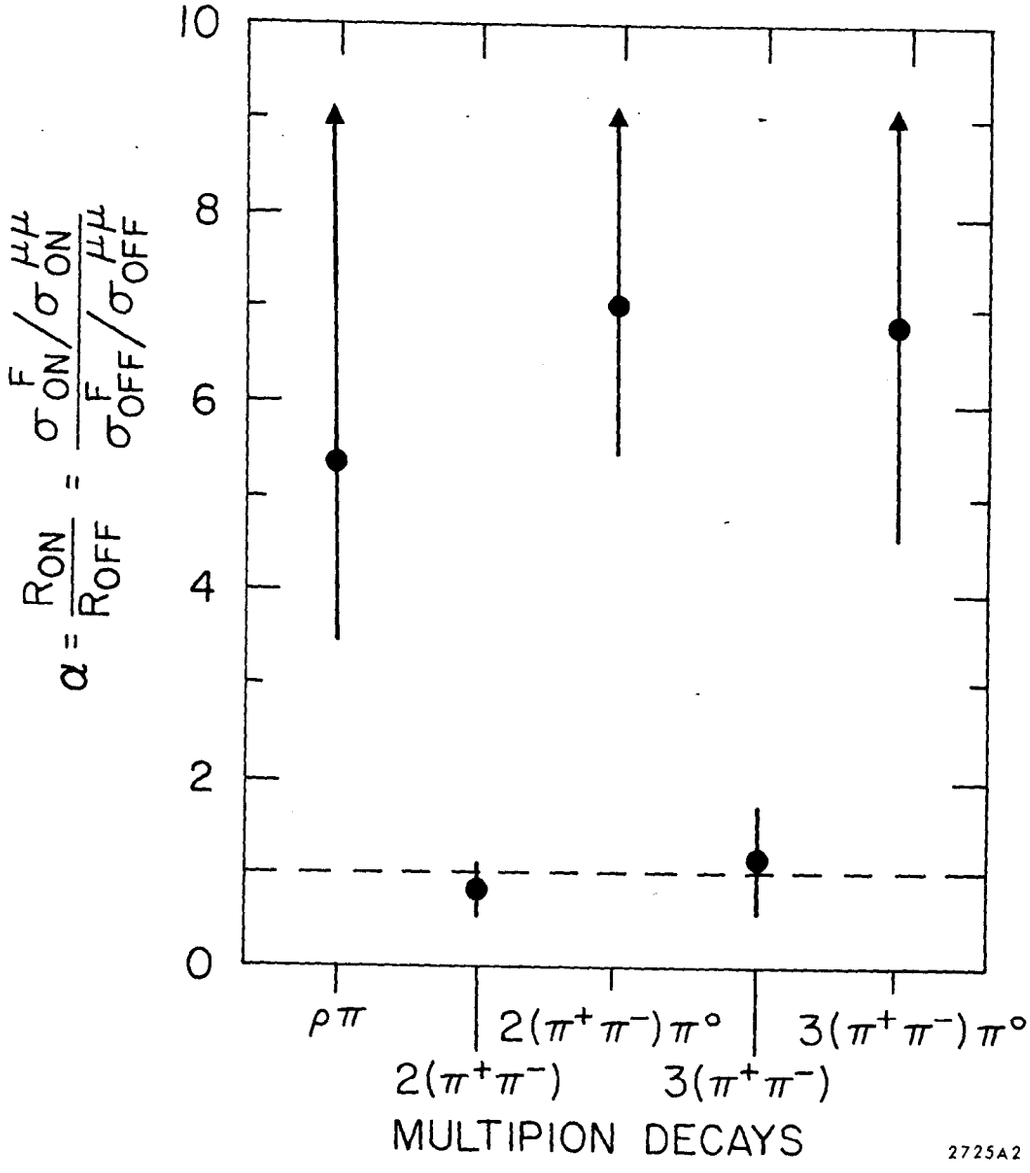

FIG. 21. α (defined in Eq. 14) versus number of pions in ψ decays.

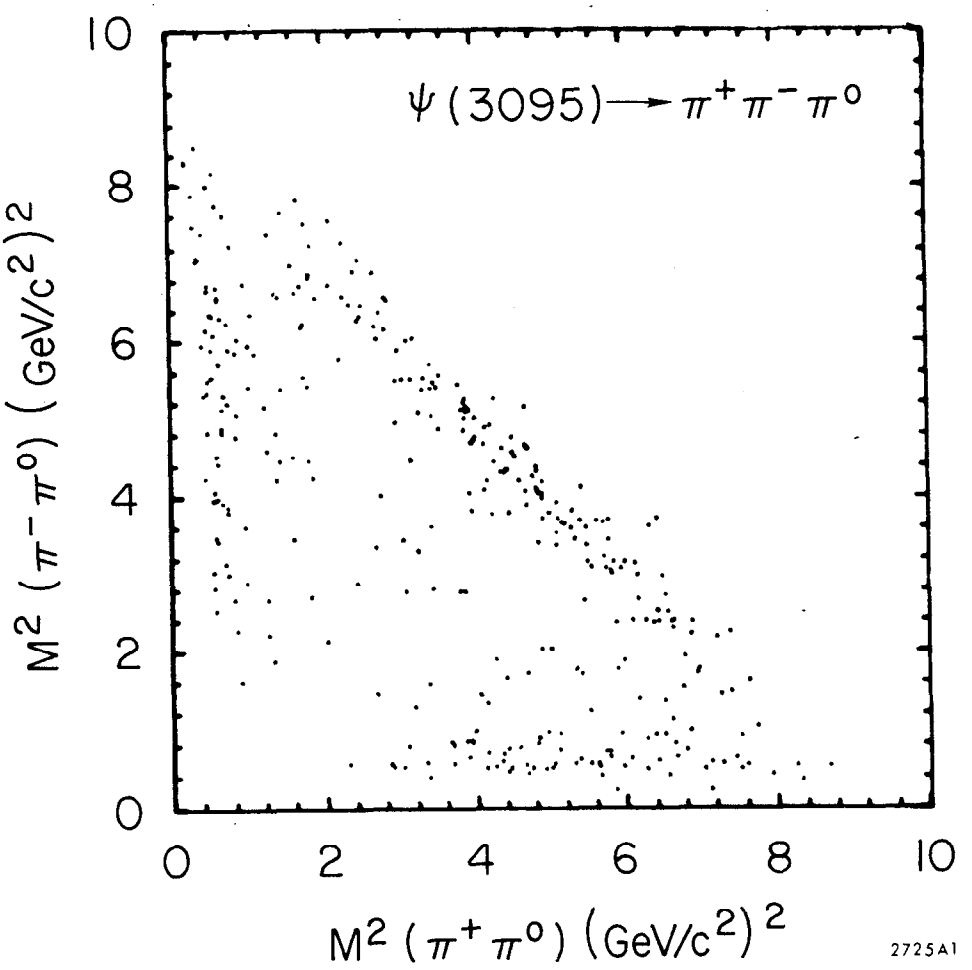

FIG. 22. Dalitz plot for $\psi \to \pi^+\pi^-\pi^0$.

If we consider the well established pseudoscalar (P), vector (V), and tensor (T) meson multiplets, then decays to PP, PT, VV, and TT meson pairs are forbidden, while decays to PV and VT pairs are allowed. Examining Table IV for decays involving K, $K^*(890)$, and $K^{**}(1420)$, we find that in each case the allowed modes are observed and the forbidden modes are not. In particular note that

$$\frac{\Gamma(K\bar{K}^*)}{\Gamma(K\bar{K})} > 30 \tag{15}$$

and

$$\frac{\Gamma(p\bar{p})}{\Gamma(k\bar{k})} > 25 \quad . \tag{16}$$

It is not true in general that heavy particles do not decay into two pseudoscalars. Shortly we will see that the $\chi(3415)$ decays into both $\pi^+\pi^-$ and K^+K^- with branching fractions of about 1%.

For the two allowed modes, PV and VT, we can proceed one step further and ask whether the branching fractions to individual channels are in accord with SU(3) symmetry. In the PV case, per channel,

$$\Gamma(\pi\rho) \quad : \quad \Gamma(KK^*) \quad : \quad \Gamma(\eta\phi) \tag{17a}$$

should be

$$1.0 \quad : \quad 1.0 \quad : \quad 0.48 \ . \tag{17b}$$

Correcting for phase space (17b) becomes

$$1.0 \quad : \quad 0.84 \quad : \quad 0.36 \ . \tag{17c}$$

The data from Table IV are

$$0.42 \pm 0.07 \quad : \quad 0.15 \pm 0.03 \quad : \quad 0.07 \pm 0.04 \ . \tag{17d}$$

Dividing by the predicted ratios (17c), we obtain

$$0.42 \pm 0.07 \quad : \quad 0.18 \pm 0.04 \quad : \quad 0.19 \pm 0.11 \ . \tag{17e}$$

Thus $\Gamma(\rho\pi)$ is about a factor of two larger than expected from $\Gamma(KK^*)$.

For the VT decays, we expect, per channel

$$\Gamma(\rho A_2) \quad : \quad \Gamma(K^*K^{**}) \quad : \quad \Gamma(\phi f') \tag{18a}$$

to be

$$1.0 \quad : \quad 1.0 \quad : \quad 1.0 \ . \tag{18b}$$

Correcting for s-wave phase space (18b) becomes

$$1.0 \quad : \quad 0.90 \quad : \quad 0.78 \ . \tag{18c}$$

The data are

$$0.30 \pm 0.10 \quad : \quad 0.34 \pm 0.13 \quad : \quad 0.08 \pm 0.05 \ . \tag{18d}$$

Dividing by the predictions, (18c), we obtain

$$0.30 \pm 0.10 \quad : \quad 0.38 \pm 0.14 \quad : \quad 0.10 \pm 0.06 \ . \tag{18e}$$

In this case there is good agreement between ρA_2 and K^*K^{**}. $\phi f'$ is low, but its predicted rate is sensitive to the assumption of s-wave phase space.

Thus, in general, the ψ does appear to behave as an SU(3) singlet. Allowed decays are observed and forbidden ones are not. Decay rates are roughly correct, but the discrepancy between $\pi\rho$ and KK^* indicates some SU(3) breaking.

Although we have not yet discussed their decays, this is probably the best place to make a few remarks on the SU(3) properties of other members of the ψ family. The only evidence we have for the ψ' is that the decay to $p\bar{p}$ has been observed and is at least four times larger than the decay to $K\bar{K}$, which has not been seen. This indicates some inhibition of the $K\bar{K}$ mode.

There are several predictions for the ψ states under the assumption that they are SU(3) singlets. These are listed in Table V.

Although the errors are large, there is no apparent deviation from the SU(3) predictions.

TABLE V. SU(3) tests for the χ states.

State	Modes	Expected ratio	Observed ratio
$\chi(3415)$	$\frac{\pi^+\pi^-}{K^+K^-}$	1	1.0 ± 0.4
$\chi(3415)$	$\frac{K^{*o}K^-\pi^+ + c.c.}{\rho^o\pi^+\pi^-}$	$\frac{4}{3}$	1.4 ± 0.8
$\chi(3510)$	$\frac{K^{*o}K^-\ \ ^+ + c.c.}{\rho^o\pi^+\pi^-}$	$\frac{4}{3}$	1.2 ± 1.2
$\chi(3550)$	$\frac{K^{*o}K^-\pi^+ + c.c.}{\rho^o\pi^+\pi^-}$	$\frac{4}{3}$	1.1 ± 0.9

VI.E. Tests of Zweig's rule

As we noted previously, the ψ is narrow because all of its decays are suppressed by Zweig's rule. The decays $\psi \to \omega\pi\pi$ and $\psi \to \phi\pi\pi$ allow the examination of this phenominological rule further since the $\phi\pi\pi$ decay is doubly suppressed, as illustrated in Fig. 23a and 23b.

From Table IV

$$\frac{\Gamma(\phi\pi\pi)}{\Gamma(\omega\pi\pi)} = 0.21 \pm 0.11 \tag{19}$$

which gives an overall suppression factor of about five. However, this overall factor is quite misleading. To understand the dynamics better, we want to study the ratio in Eq. 19 as a function of $\pi\pi$ mass, which is plotted in Fig. 24. Above 1100 MeV/c^2, there is only one observed $\phi\pi\pi$ event and the suppression factor is of order 70. But below 1100 MeV/c^2, there does not appear to be any suppression.

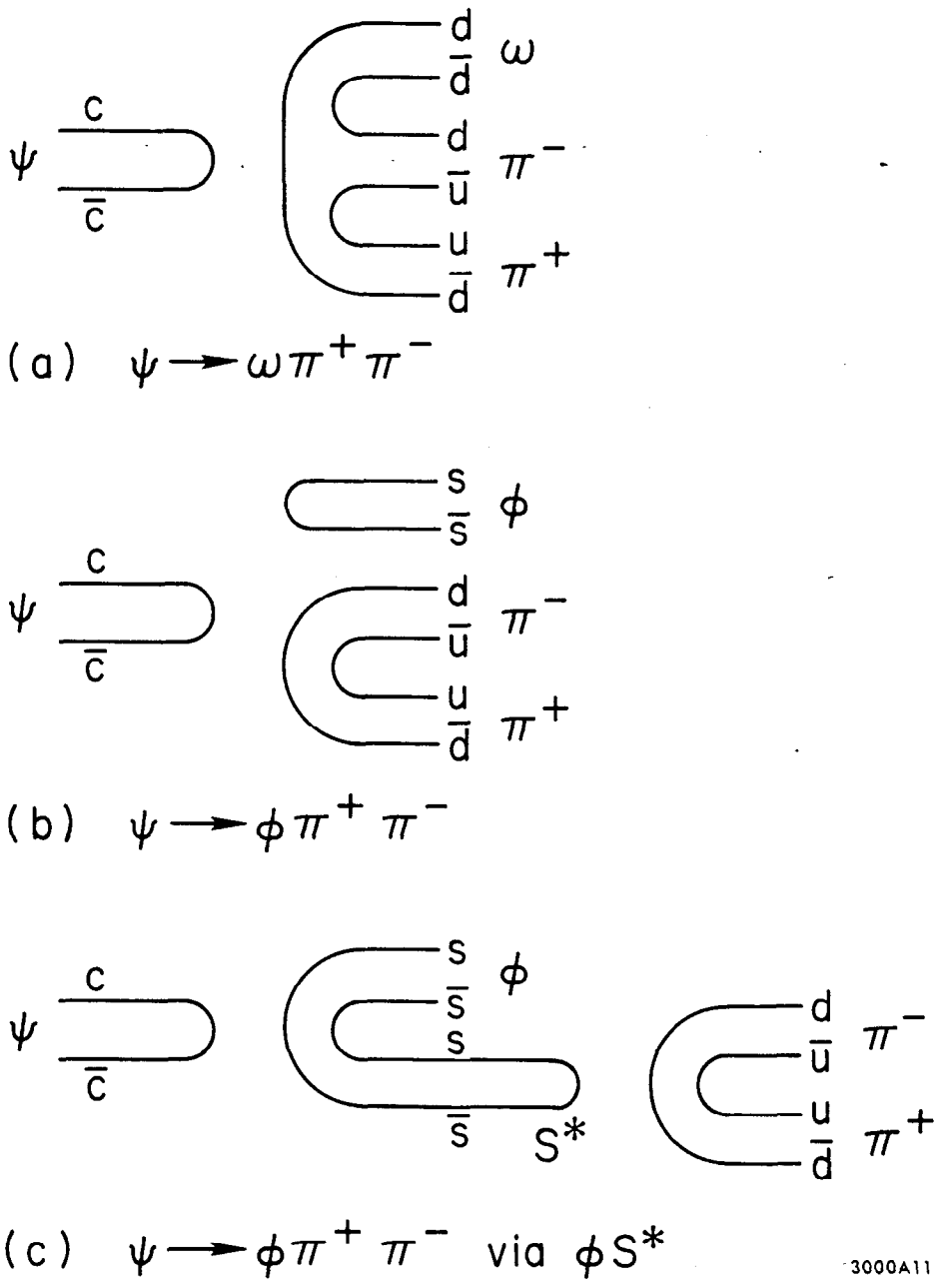

FIG. 23. Quark diagrams illustrating a) $\psi \to \omega\pi^+\pi^-$, b) $\psi \to \phi\pi^+\pi^-$, c) $\psi \to \phi S^* \to \phi\pi^+\pi^-$.

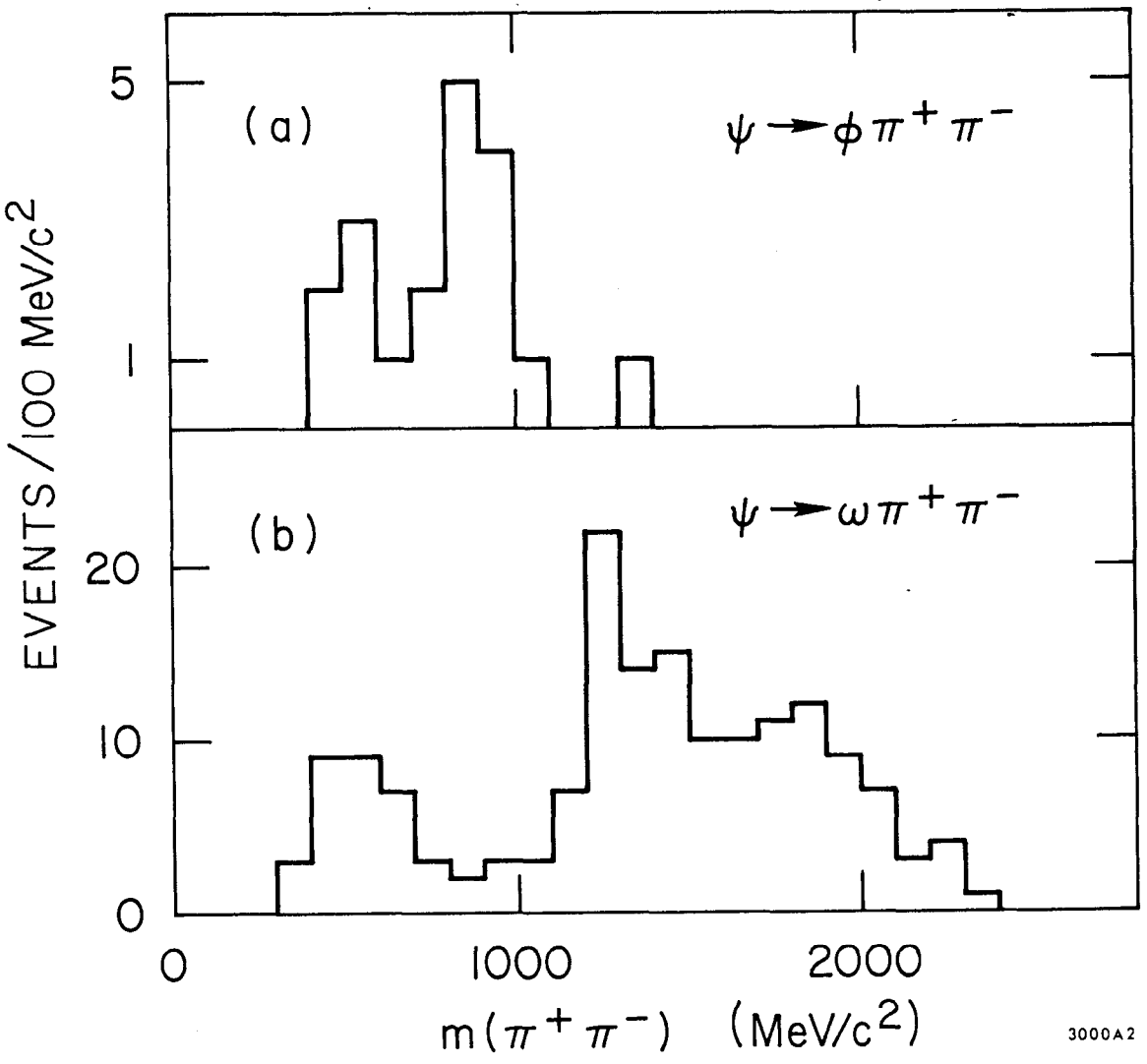

FIG. 24. Invariant mass of $\pi^+\pi^-$ in a) $\psi \to \phi\pi^+\pi^-$ and b) $\psi \to \omega\pi^+\pi^-$.

One way this could occur is shown in Fig. 23c.[69] Two pair of $s\bar{s}$ quarks could be formed with only single Zweig suppression. One pair forms a ϕ, the other a $s\bar{s}$ state near or below threshold for K pairs, for example the $S^*(993)$. Because of either phase space or kinematics, this state will be forced to decay into pions rather than kaons.

VI.F. Radiative decays

With the addition of some new data from DORIS presented at this conference,[65,66] we are now in a position to draw some interesting conclusions from ψ radiative decays. From Table IV, we note that $\psi \to \gamma\pi^0$ has not been observed and the upper limit on the branching fraction is quite small, $< 1.6 \times 10^{-4}$. $\psi \to \gamma\eta$ and $\psi \to \gamma\eta'$ are seen with branching fractions $(1.0 \pm 0.2) \times 10^{-3}$ and $(2.4 \pm 0.6) \times 10^{-3}$.

Three processes which could account for these decays are shown in Fig. 25. In Fig. 25a the photon is emitted from the light quarks. The SU(3) coupling here is a singlet going to a pair of octets. From SU(3) we would expect $\gamma\pi^0$ to be three times $\gamma\eta$. This clearly cannot be an important mechanism since the $\gamma\pi^0$ branching fraction is very small.

The second mechanism (Fig. 25b) is for the photon to be emitted from the charmed quark pair. This SU(3) coupling must be a singlet going to a pair of singlets. This diagram should be completely dominated by $\gamma\eta'$ since the η' is almost a pure SU(3) singlet, while the η is almost pure octet. If this diagram is to account for all of the radiative decays, it is hard to understand why the η to η' ratio is so large.

This brings us to an interesting suggestion.[70,71] If there is a

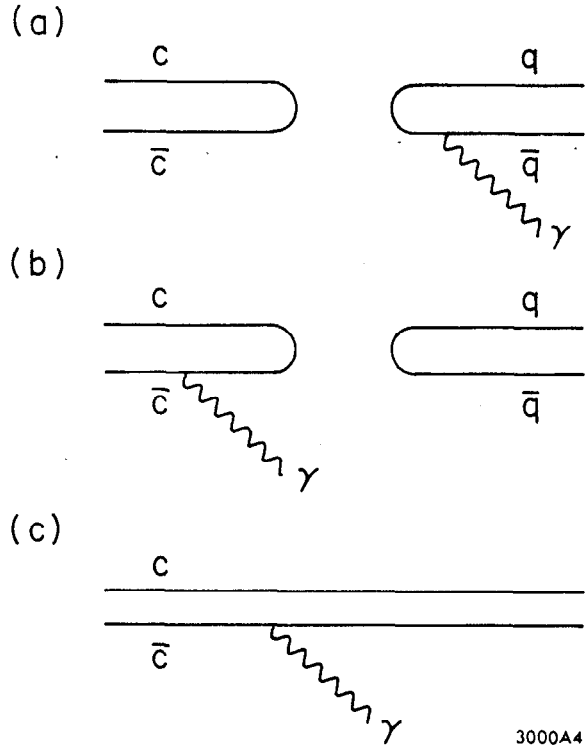

FIG. 25. Quark diagrams illustrating three mechanisms for $\psi \to \gamma\pi^0$, $\psi \to \gamma\eta$, and $\psi \to \gamma\eta'$ decays.

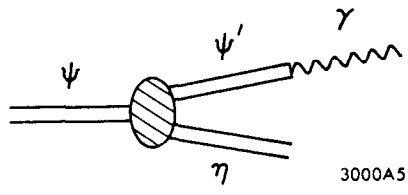

FIG. 26. Diagram for caluclating $\psi \to \gamma\eta$ from $\psi' \to \psi\eta$ using vector meson dominance.

small amount of $c\bar{c}$ mixing in the η and η' (there can be no mixing in the π^0 by isospin conservation), then the radiative decays can occur without Zweig suppression, as shown in Fig. 25c. The data on radiative decays give support to this suggestion. In Sec. VII.B additional support will come from the $\psi' \to \psi\eta$ decay.

An interesting sidelight is that part of Figs. 25b and 25c can be calculated by applying vector dominance to the decay $\psi' \to \psi\eta$, as shown in Fig. 26. This calculation gives a value which is an order of magnitude too large.[68] This should at least caution us that the use of vector dominance at the ψ mass is dangerous.

VI.G. Is anything missing?

With all of the data that have now been collected on ψ decays, it is interesting to ask whether we can account for all of the ψ decays in a reasonable way. This is attempted in Table VI.[72]

TABLE VI. Estimates of ψ decay modes. The quality of the estimate is indicated by the number of question marks following the estimate. No question mark means that the branching fraction is measured or can be derived from measurements listed in Table IV with the aid of isospin conservation. One question mark means that the branching fraction can be estimated from measurements and statistical arguments. Two question marks means a guess based on similar decays. And three question marks means that there is not enough information to even make an intelligent guess.

mode	branching fraction (%)	quality
lepton pairs	14.7	
second order electromagnetic	17.0	
3π	1.6	
5π	6.0	
7π	6.2	?
9π	2.2	?
$\geq 11\pi$	0.7	??
	16.7	
$K\bar{K}\ \pi$	0.6	
$K\bar{K}\ 2\pi$	3.1	?
$K\bar{K}\ 3\pi$	4.5	??
$K\bar{K}\ 4\pi$	2.7	?
$K\bar{K}\ n\pi,\ n \geq 5$	2.0	??
	12.9	
$2K\ 2\bar{K}$	0.3	?
$2K\ 2\bar{K}\ n\pi,\ n \geq 1$	0.7	??
	1.0	
$N\bar{N}$	0.4	
$N\bar{N}\ \pi$	0.6	
$N\bar{N}\ \eta$	0.4	
$N\bar{N}\ 2\pi$	1.7	?
$N\bar{N}\ 3\pi$	0.5	?
	3.6	
$\Lambda\bar{\Lambda}x,\ \Sigma\bar{\Sigma}x$, etc.	1.8	??
$\gamma\eta,\ \gamma\eta'$	0.3	
$\gamma x(2800)$	2.0	???
η + anything	20-30	
TOTAL	90-100	???

The decays to lepton pairs and all pion states and the decays which proceed via a second-order electromagnetic interaction (Fig. 20b) are fairly well measured. The decays involving kaons and nucleons are less certain, but can be reasonably estimated. There is certainly some double counting between the second-order e.m. decays and those involving kaons and nucleons, which we are ignoring. These decays added together account for about 70% of the total. We have not yet considered decays involving η's, about which we have no experimental information. However, based on the fraction of events involving kaons, it does not seem unreasonable that 20 to 30% of the decays should have η's in them.

Thus, although we have explicitly measured only a small fraction of hadronic decays, there is no compelling argument that there is a large component of the decays which we do not understand. However, such a situation is also not excluded by the data.

VII. Hadronic decays of the ψ'.

VII.A. Table of results

There are four classes of ψ' decays which we will discuss: a) $\psi' \to \psi$ decays, b) second-order electromagnetic decays, c) direct decays to ordinary hadrons and d) radiative decays to intermediate states (χ states). Table VII contains a compendium of world measurements of these decays.

TABLE VII. Decay Modes of $\psi'(3684)$.
(See heading for Table IV.)

Mode	Fraction (%)	Ref.	Footnotes
$e^+ e^-$	0.93 ± 0.16	25	a
$\mu^+ \mu^-$	0.93 ± 0.16	25,(73)	a
$\psi \pi^+ \pi^-$	33.0 ± 2.6	50,61,73,75-77	b
$\psi \pi^o \pi^o$	16.2 ± 2.8	50,61,73,75-77	b
$\psi \eta$	4.1 ± 0.7	50,61,73,75-77	b
$\psi \gamma + \psi \pi^o$	< 0.15	76	c
$\pi^+ \pi^-$	< 0.005	51,(49)	d
$2\pi^+ 2\pi^-$	0.08 ± 0.02	78	e
$2\pi^+ 2\pi^- \pi^o$	0.35 ± 0.15	55	
$\rho^o \pi^o$	< 0.1	55	
$K^+ K^-$	< 0.005	51,(49)	f
$K^+ K^- \pi^+ \pi^-$	0.14 ± 0.04	78	
$p \bar{p}$	0.023 ± 0.007	79,(49)	g
$\Lambda \bar{\Lambda}$	< 0.04	59	
$\Xi^- \bar{\Xi}^-$	∿ 0.02	59	h
$\gamma \gamma$	< 0.5	80,(61)	i
$\gamma \pi^o$	< 0.7	80,(61)	
$\gamma \eta$	< 0.13	61,(80)	
$\gamma \eta'$	< 0.11	66,(61)	
γ x(2800)	< 1.1	81,(67)	
γ x(2800) $\rightarrow 3\gamma$	< 0.037	61	
$\gamma \chi(3415)$	10. ± 4.	67	j
	7.5 ± 2.6	81	
$\gamma \chi(3510)$	9. ± 3.	67	k
$\gamma \chi(3550)$	8. ± 3.	67	k
$\gamma \chi(3455) \rightarrow \gamma\gamma\psi$	0.8 ± 0.4	81	l

a. $\Gamma(ee) = \Gamma(\mu\mu)$ was assumed. Without this assumption, $\Gamma(\mu\mu)/\Gamma(ee) = 0.89 \pm 0.16$ (Ref. 74). The total decay width was determined to be 228 ± 56 KeV. (Ref. 25).

Table VII continued footnotes

b. From a simultaneous fit to measurements of $\psi' \to \psi$ + anything, $\psi' \to \psi$ + neutrals, $\psi' \to \psi\pi^+\pi^-$, $\psi' \to \psi\pi^0\pi^0$, $\psi' \to \psi\eta$, and $\psi' \to \gamma\chi \to \gamma\gamma\psi$.

c. $\psi\gamma$ forbidden by C and $\psi\pi^0$ forbidden by isospin.

d. Forbidden by isospin.

e. Proceeds by second-order electromagnetic interaction. The total hadronic decay fraction via this type of interaction is (2.9 ± 0.4)% (Ref. 25).

f. Forbidden by SU(3).

g. Angular distribution of $1 + \cos^2\theta$ assumed. This is in agreement with measurements of the $\psi \to p\bar{p}$ decay.

h. Two events observed.

i. Forbidden for a spin 1 particle.

j. Angular distribution of $1 + \cos^2\theta$ assumed in agreement with spin 0 assignment and experimental measurements (Ref. 56).

k. Angular distribution assumed to be isotropic.

l. The existence of this state needs confirmation.

VII.B. $\psi' \to \psi$ decays

The ψ' decays over half the time into the ψ. These decays have now been measured at both SPEAR[73,75-77] and DORIS[50,61] with consistent results from both laboratories.

The total $\psi' \to \psi$ branching fraction can be determined by simply observing the μ pair decay of inclusive ψ's. Figure 27 shows the invariant mass distribution of the two highest momentum oppositely charged particles in each ψ' decay. (The particles are assumed to be μ's and electrons have been eliminated.)

The dominent $\psi' \to \psi$ decay, $\psi' \to \psi\pi^+\pi^-$ is visible in two different ways. Figure 28a shows the missing mass recoiling against all combinations of $\pi^+\pi^-$. Figure 28b shows the same distribution for events which satisfy a 4-C fit to $\psi' \to \mu^+\mu^-\pi^+\pi^-$.

The decay $\psi' \to \psi\eta$ is seen best in the mode in which $\eta \to \pi^+\pi^-\pi^0$ or $\pi^+\pi^-\gamma$. We search for events in which two μ's at the ψ mass and two π's are visible, but in which there is missing energy and momentum. The mass squared recoiling against the two μ's, Fig. 29 shows that all these events are consistent with the $\psi\eta$ decay mode.

Finally, the $\psi' \to \psi\pi^0\pi^0$ decay has been measured directly at DORIS[50] and indirectly at SPEAR by subtracting all other $\psi' \to \psi$ modes (including $\psi' \to \gamma\chi \to \gamma\gamma\psi$ which will be discussed in Sec. VI.E) from $\psi' \to \psi$ + anything.

There are three important conclusions to be drawn from the measurements of $\psi' \to \psi$ decays. First, the ψ' and ψ are closely related. There is much more phase space for $\psi' \to \omega\pi\pi$ than for $\psi' \to \psi\pi\pi$, yet the branching fraction for the latter decay is more than two orders of magnitude larger than that for the former.

Second, as expected for a state of charmonium, isospin is conserved

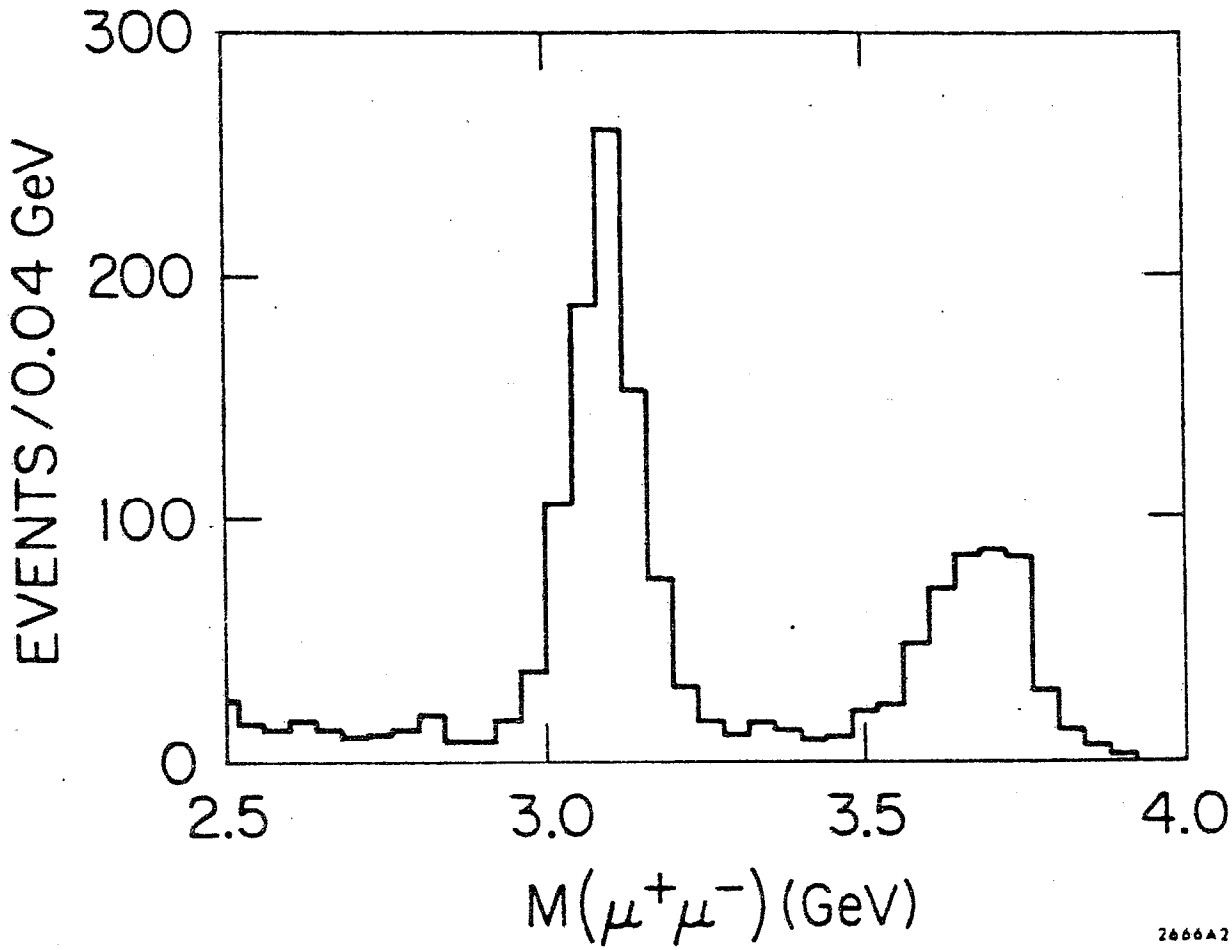

FIG. 27. $\mu^+\mu^-$ invariant mass for the highest momentum oppositely charged particle pair from each ψ' decay. Electron pairs are excluded.

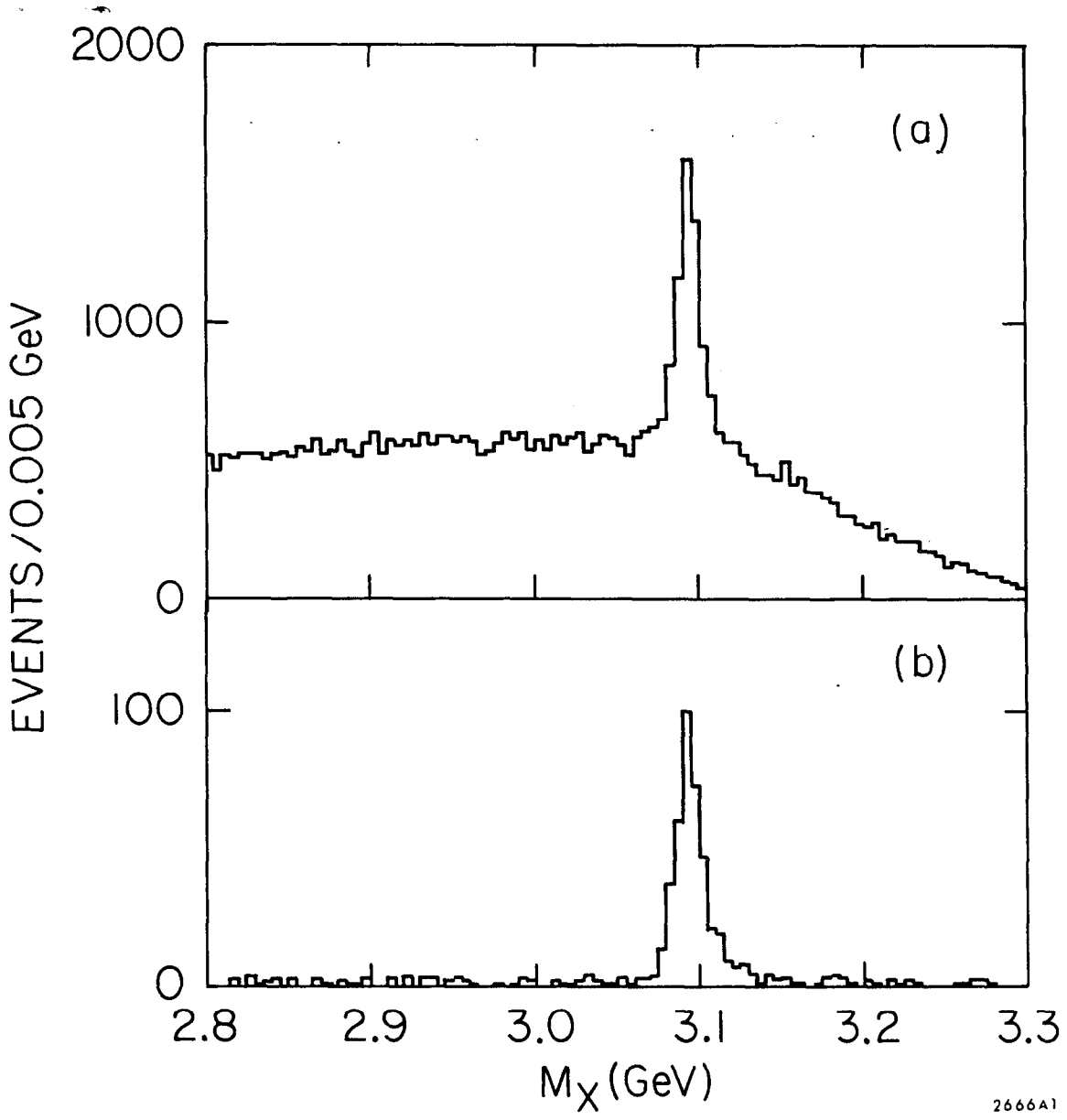

FIG. 28. Missing mass recoiling against pairs of oppositely charged particles a) in all ψ decays, and b) ψ decays with four charged particles conserving energy and momentum.

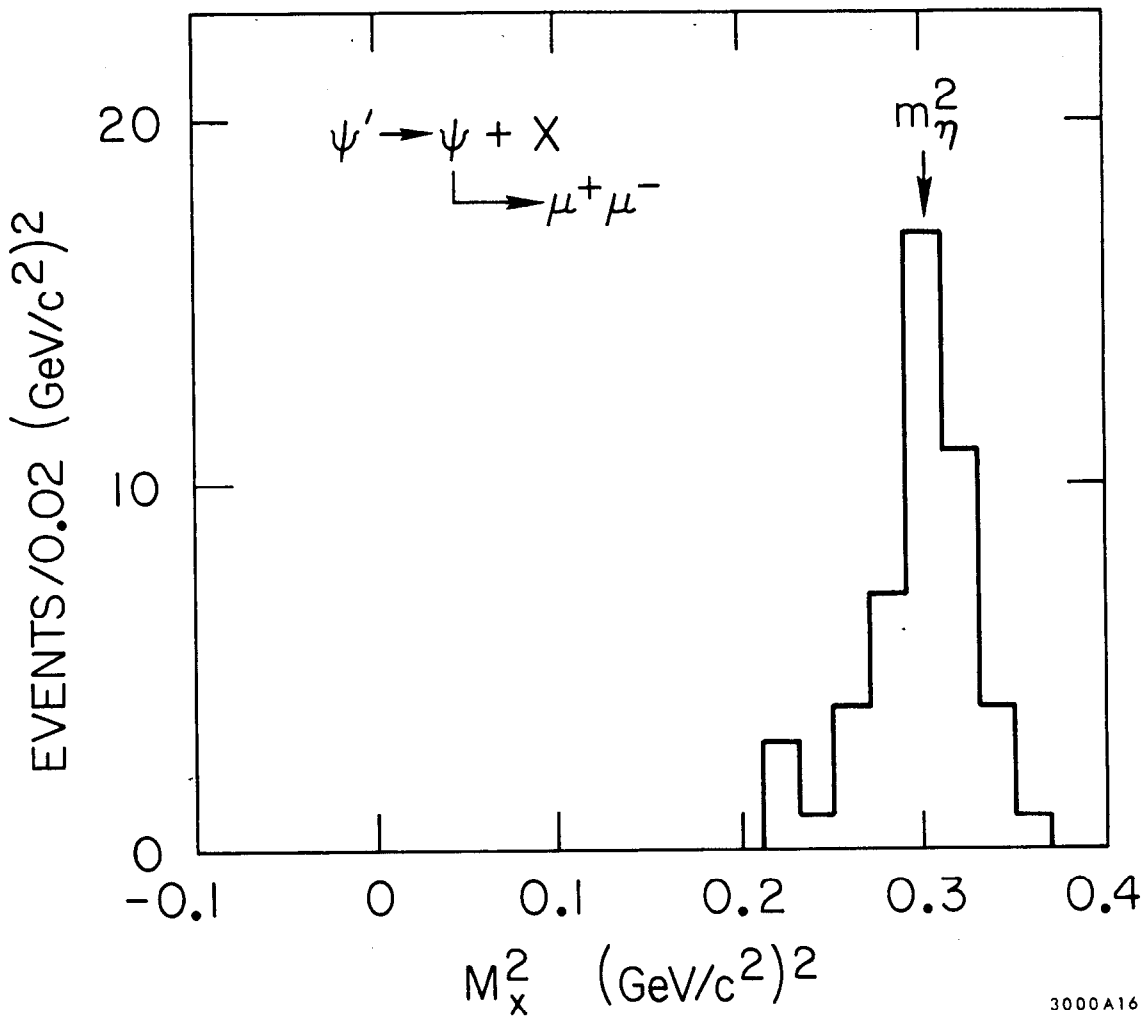

FIG. 29. Missing mass squared recoiling against the ψ in events in which the ψ and two charged pions are detected, but which are not consistent with the decay $\psi' \to \psi\pi^+\pi^-$.

in the decay and is equal to zero. This can be seen from the ratio of the $\psi\pi^0\pi^0$ mode to the $\psi\pi^+\pi^-$ mode which is equal to 0.49 ± 0.09. Correcting for phase space, we expect this ratio to be 0.52 for I = 0, 0 for I = 1, and 2.1 for I = 2. Additional evidence for isospin conservation comes from the observation of $\psi' \to \psi\eta$ but not $\psi' \to \psi\pi^0$. The latter decay is not observed at the level of 3% of the former and it is inhibited only by isospin.

The third conclusion has to do with the only real surprise in the $\psi' \to \psi$ decays, the size of $\psi' \to \psi\eta$. This decay is quite large -- it is about a 4% branching fraction -- even though it has everything working against it:

1) There is little phase space; the Q value is only 40 MeV.
2) This is a P-wave decay, so there is an angular momentum barrier.
3) The decay is SU(3) forbidden in the limit that the η is pure octet.

We have already discussed a way out of these difficulties. If there is some $c\bar{c}$ mixing in the η, $\psi' \to \psi\eta$ is no longer Zweig suppressed and its large branching fraction can easily be understood.

VII.C. Second order electromagnetic decays

The arguments of Sec. VI.C. which were applied to the ψ apply equally well to the ψ'. The branching fractions to e^+e^- and to $\mu^+\mu^-$ are each about 1%. Therefore the branching fraction for hadrons produced via an intermediate photon (Fig. 20b) should be about 3% since the non-resonant value of R in the vicinity of the ψ' is about 3.

VII.D. Direct decays to hadrons

Few direct decays of the ψ' to ordinary hadrons have been observed and only two modes, $p\bar{p}$ and $K^+K^-\pi^+\pi^-$, have been measured well. This is

partially because the direct decays are usually masked by a large background of $\psi' \to \psi\pi\pi$ decays and partially because not enough effort has been expended on finding these decays. Both the $p\bar{p}$ and $K^+K^-\pi^+\pi^-$ modes were measured in the process of working on χ decays.

Nevertheless, these two modes give us a considerable amount of information on direct ψ' decays. Table VIII shows a comparison of ψ and ψ' decays to these two modes and to lepton pairs. For all three decays the ratio of the ψ' to ψ partial widths is equal within errors. This can be understood if

$$\Gamma(\text{hadrons}) \propto |\Psi(0)|^2 , \tag{20}$$

where $\Psi(0)$ is the wave function at the origin.[38] A heuristic argument for Eq. 20 is that the charm quarks are heavy and so the interaction is fairly local.

If we assume the validity of Eq. 20, then the branching fraction for ψ' direct decay to ordinary hadrons is about 9%.

TABLE VIII. Comparison of direct ψ and ψ' decays.

mode	Γ_ψ(KeV)	$\Gamma_{\psi'}$(KeV)	$\Gamma_{\psi'}/\Gamma_\psi$
e^+e^-	5.0 ± 0.3	2.1 ± 0.3	0.42 ± 0.07
$p\bar{p}$	0.15 ± 0.01	0.05 ± 0.02	0.33 ± 0.11
$K^+K^-\pi^+\pi^-$	0.50 ± 0.16	0.32 ± 0.09	0.64 ± 0.27

VII.E. $\psi' \to \gamma\chi$ decays

If we consider the ψ the triplet S ground state of charmonium and the ψ' a radially excited state of the ψ, other states should exist which could be reached by radiative transitions from the ψ'.[82-85] The expected scheme

is shown in Fig. 30. There are three triplet P states and two singlet S states. The states above the ψ could decay radiatively to the ψ or could decay directly to ordinary hadrons. As we will discover in the following sections, the P states are well established. There are also candidates for the two pseudoscalar S states, but they are in need of further experimental confirmation.

We will use χ, a name suggested over a decade ago by Bjorken and Glashow for states of charmonium,[86] as a generic name for all these new C-even states. The name P_C was originally suggested by the DASP collaboration[87] for the state we now identify as the $\chi(3510)$; this name is also common in the literature.

The $\psi' \to \gamma\chi$ decays have been detected by three techniques: 1) by detecting the hadronic decay of the χ's, 2) by detecting the ψ and one or both of the cascade photons in $\psi' \to \gamma\chi \to \gamma\gamma\psi$, and 3) by detecting monochromatic photons. We will now discuss each of these techniques in turn.

VII.E.1. χ decays to hadrons

As an example of this technique we will go through the steps used in isolating the $\chi \to 2\pi^+2\pi^-$ decays. The search begins in Fig. 31, which contains scatter plots of missing mass squared (m_x^2) versus missing momentum (p_x) for four-prong events from ψ and ψ' decays.[88] In the ψ case (Fig. 31b) a dense band of events exists near $m_x^2 = 0$ extending across the entire p_x range. These events correspond to the five-pion decay of the ψ. The ψ' decays shown in Fig. 31a after subtraction of $\psi' \to \psi\pi^+\pi^-$ decays appear quite different. The band is absent, but instead there is a cluster of events in the p_x region between 100 and 300 MeV/c.

To investigate this further, we select the events in this region ($100 < p_x < 300$ MeV/c) and plot the projection of these data on the m_x^2

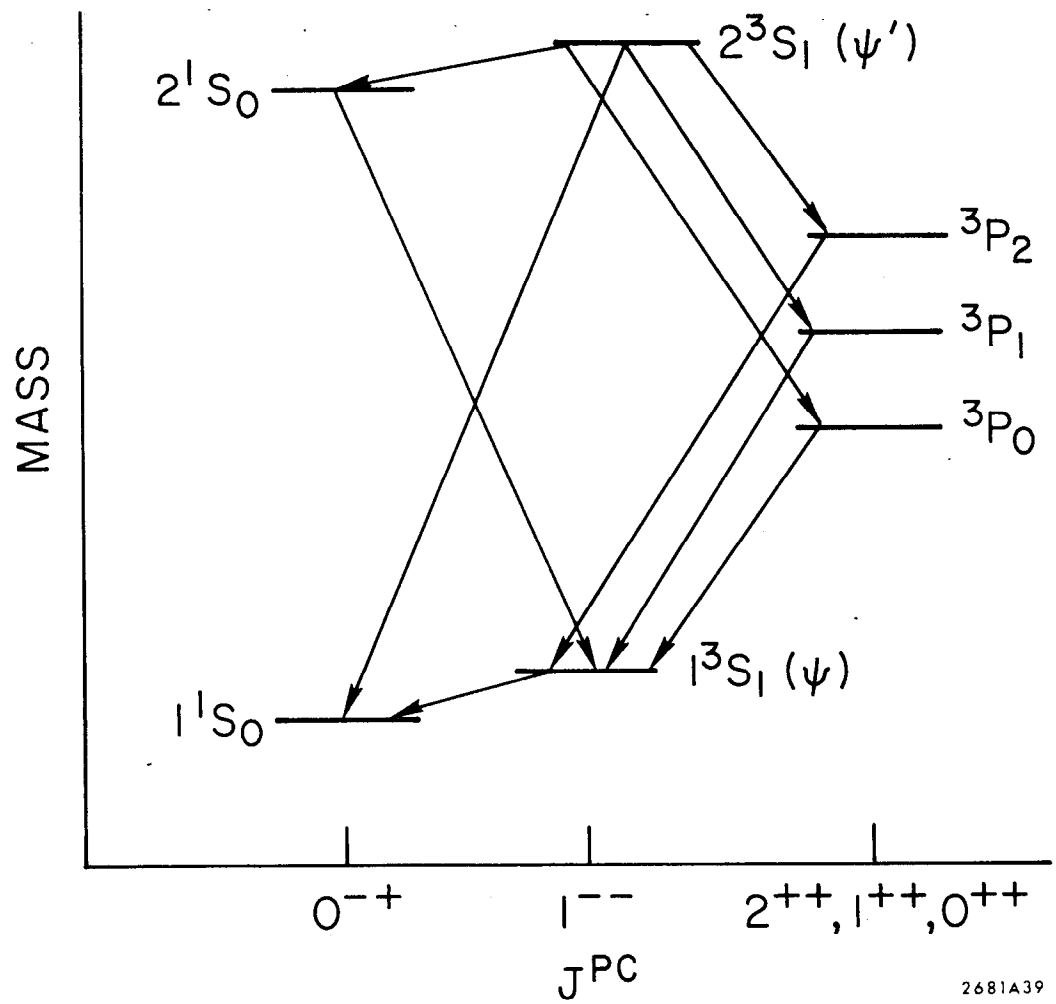

FIG. 30. States and radiative transitions expected from bound fermion-antifermion system.

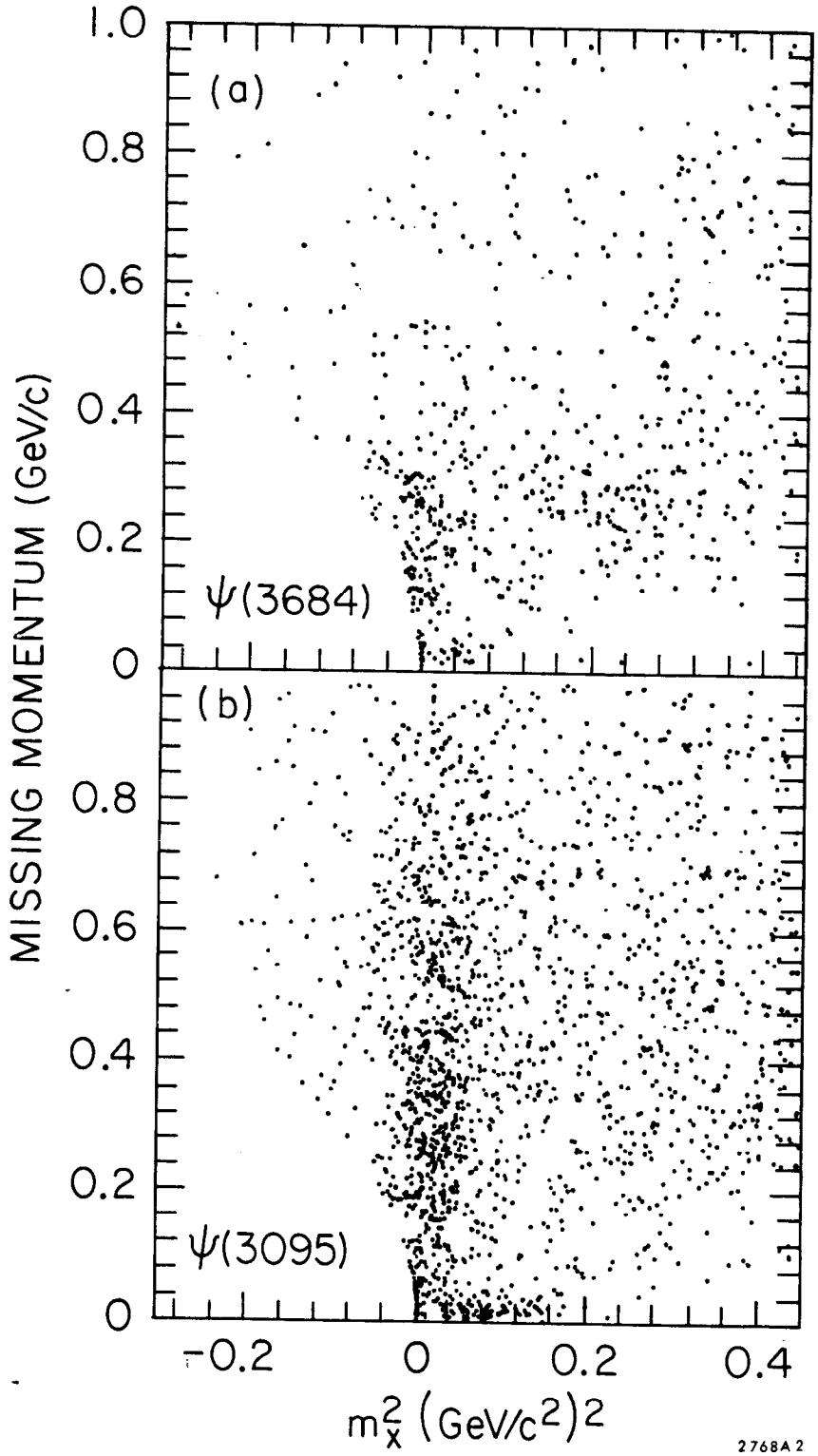

FIG. 31. Scatter plots of missing momentum versus missing mass squared for four prong events in a) ψ' decays and b) ψ decays.

axis. The results are shown in Fig. 32 for the ψ' and ψ. In the case of the ψ (Fig. 32b) the m_x^2 distribution is consistent with a missing π^o, but inconsistent with a missing γ. In the ψ' decays (Fig. 32a) the exact opposite is true -- the missing neutral is consistent with being a γ and is not consistent with being a π^o. Thus, we have the exceptional circumstance that in this p_x range we are observing a $4\pi\gamma$ final state.

We now select those events near $m_x^2 = 0$ ($-0.03 < m_x^2 < 0.03$ GeV/c^2), make a one-constraint fit, and plot the resulting 4π mass in Fig. 33a. Events with masses above 3.60 GeV/c^2 are consistent with the second order electromagnetic decay $\psi' \to 4\pi$. There are three other clear peaks at masses of about 3415, 3500, and 3550 MeV/c^2 each of which we identify with a new χ state.[78,79]

Figures 33b, 33c, and 33d show the mass plots for χ decays to $K^+K^-\pi^+\pi^-$, $3\pi^+3\pi^-$, and $\pi^+\pi^-$ or K^+K^-, all obtained by similar techniques. The same three states are found in these plots, but not as clearly in all cases. In the $K^+K^-\pi^+\pi^-$ mode the $\chi(3510)$ is weak. In the $3\pi^+3\pi^-$ mode the $\chi(3510)$ and $\chi(3550)$ are not resolved. In the $\pi^+\bar{\pi}$ or K^+K^- mode, the $\chi(3415)$ is quite clear and there are eleven events in the vicinity of the $\chi(3550)$ with an estimated background of only two or three events. There are only two events in the vicinity of the $\chi(3510)$ and these are consistent with backgrounds. These decays into two pseudoscalars will be important when we consider the spin assignments of the χ states in Sec. VIII.B.

VII.E.2. χ decays to $\gamma\psi$

Two methods have been used to detect the $\psi' \to \gamma\chi \to \gamma\gamma\psi$ cascade. In both methods the ψ is observed in its muon pair decay, so that we have a final state corresponding to $\psi' \to \gamma\gamma\mu^+\mu^-$.

In the first method, which has been used in the SPEAR magnetic de-

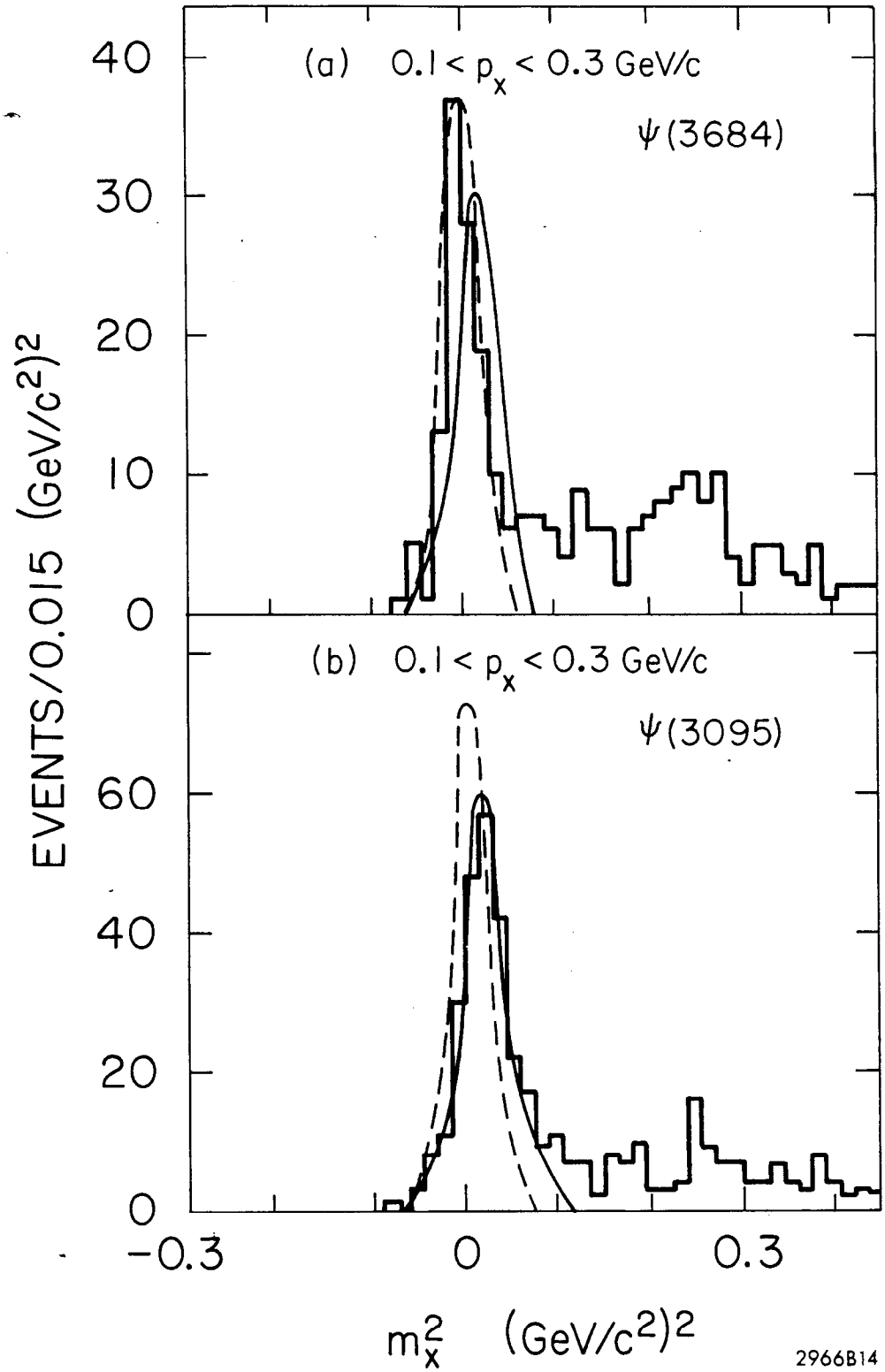

FIG. 32. Missing mass squared for four prong events with missing momentum in the range 100 to 300 MeV/c for a) ψ' decays and b) ψ decays. The solid and dashed lines give the predicted resolution functions for a missing π^0 and γ, respectively.

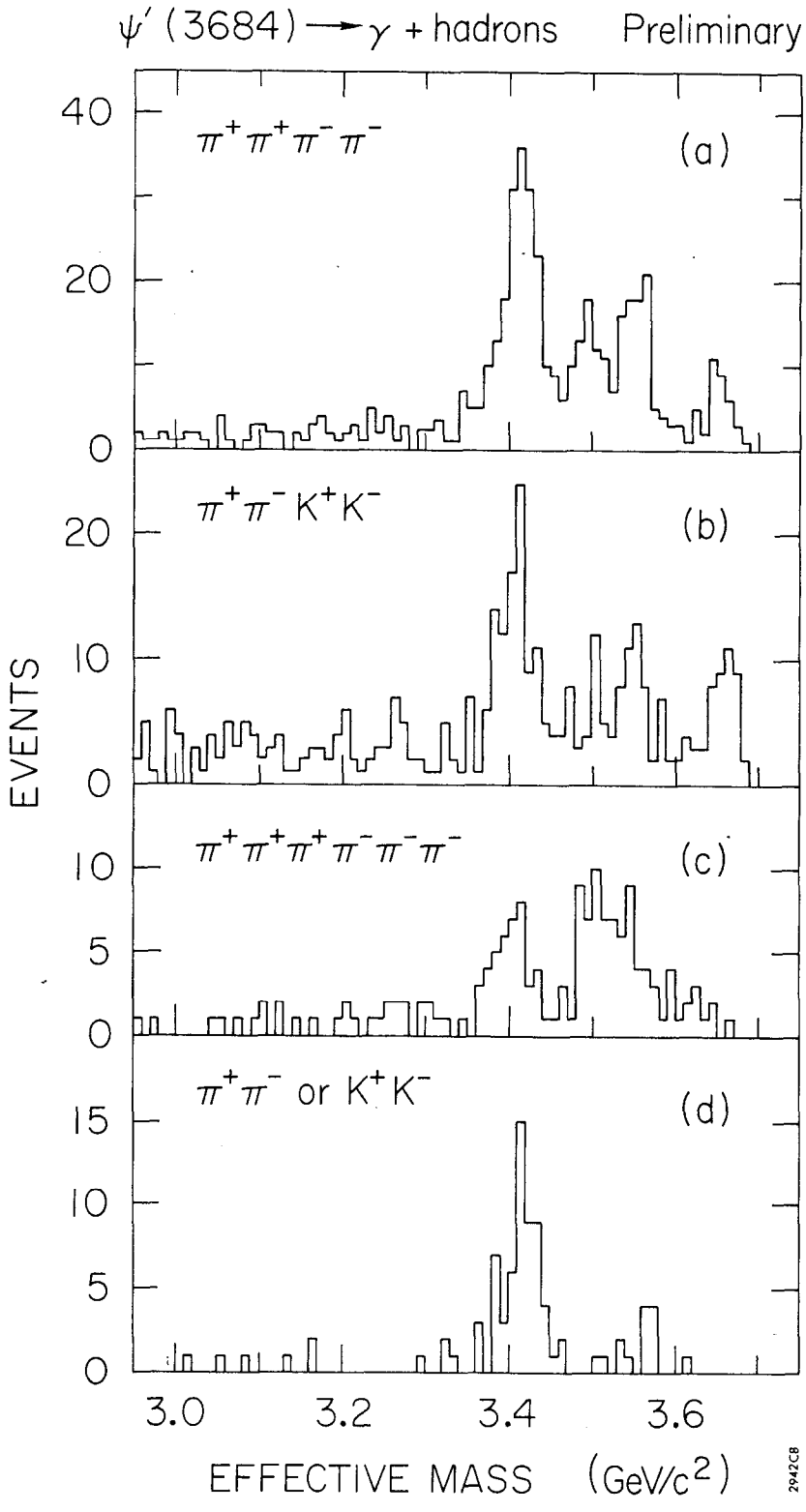

FIG. 33. Invariant χ mass distributions for $\psi' \to \gamma\chi$ for a) $2\pi^+2\pi^-$ b) $\pi^+\pi^-K^+K^-$ c) $3\pi^+3\pi^-$, and d) the sum of $\pi^+\pi^-$ and K^+K^-.

tector, we detect $\mu^+\mu^-$ and observe a conversion of one of the photons in the 0.052 radiation lengths of material surrounding the beam pipe.[90] A 1-C fit is then performed to the event. A computer reconstruction of this type of event is shown in Fig. 34.

In the second method, which has been used both at SPEAR[90] and at DORIS,[61] both photons are detected in shower counters and the angle measurements are used to give a 2-C fit. In the SPEAR magnetic detector, the azimuthal angle is determined by which shower counter is hit and the polar angle is determined by the relative pulse height at the two ends of the counter. This second method provides worse resolution, but much higher statistics than the first method. It will be useful in Sec. VIII.B where we discuss the angular distributions.

Whichever method is used, there are two solutions for each event since we do not know a priori which photon was emitted first. This two-fold ambiguity can be resolved by observing the widths of the reconstructed χ masses since the first photon will be monochromatic, while the second is Doppler shifted by the motion of the χ.

Figure 35 shows the $\gamma\psi$ masses obtained by the first method at SPEAR.[81] There are four clusters of events. The $\chi(3510)$ and $\chi(3550)$ are clearly visible and the two-fold ambiguity is resolved in favor of the higher mass states in agreement with the observation of χ's from their hadronic decays. There is a single event consistent with coming from the $\chi(3415)$.

The new element in Fig. 35 is the cluster of four events at 3454 MeV/c^2. Since the expected background in all of Fig. 35 is only one event, it seems unlikely that this cluster is due to background. Nevertheless, these four events are the only evidence for this possible state; it clearly is on shaky experimental ground and badly needs confirmation. We will tentatively

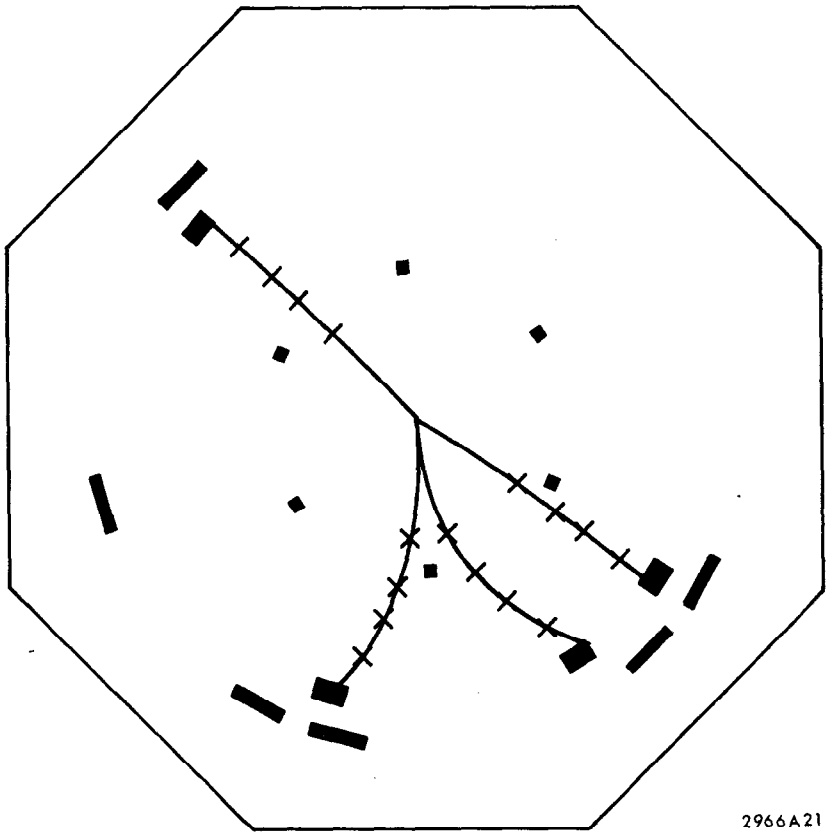

FIG. 34. Computer reconstruction of a $\psi' \to \gamma\chi \to \gamma\gamma\psi \to \gamma\gamma\mu\mu \to \gamma e^+e^-\mu^+\mu^-$ cascade. The short boxes respresent trigger counters and the long boxes represent shower counters. The unconverted γ is detected by the isolated shower counter on the left.

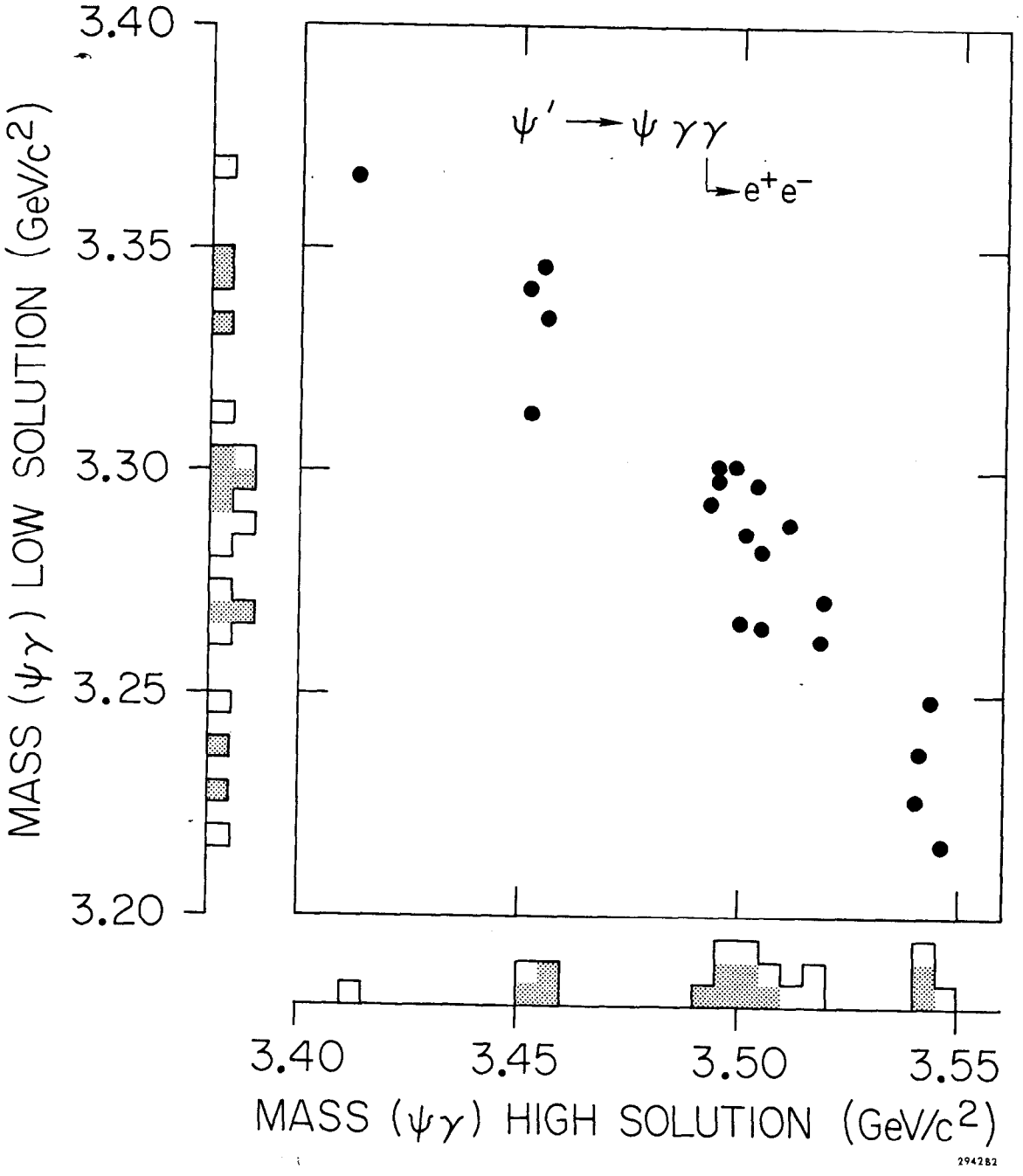

FIG. 35. Scatter plot of the two solutions for the mass of χ states in $\psi' \rightarrow \gamma\chi \rightarrow \gamma\gamma\psi$ events.

dub it the $\chi(3455)$ and discuss it, but the reader is forewarned of its weak status.

The latest data from DORIS[91] show the same pattern as Fig. 35, but with fewer events and worse resolution. There are five events at the $\chi(3510)$, one event each consistent with coming from the $\chi(3415)$ and $\chi(3550)$, and one event ambiguous between the $\chi(3510)$ and the $\chi(3455)$.

VII.E.3. Monochromatic photons

In order to measure the branching ratios for $\psi' \to \gamma\chi$, it is necessary to detect the monochromatic photons. Two measurements of this type have now been performed. The first comes from the magnetic detector at SPEAR.[81] Photons were detected by observing conversions in the material around the beam pipe. For low energy photons, the rms energy resolution is about 2% for this technique. Photon energy spectra from ψ and ψ' decays are shown in Fig. 36. A peak is seen in the ψ' spectrum at 261 MeV, corresponding to the $\chi(3415)$. The branching fraction for $\psi' \to \gamma\chi(3415)$ from these data is 0.075 ± 0.026. The other χ states correspond to lower photon energies and are not visible because of rapidly falling acceptance in this region.

A special experiment was conducted at SPEAR to search for monochromatic photons by a collaboration from Maryland, Pavia, Princeton, San Diego, SLAC, and Stanford (MPPSDSS).[67] A sketch of the apparatus is shown in Fig. 37. Arrays of large NaI crystals were used to detect the photons with about 5% rms energy resolution. The data from ψ and ψ' decays are shown in Fig. 38. There are no significant peaks in the ψ spectrum, but four clear peaks are apparent in the ψ' spectrum. The first three correspond to the $\chi(3550)$, $\chi(3510)$ and $\chi(3415)$, and the last is from the Doppler broadened photon in the $\chi(3510) \to \gamma\psi$ decay. The branching ratios for $\psi' \to \gamma\chi$ are 0.10 ± 0.04, 0.09 ± 0.03, and 0.08 ± 0.03 for the $\chi(3415)$, $\chi(3510)$, and $\chi(3550)$, respectively. The branching fraction for $\psi' \to \gamma\chi(3415)$ determined by these

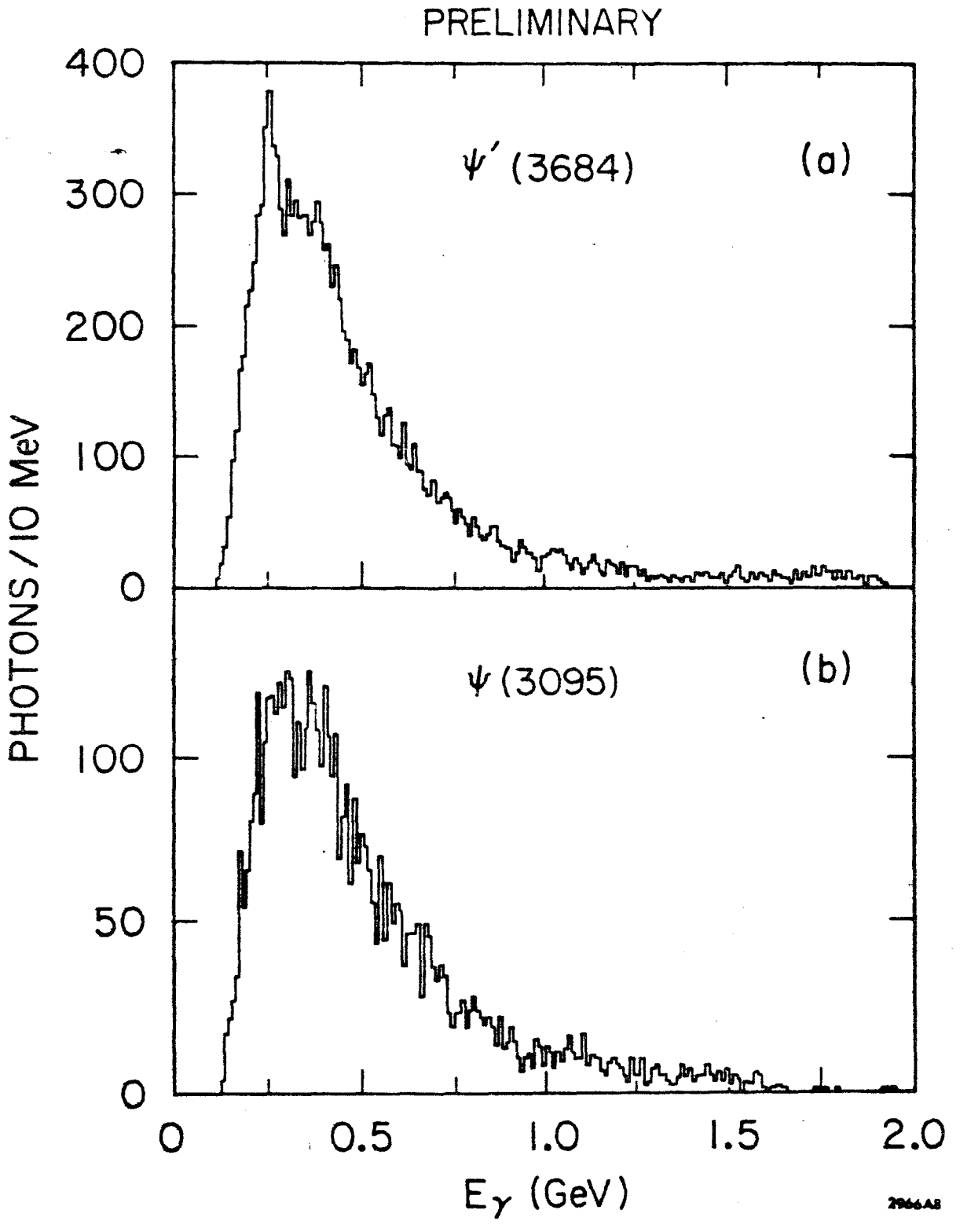

FIG. 36. Inclusive photon energy distributions for a) ψ decays and b) ψ' decays.

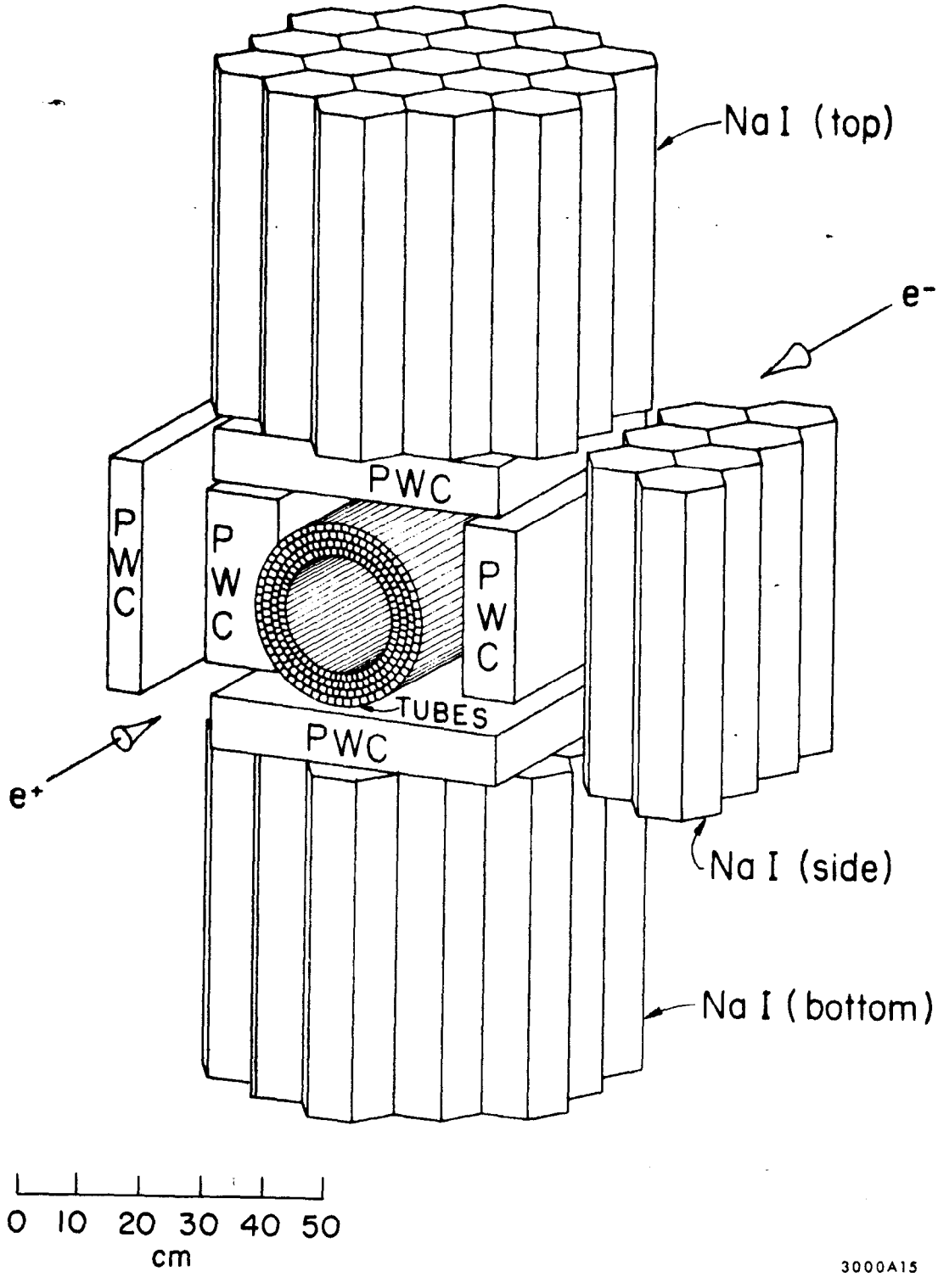

FIG 37. MPPSDSS experiment detector.

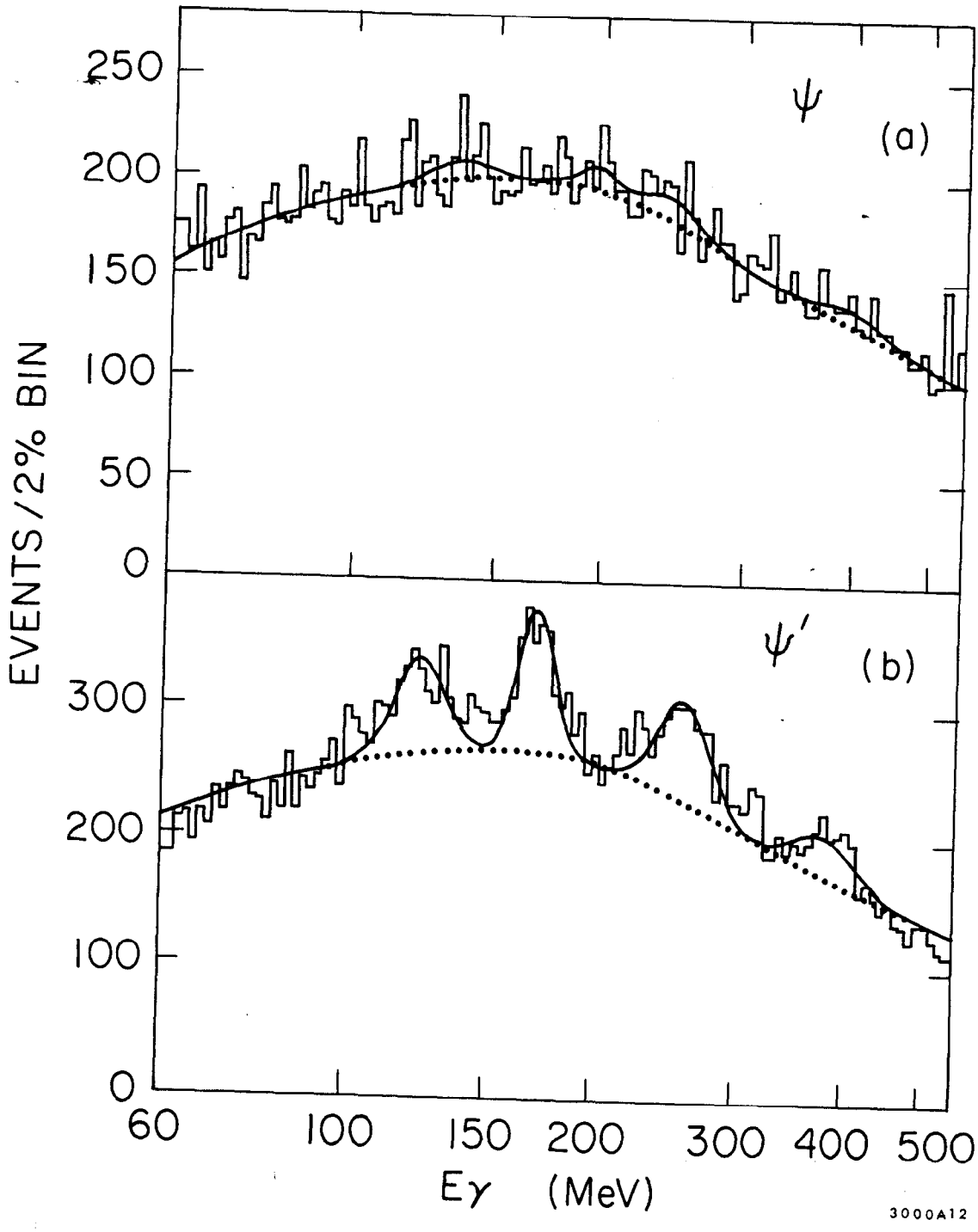

FIG. 38. Inclusive photon energy distributions for a) ψ decays and b) ψ' decays measured by the MPPSDSS experiment.

two experiments agree within errors. For the remainder of this lecture, we use the MPPSDSS branching fractions so that we have a consistent set of values.

VII.F. Is anything missing?

A little over a year ago, before the χ states and direct ψ' decays were found, there was a large fraction of ψ' decays that could not be accounted for.[74] It is now interesting to ask whether the situation has been rectified. The accounting is given in Table IX. There is much less guess work here than was necessary for the ψ (Table VI). We can account for (95 ± 12)% of the ψ' decays. There is still room for new decay modes but they are no longer mandated by the data.

TABLE IX. Summary of ψ' decay modes.

mode	branching fraction (%)
lepton pairs	1.9 ± 0.3
hadrons via second-order e.m. interaction	2.9 ± 0.4
direct decays to ordinary hadrons	9 ± 5
$\psi\pi\pi$, $\psi\eta$	53.3 ± 4.4
$\gamma\chi$	28 ± 10
TOTAL	95 ± 12

VIII. χ states

VIII.A. Masses and branching ratios

Table X lists the mass determinations of the χ states. The average values are 3414 ± 4, 3454 ± 7, 3508 ± 4, and 3552 ± 6 MeV/c^2.

Tables XI, XII, and XIII give a compendium of χ branching ratios.

TABLE X. Mass Determinations of the χ States

Masses are referenced to $m_{\psi'} = 3684$ MeV/c^2. See footnote b.

State	Mass (MeV/c^2)	ψ' Decay Mode	Ref.	footnotes
$\chi(3415)$	3415 ± 10	γ + hadrons	78	
	3413 ± 5	monochromatic γ	81	
	3413 ± 10	$\gamma\gamma\psi$	81	a
	3418 ± 7	monochromatic γ	67	
	3412 ± 8	$\gamma\gamma\psi$	61	a,b
average	3414 ± 4			
$\chi(3455)$	3454 ± 7	$\gamma\gamma\psi$	81	c
$\chi(3510)$ or P_c	3500 ± 10	γ + hadrons	78	
	3504 ± 7	$\gamma\gamma\psi$	81	
	3512 ± 7	monochromatic γ	67	
	3512 ± 7	$\gamma\gamma\psi$	61	b
average	3508 ± 4			
$\chi(3550)$	3550 ± 10	γ + hadrons	78	
	3543 ± 7	$\gamma\gamma\psi$	81	
	3561 ± 7	monochromatic γ	67	
average	3552 ± 6			d

a. A total of three events have been observed in $\chi(3415) \rightarrow \gamma\psi$, two at DESY and one at SLAC.

b. DESY mass assignments have been increased by 4 MeV/c^2 to correct for the difference in ψ' mass measurements between SLAC and DESY.

c. The existence of this state needs confirmation.

d. Error increased by 30% due to high χ^2.

TABLE XI. Decay Modes of the $\chi(3415)$

The branching fraction for $\psi' \to \gamma\chi(3415)$ is assumed to be 0.10 (Ref. 67). All the values and errors in this Table will scale inversely with this value. See heading for Table IV.

Mode	Fraction (%)	Ref.	footnote
$\gamma\psi$	5. ± 3.	61,81	a
$\pi^+\pi^-$	0.7 ± 0.2	78,(61,88)	
K^+K^-	0.7 ± 0.2	78,(61,88)	
$2\pi^+ 2\pi^-$	3.2 ± 0.6	78,(88)	
$K^+K^-\pi^+\pi^-$	2.7 ± 0.7	78,(88)	
$3\pi^+ 3\pi^-$	1.4 ± 0.5	78,(88)	
$\rho^o\pi^+\pi^-$	1.2 ± 0.4	78	
$K^{o*} K^+ \pi^+$	1.7 ± 0.8	78	
$\gamma\gamma$	< 0.013	61	

a. A total of three events have been observed in $\chi(3415) \to \gamma\psi$, two at DESY and one at SLAC.

TABLE XII. Decay Modes of the $\chi(3510)$ or P_c

The branching fraction for $\psi' \to \gamma\chi(3510)$ is assumed to be 0.09 (Ref. 67). All the values and errors in this Table will scale inversely with this value. See heading for Table IV.

Mode	Fraction (%)	Ref.	footnotes
$\gamma\psi$	30. ± 8.	61,81(87)	
$\pi^+\pi^-$ and K^+K^-	< 0.17	78,(61)	a
$2\pi^+ 2\pi^-$	1.2 ± 0.5	78,(88)	
$K^+K^-\pi^+\pi^-$	0.7 ± 0.3	78,(88)	
$3\pi^+ 3\pi^-$	∿ 1.4	78,(88)	b
$\rho^o\pi^+\pi^-$	0.29 ± 0.24	78	
$K^{o*} K^- \pi^+$	0.35 ± 0.21	78	
$\gamma\gamma$	< 0.015	61	c

a. Forbidden for a $J^{PC} = 1^{++}$ state

b. $\chi(2510) \to 3\pi^+ 3\pi^-$ and $\chi(3550) \to 3\pi^+ 3\pi^-$ are not resolved experimentally. The total combined branching fraction for these two states is $\psi' \to \gamma\chi \to \gamma 3\pi^+ 3\pi^- = (2.5 \pm 0.8) \times 10^{-3}$.

c. Forbidden for a spin 1 particle.

TABLE XIII. Decay Modes of the $\chi(3550)$

The branching fraction for the $\psi' \to \gamma\chi(3550)$ is assumed to be 0.08 (Ref. 67). All the values and errors in this Table will scale inversely with this value. See heading in Table IV.

Mode	Fraction (%)	Ref.	footnote
$\gamma\psi$	12.5 ± 7.5	81	
$\pi^+\pi^-$ and K^+K^-	0.29 ± 0.15	78	
$2\pi^+ 2\pi^-$	2.0 ± 0.5	78,(88)	
$K^+K^-\pi^+\pi^-$	1.8 ± 0.5	78,(88)	
$3\pi^+ 3\pi^-$	$\sim$ 1.6	78,(88)	a
$\rho^o\pi^+\pi^-$	0.62 ± 0.36	78	
$K^{o*} K^- \pi^+$	0.66 ± 0.36	78	

a. $\chi(3510) \to 3\pi^+ 3\pi^-$ and $\chi(3550) \to 3\pi^+ 3\pi^-$ are not resolved experimentally. The total combined branching fraction for these two states is $\psi' \to \gamma\chi \to \gamma 3\pi^+ 3\pi^- = (2.5 \pm 0.8) \times 10^{-3}$.

VIII.B. Spins and parities

Although we have not explicitly determined the spin of any of the χ states, we now have enough information to give an experimentally preferred assignment under the mild, but powerful, assumption that we are dealing with the low lying states of a fermion-antifermion system.

We will assume that the possible spin-parity states are those shown in Fig. 30, 0^-, 0^+, 1^+, and 2^+. We will then go through a series of arguments which will exlcude certain spin-parity assignments for certain states. At the end, if we make the additional assumption that each of the the four spin states should be assigned to one of the four χ states, we obtain a unique solution.

The first piece of evidence for spin assignments comes from χ decays to two pseudoscalars, $\pi^+\pi^-$ or K^+K^-. The possible J^{PC} states for two pseudoscalars are 0^{++}, 1^{++}, 2^{++}, etc. The χ states have **even** C since they are reached by radiative transitions from the ψ'. Therefore any χ state which decays to $\pi^+\pi^-$ or K^+K^- must have $J^P = 0^+$, 2^+, etc. In Fig. 33, there is overwhelming evidence that the $\chi(3415)$ decays to $\pi^+\pi^-$ or K^+K^- and there is strong evidence for the $\chi(3550)$ decay to $\pi^+\pi^-$ or K^+K^-.

The other technique which can be used to determine χ spins is a study of angular distributions of the photons. The most information comes from the $\psi' \to \gamma\chi \to \gamma\gamma\psi \to \gamma\gamma\mu\mu$ cascade.[92-94] There are five independent angles as illustrated in Fig. 39. For spin 0, the distribution is unique,

$$W(\theta, \phi, \vartheta, \theta', \phi') \propto (1 + \cos^2\Theta)(1 + \cos^2\Theta') \ . \qquad (21)$$

For other spins, the distributions are quite complex and depend on which multipoles are excited. A study has been made at SPEAR of these distributions for the $\chi(3510)$ using the second method of detecting cascade events

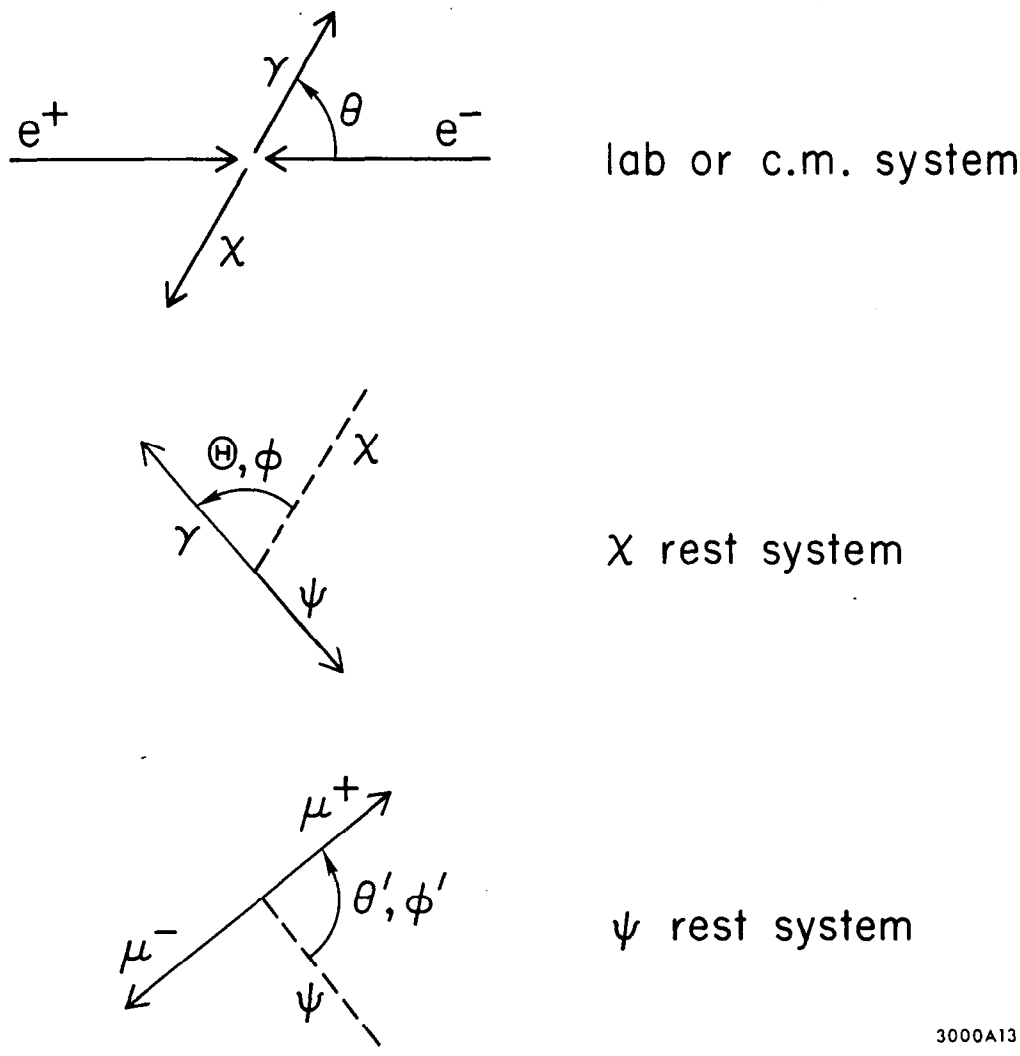

FIG. 39. Definition of angles for the cascade decay $\psi' \to \gamma\chi \to \gamma\gamma\psi \to \gamma\gamma\mu^+\mu^-$.

discussed in Sec. VII.E.2.[77] Preliminary results indicate that the observed distributions completely exclude spin 0. Work is now in progress to determine whether spin 1 or 2 is favored and which multipoles are involved in the decay.

The DESY-Heidelberg collaboration has also concluded that the $\chi(3510)$ spin is not zero by just studying the θ distribution.

The angular distribution of the photon in the production of the $\chi(3415)$ and the $\chi(3550)$ has been studied in $\chi \to 4\pi$ and $\chi \to K^+K^-\pi^+\pi^-$ decays.[78] Figure 40 shows the θ distributions when χ's are detected in these modes. The angular distribution must be of the form

$$W(\theta) \propto 1 + \alpha \cos^2\Theta \ , \tag{22}$$

and from Eq. 21 $\alpha = 1$ for spin 0. Fits for α to the data of Fig. 40 give

$$\alpha = 0.21 \begin{smallmatrix} +\,0.39 \\ -\,0.31 \end{smallmatrix} \text{ for } \chi(3550), \tag{23a}$$

$$\alpha = 0.25 \begin{smallmatrix} +\,0.56 \\ -\,0.38 \end{smallmatrix} \text{ for } \chi(3510) \ , \tag{23b}$$

and

$$\alpha = 1.37 \begin{smallmatrix} +\,0.51 \\ -\,0.41 \end{smallmatrix} \text{ for } \chi(3415) \ , \tag{23c}$$

Thus, the $\chi(3415)$ is consistent with spin 0, but the $\chi(3550)$ is inconsistent with spin 0 to about two standard deviations.

All of these arguments are summarized in Table XIV. A number of conclusions can be drawn: Without any assumptions, none of the three well established states, $\chi(3415)$, $\chi(3510)$, or $\chi(3550)$, can be a pseudoscalar. Also if the $\chi(3550)$ has a spin below 4, its spin-parity must be 2^+. If we assume that the four candidate spin states each correspond to

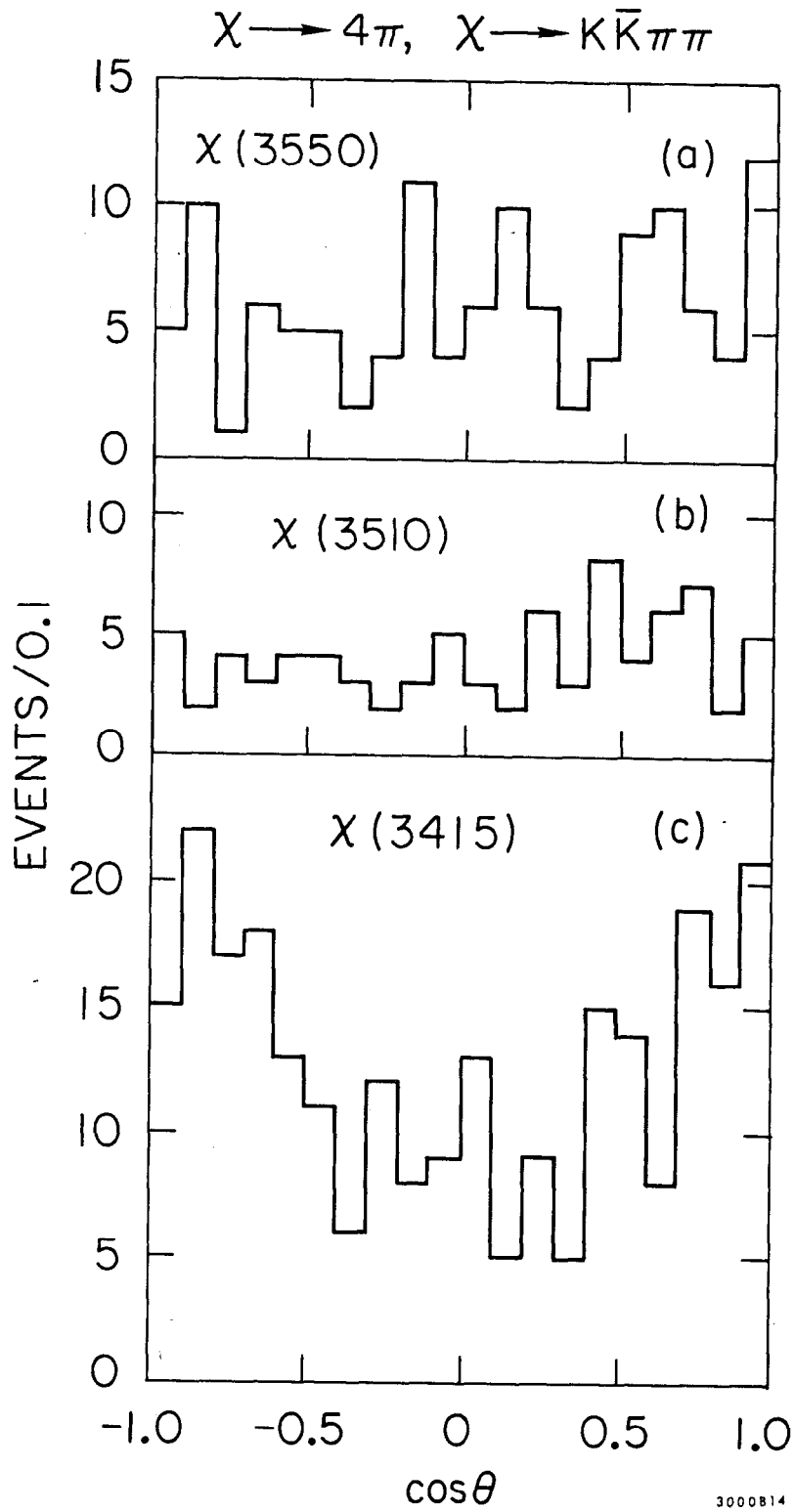

FIG. 40. Distribution of cos ϕ for $\psi' \to \gamma\chi$, $\chi \to 2\pi^+2\pi^-$ or $K^+K^-\pi^+\pi^-$.

one of the four χ states, there is a unique assignment:

State	J^P
$\chi(3550)$	2^+
$\chi(3510)$	1^+
$\chi(3445)$	0^-
$\chi(3415)$	0^+ .

Note that the $\chi(3455)$ has been assigned to be a pseudoscalar, not because we know anything about it, but because that was the only slot left. There are other possibilities. Jaffe suggested that this state could be an exotic[96] and Harari suggested that it could be a singlet D state, $J^{PC} = 2^{-+}$.[97]

TABLE XIV. Spin assignments of the χ states. The preferred assignments depend on assumptions discussed in the text.

State/J^P	0^-	0^+	1^+	2^+
$\chi(3550)$	excluded by $\chi \to \pi^+\pi^-$ or K^+K^- and by angular distribution in $\psi' \to \gamma\chi \to \gamma$ hadrons	excluded by angular distribution in $\psi' \to \gamma\chi \to \gamma$ hadrons	excluded by $\chi \to \pi^+\pi^-$ or K^+K^-	preferred
$\chi(3510)$	excluded by angular distribution in $\psi' \to \gamma\chi \to \gamma\gamma\psi$	excluded by angular distribution in $\psi' \to \gamma\chi \to \gamma\gamma\psi$	preferred	
$\chi(3455)$	preferred			
$\chi(3415)$	excluded by $\chi' \to \pi^+\pi^-$ or K^+K^-	preferred	excluded by $\chi \to \pi^+\pi^-$ or K^+K^-	

VIII.C. Comparisons to theoretical models.

The data on P states appear to be in reasonable agreement with most charmonium models. First, the order of the states is correct. In all models the 2^+ state should be heaviest and the 0^+ state should be lightest. Second, the ratio of $\psi' \to \gamma\chi$ partial widths is in agreement with simplest assumption: that they should be proportional to the phase space factor for dipole transitions. We expect:

$$\begin{array}{lccccc} & \Gamma(\psi' \to \chi(3550)) & : & \Gamma(\psi' \to \chi(3510)) & : & \Gamma(\psi' \to \chi(3415) \\ = & 5k^3 & : & 3k^3 & : & k^3 \\ = & 1.0 & : & 1.4 & : & 1.6 \quad , \end{array} \tag{24a}$$

where k is the available momentum and the coefficients are spin factors. With large errors the observed values are:

$$1.0 \quad : \quad 1.1 \quad : \quad 1.25 \ . \tag{24b}$$

The $\chi(3510)$ has a larger branching fraction to $\gamma\psi$ than either the $\chi(3415)$ or $\chi(3550)$, presumably due to a suppression of $\chi(3510) \to$ hadrons. This behavior was expected for 1^+ P state in models in which C-even states decays to hadrons via two massless vector gluons.[98] Since a spin 1 particle cannot decay into two massless vector particles, these decays are suppressed.

The assignment of the $\chi(3455)$ as the η_c' appears to be in strong disagreement with models where it decays via two vector gluons. Chanowitz and Gilman[99] point out that from $\psi' \to \gamma\eta_c$ has the same matrix element as $\eta_c' \to \gamma\psi$. Accounting for phase space,

$$\Gamma(\chi(3455) \to \gamma\psi) \simeq \tfrac{1}{4}\Gamma(\psi' \to \gamma\eta_c) \quad , \tag{25}$$

from which we can conservatively deduce

$$\Gamma(\chi(3455) \to \text{all}) < 5 \text{ KeV} \quad , \tag{26}$$

whereas one expects a width of several MeV in these models.

IX. The X(2800)

Two experiments at DORIS have reported evidence for a state at about 2800 MeV/c^2 which is detected in the sequence $\psi \to \gamma X \to \gamma\gamma\gamma$.[61,62] Only the photon angles are measured and a 1-C fit is performed. Backgrounds are $\psi \to \gamma\eta$, $\psi \to \gamma\eta'$, and radiative (non-resonant) two photon production.

The original data were not completely conclusive, so additional data were collected at DORIS. Peter Schmuser will report the new DASP results in the topical conference,[65] so we will not cover the details here.

Unfortunately, the new DASP results are still not completely conclusive. There is a slightly over three standard deviation signal, but this level of significance is generally not considered sufficient to establish a new particle. New results from the DESY-Heidelberg group are not available yet; these results may help to clarify the situation.

No experiment at SPEAR has been sensitive to the three photon mode. Originally, it was reported that $\psi \to \gamma\chi \to \gamma p\bar{p}$ with a branching fraction o about 2×10^{-4}, based on the observation of two events.[61] This result was later withdrawn, but in the meantime a search was made for the $\gamma p\bar{p}$ decay mode in the SPEAR magnetic detector. The background is $\psi \to p\bar{p}\pi^0$ since a π^0 and photon will not be completely separable by missing mass. The data are shown in Fig. 41. There is no sign of the X(2800) and an upper limit on the branching fraction for $\psi \to \gamma X \to \gamma p\bar{p}$ can be set at 4×10^{-5}. Searches for X(2800) decays into other hadronic modes have all been unsuccessful, but none of the limits are small enough to be conclusi

The status of the X(2800) and the X(3455) are quite similar. We

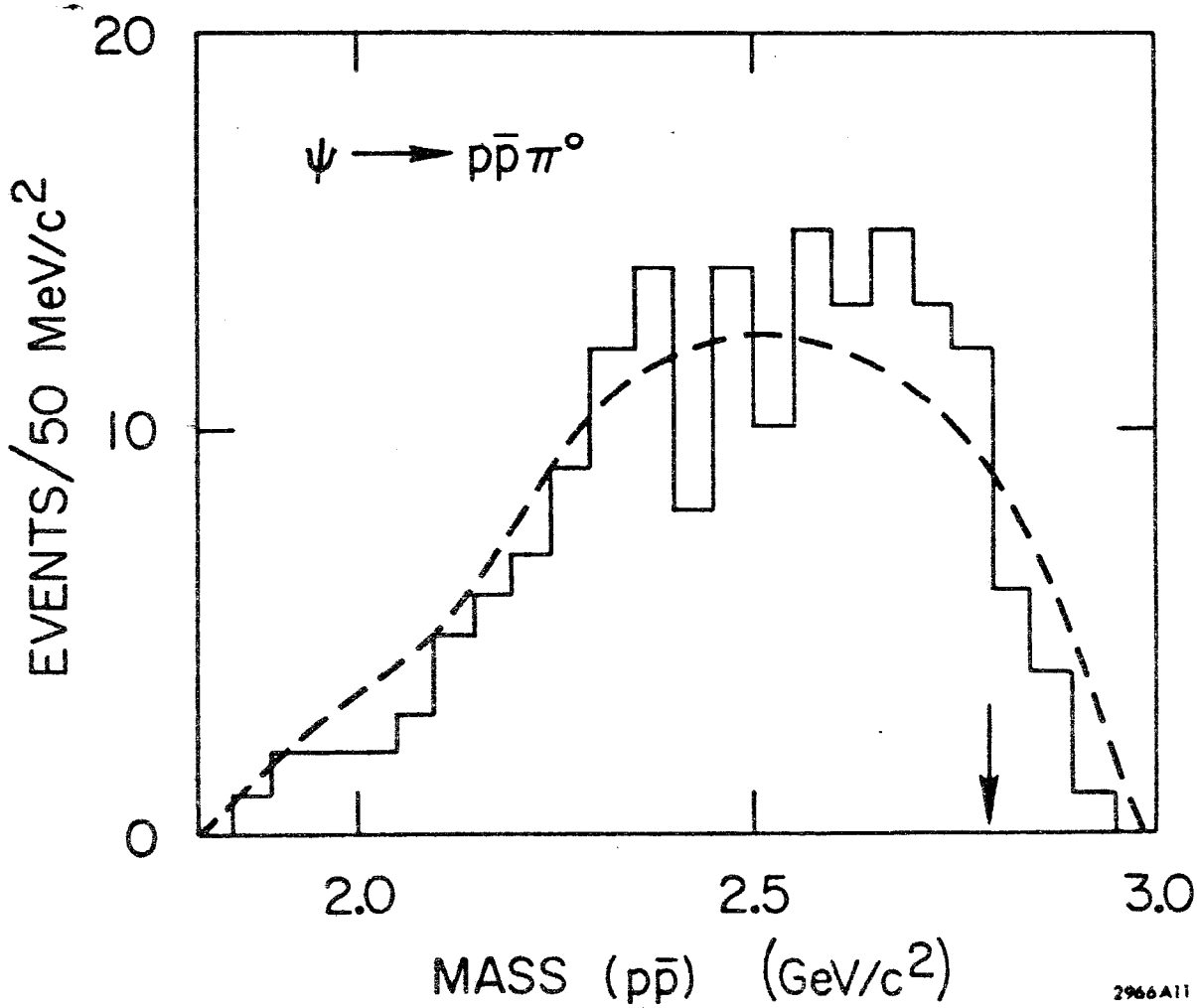

FIG. 41. Invariant mass of $p\bar{p}$ in $\psi \to p\bar{p}\pi^0$ or $p\bar{p}\gamma$ decays.

have enough evidence to take these states seriously, but not enough to establish them. Confirmation of both is badly needed.

X. Summary

In less than two years after the discovery of the ψ, we have learned a a great deal about it and its relatives. In some cases we understand a state of charmonium better than its analogue in light quarks. An attempt to summarize as much of this information as possible on one page is made in Fig. 42.

As we look to future work in this field it is clear that a great deal of it should and will go into understanding the structure of the charmonium states in the 4 GeV region and into studying the spectroscopy of charmed particles. There is, however, more work that should be done on ψ and ψ' decays. Below is a list in no particular order. Some of these items can be worked on now, others will have to await better detectors.

1) The status of the 0^- states is clearly the outstanding question. The masses and transition widths to these states are crucial parameters for charmonium calculations.

2) Although we now have a preferred set of χ spin assignments, it is important to determine the spins directly without imposing assumptions on the possible values.

3) There is still a missing P state, the singlet 1^{+-} state. The best way of finding it may be in the $\chi(3550) \to \gamma\ 1^{+-}$ decay.

4) The direct ψ' decays to ordinary hadrons needs much more study. Much more can be done with just the present data.

5) The suggestions that there is $c\bar{c}$ mixing with the lighter quarks in the pseudoscalar states should be followed up. We have seen evidence

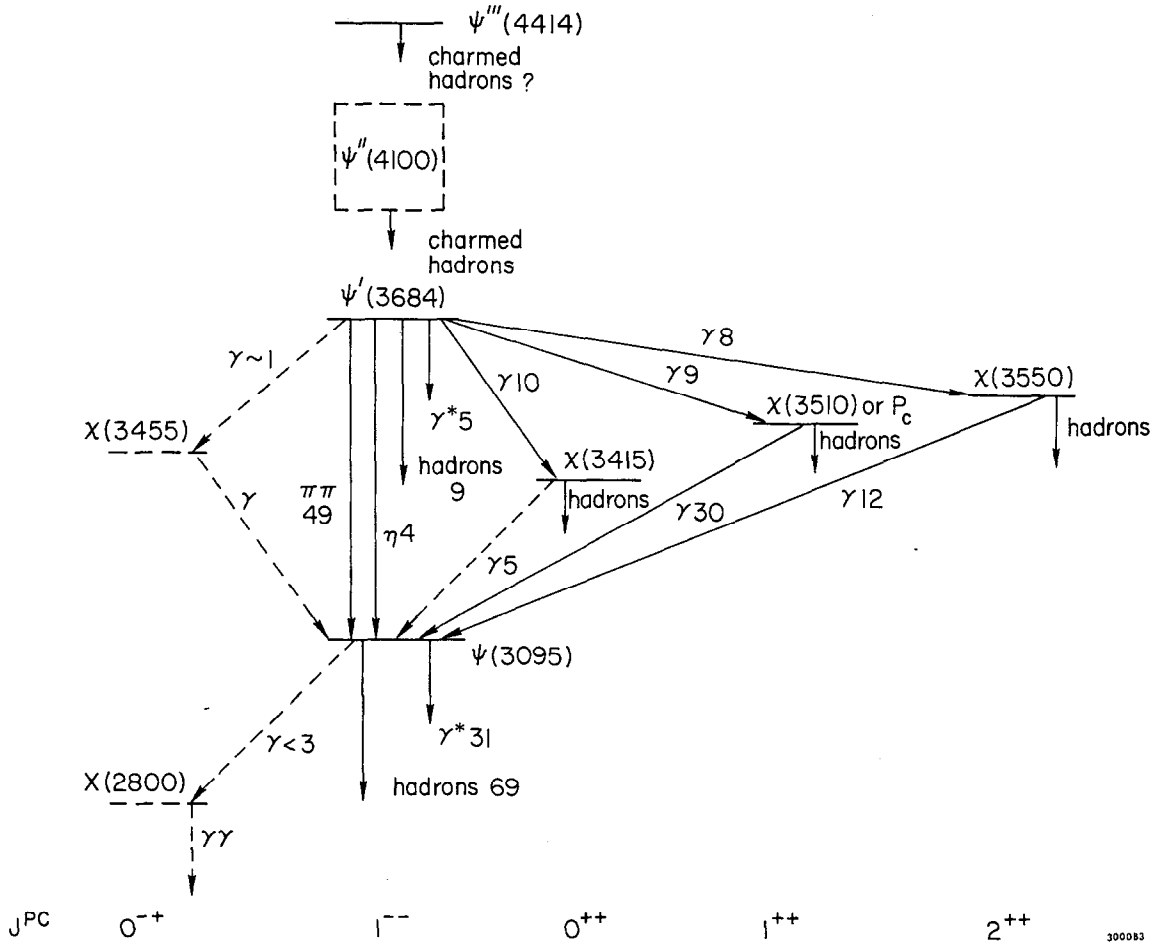

FIG. 42. Summary of observed charmonium states and transitions. Uncertain states and transitions are indicated by dashed lines. Numbers indicate branching fractions in per cent.

for it in radiative ψ decays and in the rate of $\psi' \to \psi\eta$. Inclusive and exclusive state studies of η and η' production in ψ decays would be useful for the further study of this possible mixing.

6) Finally there is a great deal of bread and butter physics to be done. We can imagine mega- and multimega-event runs with powerful second generation detectors. Systematic measurements of all ψ and ψ' decay modes from these data could have three separate objectives:

a) To study the dynamics of charmonium annihilation.

b) To study ordinary hadron spectroscopy from a new perspective. In Sec. IV.D, we saw that ψ decays to PV and VT mesons were allowed and that all channels were populated approximately equally. The scalar (S) and axial vector (A^+, A^-) multiplets of ordinary mesons are not well understood yet. By studying the allowed VS, VA^+, and PA^- ψ decays we may gain new insight into them. Note that the possible ϕS^* decay discussed in Sec. IV.E is a VS type decay; by SU(3) all the others should be present too.

c) And finally, to look for surprises which may provide the germ of the next level of understanding.

REFERENCES

1. G. Goldhaber et al., Phys. Rev. Lett. 37, 255(1976).

2. I. Peruzzi et al., Phys. Rev. Lett. 37, 569(1976).

3. D. Hitlin, these proceedings.

4. G. Goldhaber, these proceedings.

5. V.L. Auslander et al., Phys. Lett. B25, 433(1967).

6. V.L. Auslander et al., Sov. J. Nucl. Phys. 9, 114(1969).

7. V.E. Balakin et al., Phys. Lett. B34, 328(1971).

8. L.M. Kurdadze et al., Phys. Lett. B42, 515(1972).

9. J.-E. Augustin et al., Phys. Lett. B28, 508(1969).

10. J.-E. Augustin et al., Phys. Lett. B28, 513(1969).

11. J.-E. Augustin et al., Phys. Lett. B28, 517(1969).

12. J.C. Bizot et al., Phys. Lett. B32, 916(1970).

13. D. Benakas et al., Phys. Lett. B39, 289(1972).

14. G. Cosme et al., Phys. Lett. B40, 685(1972).

15. D. Benakas et al., Phys. Lett. B42, 507(1972).

16. B. Bartoli et al., Phys. Rev. D6, 2374(1972).

17. C. Bacci et al., Phys. Lett. B44, 533(1973).

18. M. Grilli et al., Nuovo Cimento 13A, 593(1973).

19. F. Ceradini et al., Phys. Lett. B47, 80(1973).

20. M. Bernardini et al., Phys. Lett. B51, 200(1974).

21. A. Litke et al., Phys. Rev. Lett. 30, 1189(1973).

22. G. Tarnospolsky et al., Phys. Rev. Lett. 32, 432(1974).

23. J.-E. Augustin et al., Phys. Rev. Lett. 34, 764(1975).

24. A.M. Boyarski et al., Phys. Rev. Lett. 34, 1357(1975).

25. V. Lüth et al., Phys. Rev. Lett. 35, 1124(1975).

26. J. Siegrist et al., Phys. Rev. Lett. 36, 700(1976).

27. R.F. Schwitters in Proceedings of the 1975 International Symposium on Lepton and Photon Interactions at High Energies (Stanford University, 1975). p. 5.

28. S. Okubo, Phys. Lett. 5, 165(1963).

29. G. Zweig, unpublished work (1964).

30. J. Iizuka, Suppl. Prog. Theor. Phys. 37-38, 21(1966).

31. J.D. Jackson, these proceedings.

32. D.R. Yennie, Phys. Rev. Lett. 34, 239(1975).

33. A.M. Boyarski et al., Phys. Rev. Lett 34, 762(1975).

34. G.S. Abrams et al., Phys. Rev. Lett. 33, 1453(1974).

35. H.L. Lynch, SLAC report number SLAC-PUB-1750, (1976).

36. D.C. Hom et al., Phys. Rev. Lett. 36, 1236(1976).

37. D. Eartly, G. Giacomelli, and K. Pretzl, Phys. Rev. Lett. 36, 1355(1976).

38. T. Appelquist and H.D. Politzer, Phys. Rev. Lett. 34, 43(1975).

39. J.-E. Augustin et al., Phys. Rev. Lett. 34 233(1975).

40. G.J. Feldman and M.L. Perl, Phys. Rep. 19C 233(1975), Appendix A.

41. W. Braunschweig et al., Phys. Lett. 53B, 393(1974).

42. W. Braunschweig et al., Phys. Lett. 56B, 491(1975).

43. R. Baldini-Celio et al., Phys. Lett. 58B, 471(1975).

44. B. Esposito et al., Lett. Nuovo Cimento 14, 73(1975).

45. C. Bemporad in Proceedings of the 1975 International Symposium on Lepton and Photon Interactions at High Energies (Stanford University, 1975), p. 113.

46. R.L. Ford et al., Phys. Rev. Lett. 34, 604(1975).

47. L. Criegee et al., DESY report 75/32 (1975).

48. A.D. Lieberman in Proceedings of the 1975 International Symposium on Lepton and Photon Interactions at High Energies (Stanford University, 1975), p. 55

49. W. Brauschweig et al., Phys. Lett. 63B, 487(1976).

50. G. Wolf, Proceedings of the International Meeting on Storage Ring Physics., Flaine, France, Feb. 22-28, 1976 (to be published).

51. G.J. Feldman, internal SLAC-LBL memorandum (quoted in ref. 50).

52. B. Jean-Marie et al., Phys. Rev. Lett. 36, 291(1976).

53. F. Vannucci, internal SLAC-LBL memorandum.

54. F. Vannucci et al., SLAC report SLAC-PUB-1724 (1976).

55. G.S. Abrams in Proceedings of the 1975 International Symposium on Lepton and Photon Interactions at High Energies (Stanford University, 1975) p. 25.

56. G. Goldhaber, LBL report number LBL-4884 (1976).

57. I. Peruzzi and M. Piccolo, and S.M. Alam, SLAC-LBL internal memoranda.

58. G. Goldhaber, LBL report number LBL-4224 (1975).

59. G. Goldhaber, SLAC-LBL internal memorandum.

60. C. Bacci et al., Lett. Nuovo Cimento 12, 269(1975).

61. B. Wiik in Proceedings of the 1975 International Symposium of Lepton and Photon Interactions at High Energies (Stanford University, 1975), p. 69.

62. J. Heintze in Proceedings of the 1975 International Symposium on Lepton and Photon Interactions at High Energies (Stanford University, 1975), p. 97.

63. R. Baldini-Celio, Phys. Lett. 58B, 475(1975).

65. P. Schmuser, these proceedings.

66. W. Bartel et al., DESY report number 76/40 (1976).

67. D.H. Badtke et al., paper submitted to the XVIII International Conference on High Energy Physics, Tbilisi, USSR, July 15-21, 1976; D.E. Lyon and J.G. Smith, private communications.

68. F.J. Gilman, SLAC report SLAC-PUB-1600 (1975).

69. This mechanism was first suggested to us by F.J. Gilman.

70. R.N. Cahn and M.S. Chanowitz, Phys. Lett. 59B, 277(1976).

71. H. Harari, Phys. Lett. 60B, 172(1976).

72. I am grateful to F.J. Gilman for pointing out several calculational errors in the original table.

73. E. Hilger et al., Phys. Rev. Lett. 35, 625(1975).

74. V. Lüth, SLAC report SLAC-PUB-1599 (1975).

75. G.S. Abrams, et al., Phys. Rev. Lett. 34, 1181(1975).

76. W. Tanenbaum et al., Phys. Rev. Lett. 36, 402(1976).

77. W. Tanenbaum, SLAC-LBL internal memorandum and private communication.

78. F.M. Pierre, LBL report number LBL-5324.

79. G.J. Feldman, SLAC-LBL internal memorandum.

80. E.B. Hughes et al., Phys. Rev. Lett. 36, 76(1976).

81. J.S. Whitaker et al., SLAC report SLAC-PUB-1817 (1976).

82. C.G. Callan et al., Phys. Rev. Lett 34, 52(1975).

83. T. Appelquist et al., Phys. Rev. Lett. 34, 365(1975).

84. E. Eichten et al., Phys. Rev. Lett. 34, 369(1975).

85. B.J. Harrington et al., Phys. Rev. Lett. 34, 706(1975).

86. J.D. Bjorken and S.L. Glashow, Phys. Lett. 11, 255(1964).

87. W. Braunschweig et al., Phys. Lett. 57B, 407(1975).

88. G.J. Feldman et al., Phys. Rev. Lett. 35 821(1975).

89. G.H. Trilling, these proceedings.

90. W. Tanenbaum et al., Phys. Rev. Lett. 35, 1323(1975).

91. S. Orito, Invited talk at the New Physics Meeting, Rutherford Laboratory, Chilton, Didcot, England, February 18-20, 1976.

92. G. Karl, S. Meshkov, J.L. Rosner, Phys. Rev. D13, 1203(1976).

93. L.S. Brown and R.N. Cahn, Phys. Rev. D13, 1195(1976).

94. P.K. Kabir and A.J.G. Hey, Phys. Rev. D13, 3161(1976).

95. H. Rieseberg, Invited talk at the 2nd International Conference at Vanderbilt University on New Results in High Energy Physics, Nashville, Tennessee, March 1-3, 1976.

96. R.L. Jaffe, comments during the discussion period.

97. H. Harari, CERN report Th.2222-CERN (1976).

98. R. Barbieri, R. Gatto, and E. Remiddi, Phys. Lett. 61B, 465(1976).

99. M.S. Chanowitz and F.J. Gilman, Phys. Lett. 63B, 178(1976).